UNIVERSITY OF KELANIYA

INTERNATIONAL PROCEEDINGS OF MULTIDISCIPLINARY

RESEARCH AND APPLICATIONS

SELECTED PAPERS FROM
INTERNATIONAL CONFERENCE ON APPLIED AND PURE SCIENCES

ICAPS 2021-KELANIYA

Volume 01

University of Kelaniya

International Proceedings of Multidisciplinary Research and Applications

Volume I

"Green Technology Towards a Knowledge-based Economy"

Faculty of Science
University of Kelaniya
Sri Lanka

Selected papers from

International Conference on Applied and Pure Sciences

ICAPS 2021- Kelaniya

29 October 2021, Faculty of Science, University of Kelaniya Sri Lanka

"Green Technology Towards a Knowledge-based Economy"

Contents

EDITORIAL BOARD

Dr. K. K. K. R. Perera
University of Kelaniya
Dr. K. M. D. C. Jayathilaka
University of Kelaniya
Dr. R. P. Wanigatunga
University of Kelaniya
Dr. D. M. P. V. Dissanayaka
University of Kelaniya

International Editorial Members

Prof. R. C. Woods
University of South Alabama, USA
Prof. F. Konietschke
Charité - Universitätsmedizin Berlin, Charitéplatz 1, Berlin, Germany
Prof. C. R. De Silva
Western Carolina University, Cullowhee, NC 28723
Dr. R. Raghavan
Department of Fisheries Resource Management, KUFOS, Kochi, India
Dr. M. P. Ginige
CSIRO Land and water, Australia
Dr. E. E. L. Mbamyah
Faculty of Medicine and Biomedical Sciences, University of Yaounde1, Cameroon
Dr. H. Kalutarage
School of computing, Robert Gordon University, Aberdeen, UK
Dr. S. Panda
National Institute of Technology Calicut, Kerala, India
Asst. Prof. I. R. Churchill
State University of New York SUNY at Oswego, Oswego, NY
Dr. C. D. Hirwa
Rwanda Agricultural and Animal Resource Development Board, Animal Resources Department, Rwanda

Organizing Committee

Faculty of Science, University of Kelaniya

Dean, Faculty of Science
Prof. S. R. D. Kalingamudali

Conference Chair
Prof. P. A. S. R. Wickramarachchi

Conference Secretary
Dr. D. A. D. A. Daranagama

Track Coordinators
Dr. H. A. C. C. Perera **-** *Biological Sciences*
Dr. C. C. Kadigamuwa - *Physical Sciences*
Dr. I. V. N. Rathnayake - *Multidisciplinary Research*
Dr. A. S. Withanaarachchi - *Software Intensive Systems*

Conference Management Tool Administrators
Dr. I. U. Hewapathirana - *Chair*
Mr. T. D. Kodituwakku

Web Development & Publicity Committee
Dr. W. A. C. Weerakoon - *Chair*
Ms. N. M. T. De Silva
Ms. N. Harischandra

Finance Committee
Ms. N. A. S. N. Wimaladharma - *Chair*
Dr. T. M. M. De Silva

Publication Committee
Prof. W. J. M. Samaranayake – *Chair*
Prof. M. D. M. D. W. M. M. K. Yatawara
Dr. A. L. A. K. Ranaweera
Dr. F. S. B. Kafi

Technical committee
Dr. B. M. T. Kumarika – *Co chair*
Ms. B. B. U. P. Perera – *Co chair*
Dr. S. P. Pitigala
Dr. K. N. S. Warnajith
Dr. W. A. C. Weerakoon
Ms. W. G. D. M. Samankula
Ms. N. M. T. De Silva

Event Management committee
Prof. M. D. M. D. W. M. M. K. Yatawara - *Co chair*
Prof. C. S. K. Rajapakse - *Co chair*
Ms. N. A. S. N. Wimaladharma
Dr. T. M. M. De Silva

Reviewer Panel

Prof. C. R. De Silva
Western Carolina University, USA

Prof. R. M. Dharmadasa
Industrial Technology Institute

Prof. F. Koneitschke
Charité - Universitätsmedizin Berlin, Germany

Prof. M. G. Kularathna
University of Kelaniya

Prof. G. A. K. S. Perera
Wayamba University of Sri Lanka

Prof. V. P. S. Perera
The Open University of Sri Lanka

Prof. S. M. W. Ranwala
University of Colombo

Prof. R. M. K. T. Rathnayaka
Sabaragamuwa University of Sri Lanka

Prof. S. P. Senanayake
University of Kelaniya

Prof. S. A. Wijesundara
National Institute of Fundamental Studies

Prof. R. C. Woods
University of South Alabama, USA

Dr. R. A. B. Abeygunawardana
University of Colombo

Dr. R. Amarakoon
University of Kelaniya

Dr. S. Chelvendran
Industrial Technology Institute

Dr. W. S. Dandeniya
University of Peradeniya

Dr. W. A. R. De Mel
University of Ruhuna

Dr. T. M. M. De Silva
University of Kelaniya

Dr. N. C. Ganegoda
University of Sri Jayewardenepura

Dr. M. P. Ginige
CSIRO Land and water, Australia

Dr. A. P. Hewaarachchi
University of Kelaniya

Dr. D. Kasthurirathna
Sri Lanka Institute of Information Technology

Dr. R. Liyanage
National Institute of Fundamental Studies

Dr. D. A. Meedeniya
University of Moratuwa

Dr. E. J. K. P. Nandani
University of Ruhuna

Dr. M. Nkoua
University Marien, Ngouabi

Dr. A. Pallewatta
University of Kelaniya

Dr. S. Panda
National Institute of Technology Calicut, India

Dr. W. N. N. K. Perera
University of Sri Jayewardenepura

Dr. L. P. N. D. Premarathna
University of Kelaniya

Dr. W. D. C. Udayanga
University of Kelaniya

Dr. G. S. Wijesiri
University of Kelaniya

Mr. H. Wijekoon
Czech University of Life Sciences Prague, Czechia

List of Full Papers

Conference Paper No: BF-03

Formulation and quality evaluation of fruit and vegetable-based energy drink

R.M.N.A. Wijewardane*[1], J.A.A.S. Jayaweera[2] and G.A.A.R. Perera[2]

[1]National Institute of Postharvest Management, Research and Development Center, Jayanthi Mawatha, Anuradhapura, Sri Lanka
[2]Department Export Agriculture, Uva Wellassa University, Badulla
nilanthiwijewardana@yahoo.com*

Abstract

Among specific food products, sports drinks, as well as energy drinks, have become very popular in the last few decades. Although energy drinks currently available are particularly rich with stimulants like caffeine those are very important to the people like athletes, students, and elderly people. The long-term exposure to various components of energy beverages may cause adverse health effects. The present study aims to develop a nutritionally rich natural energy drink formulation using locally available fruits and vegetables without adding stimulants like caffeine. Different combination of energy drink formulations were prepared using different combinations of beetroot, watermelon, pomegranate, orange juices, and king coconut water. Different combinations of energy drink formulations were evaluated based on physicochemical properties, energy content, and organoleptic properties. The best performing formulation was treated with Sodium metabisulphite (SMS) and Sodium Benzoate (SB) with a control (no added preservative) and stored under room temperature (30°C) vs. the refrigerated condition (4±2°C). Data obtained in triplicate (n=3) and the results were analyzed by completely randomized using ANOVA. Mean separation was done using Least Significant Difference (LSD) at $\alpha= 0.05$. The selected best formula contained beetroot (40%), watermelon (20%), pomegranate (30%) and orange (5%) juices, and king coconut water (5%) by volume with 50 ppm of sodium benzoate as a preservative. The content of energy is 54.74 kcal.g^{-1} and 12.37 g of carbohydrate per 100 mL of beverage. Therefore the product can be stored at refrigerated conditions (4±2°C) for a period of two months without deteriorating the quality.

Keywords

Energy drink, Fruits, Nutrition, Storage, Vegetables

Introduction

Energy drinks have been promoted as a healthy beverage within many sub populations, such as, athletes and students, etc. The high concentration of ingredients in the drink that stimulate the body and mind is the cause of many complications. The performance of most of these energy drinks should be monitored because of the unbalanced ingredients, especially sugar and caffeine in their compositions. There are healthier alternative energy drinks that contain significantly lower, sugars, and calories. It is important to consume natural sugars found in fruits, vegetables while avoiding added sugars. Energy drinks are non-alcoholic beverages and most of the synthetic functional beverages contain caffeine as the main active ingredient (Aranda et al., 2006). Now energy drinks are available in more than 140 countries. Most of the consumers of these drinks are children, adolescents, and young adults (Seifert, 2011). Sri Lanka produces about 602,000 metric tons of vegetables and 855,000 metric tons of fruits annually. This comprises of over 40 vegetables and 50 fruit varieties grown in different agro-climatic regions. It is estimated that 30% - 40% of all fruits and vegetables are wasted between harvest and marketing due

to poor post-harvest handling. The increased recognition of fruits and vegetables as important components of a healthy diet has undoubtedly benefitted the industry of the same. The overall trend in new fruit and vegetable products is "added value", thus, providing increased convenience to the consumer by having a much greater variety of readily prepared fruit and vegetable products. In this paper, the energy drink developed comprising of the following major constituents: Beetroot (*Beta vulgaris*), Watermelon (*Citrullus lanatus*), Pomegranate (*Punica granatum*), Orange (*Citrus centifolia*), King Coconut water (KCW) (*Cocos nucifera*).

Methodology

Formulation of energy drink

The experiment was carried out at the National Institute of Postharvest Management, Research and Development Center, Anuradhapura, Sri Lanka. Fruits were obtained from local markets which were superior in quality without significant sign of quality deteriorations. Here, the energy drink was developed as compose of the following major constituents: Beetroot (*Beta vulgaris*), Watermelon *(Citrullus anatus)*, Pomegranate *(Punica granatum),* Orange *(Citrus crenatifolia),* King Coconut water (*Cocos nucifera*) (Table 1).

Sample preparation

The fruits were washed and disinfected by immersing 50 ppm sodium hypochlorite for 15 min. The juice was extracted using juice extractor Fengxiang®, FC-310: China. Raw juices were clarified by bentonite using concentrations of 3 gL^{-1}. The juice was centrifuged at 6000 rpm in a HERMLE centrifugation unit (model Z326k) for 20 minutes at 4 °C temperature. The Juice blend was pasteurized 96 °C 15 min. The hot filling was done using pre-sterilized bottles by maintaining the headspace about 1 inch and capping was done using a manually operated bottle sealing machine. (Palet 3.2 Manual cap Sealing machine). Bottles were kept in the refrigerator (4 ±2 °C) and room temperature (30 °C) separately. The better performing treatment was selected based on physico chemical, organoleptic properties, and energy content of the prepared juice blends.

Table 1. Composition of the energy drinks formulations

Treatment	Beetroot Juice	Watermelon Juice	Pomegranate Juice	Orange Juice	KCW
Treatment 01	40	20	30	5	5
Treatment 02	40	30	20	5	5
Treatment 03	40	40	10	5	5

Two different chemical preservatives such as Sodium Metabisulphite (SMS), Sodium benzoate (SB) were used to enhance the keeping quality of juice blends and another sample was kept as a control without adding any chemical preservatives. The treatments were stored under room temperature (30°C) and refrigerator condition (4 ±2°C) for 8 weeks. The physicochemical properties, microbiological quality, and sensory evaluation were done once in the two-week interval.

Measurement of total soluble solids (TSS), colour, pH and titratable acidity, proximate composition, organoleptic properties, and energy calculation

TSS of the extracted juice was measured by a temperature-compensated digital refractometer (3,810. Atago PAL-1) and is expressed as a percentage. TA was determined as per AOAC (2000). Juice pH was measured by a pH meter (230A+, Thermoorin). Product colour was measured by using Hunter lab color difference meter (CR 400, Konica Minolta) and the values of L*, a*, b* were recorded. The total plate count and yeast and mold count were done as described in AOAC (2000). A proximate composition such as moisture, fat, crude fiber, crude protein, and ash content were determined using the method described in AOAC (2000). The energy value of energy drink formulations was calculated based on their content of crude protein, fat, and carbohydrate using the formula described by Crisan and Sands (1978). Three different formulations (Table. 01) were subjected to evaluate the sensory properties such as external appearance, internal appearance, colour, aroma, taste, texture, and overall acceptability by 30 semi-trained panelists using 5 point Hedonic scale. Different energy drink formulations were stored at two different temperatures such as ambient (30 °C, RH 70%) and refrigerated storage (4 °C ± 2 °C).

Experimental design and analysis

Data obtained were in triplicate (n=3) and the results were assessed by completely randomized design using ANOVA by SAS statistical package. Mean separation was done by using Least Significant Difference (LSD) at $\alpha = 0.05$.

Results and Discussion

Table 2. Effect of different juice combinations on changes in chemical properties of energy drink formulations

Treatment	TSS	TA	pH
Product 01	10.03 ± 0.15	0.25 ± 0.00	4.06 ± 0.04
Product 02	9.73 ± 0.05	0.25 ± 0.00	4.08 ± 0.05
Product 03	9.50 ± 0.00	0.27 ± 0.03	4.34 ± 0.01

Product 1 recorded the highest TSS content compared with other treatments and there was no any significant different ($\alpha = 0.05$) in TA and pH between treatment 2 and 3. Treatment 3 was significantly different from other two treatments (Table 2).

Table 3. Effect of different juice combinations on proximate composition of energy drink formulations

Proximate composition	Product 01	Product 02	Product 03
Moisture content	86.30 ± 0.30	86.67 ± 0.01	87.20 ± 0.00
Crude Fat (Ether extract)	0.18 ± 0.01	0.17 ± 0.00	0.16 ± 0.01
Crude fiber	0.17 ± 0.01	0.21 ± 0.01	0.24 ± 0.01
Ash	0.07 ± 0.01	0.070 ± 0.00	0.06 ± 0.01
Protein	0.88 ± 0.00	0.90 ± 0.02	0.98 ± 0.00
Carbohydrate	12.37 ± 0.01	11.96 ± 0.02	11.35 ± 0.01

Table 4. *Calorific values of the energy drink formulations*

Treatments	Energy (kcalg⁻¹)	Energy (kJg⁻¹)
Product 1	$(12.37 * 4) + (0.88*4) +$ $(0.186*9)$ $= 54.74$	$(12.37* 17) + (0.88*17) +$ $(0.18*37)$ $= 232.35$
Product 2	$(11.96*4) + (0.90*4) + (0.17*9)$ $= 53.70$	$(11.96*17) + (0.90*17) +$ $(0.17*37)$ $= 220.75$
Product 3	$(11.35 *4) + (0.98*4) + (0.16*9)$ $= 50.78$	$(11.35 *17) + (0.98*17) +$ $(0.16*37)$ $= 215.61$

Table 4 recorded that, the highest energy value was recorded by the product one when compare to other treatments.

Sensory analysis

Figure 1 illustrated that, 20% watermelon incorporated energy drink gave the highest estimated median 8.6, 8, 8.6, 8.6 were recorded for appearance, colour, taste and aroma respectively. Therefore the overall acceptability of 20% watermelon incorporated energy drink were recorded the highest estimated median (8.5) and highest sum of rank (76) by accepting as a better formulation for storage.
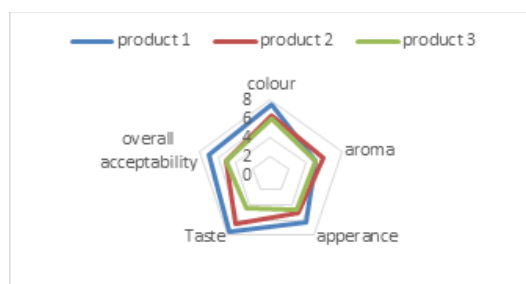
Figure 1. *Effect of different concentration of fruit juices on organoleptic properties of energy drink*
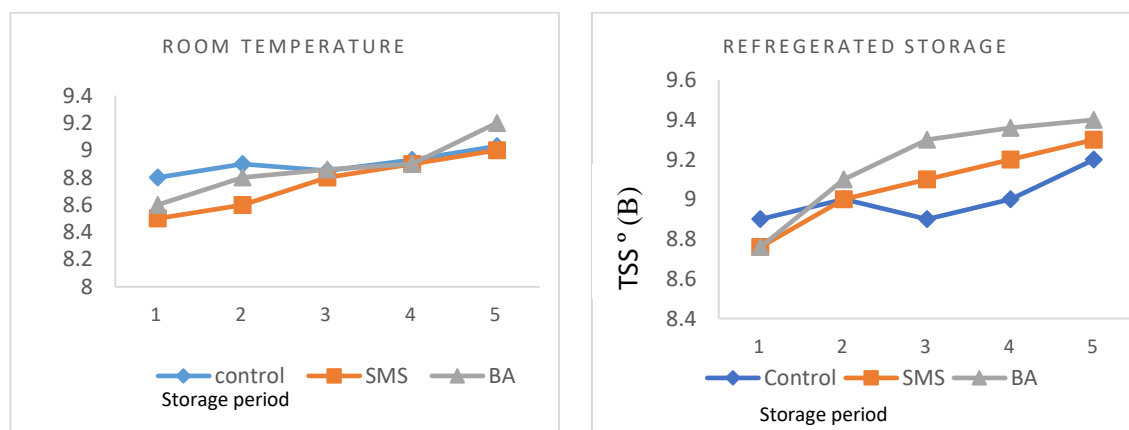
Figure 2. *Effect of SMS and Sodium Benzoate application on TSS of energy drink under room temperature and the refrigerated storage*

The results in figure 2 showed that total soluble solid content in beverage was increased during the storage period which is preserved using two different chemical preservatives (SMS and SB) and control. Total soluble content was gradually increased with the storage period probably due to the conversion of polysaccharides into sugars in the presence of organic acids. Tandon et al. (2003) also reported no significant changes in the total soluble solids during storage. Bull et al. (2004) reported that the °Brix of thermally processed orange juice did not change significantly during storage time.

The figure 3 and 4 shows the changes of pH and titratable acidity respectively in products treated with SMS, SB, and control sample at room temperature. pH values of energy drinks were gradually decreased up to the 8th week. Chemical degradation and chemical reactions may be the possible reasons for these changes. The changes of acidity of three treatments at refrigerator condition were exhibited the gradually increased due to decrease of pH. This Increasing trend was earlier observed by Chauhan et.al 2012. pH decreased and acidity increased due to the degradation of carbohydrates in fruit juices (Ahmad et.al 2011). Brix, pH, and Acidity are three parameters extremely important as they decide the quality of RTS beverages (Patil et. al. 2009). The results compromise with Bull et al. (2004) who studied the thermally processed Valencia and Navel orange juice found no significant modifications of total titratable acidity throughout the storage time
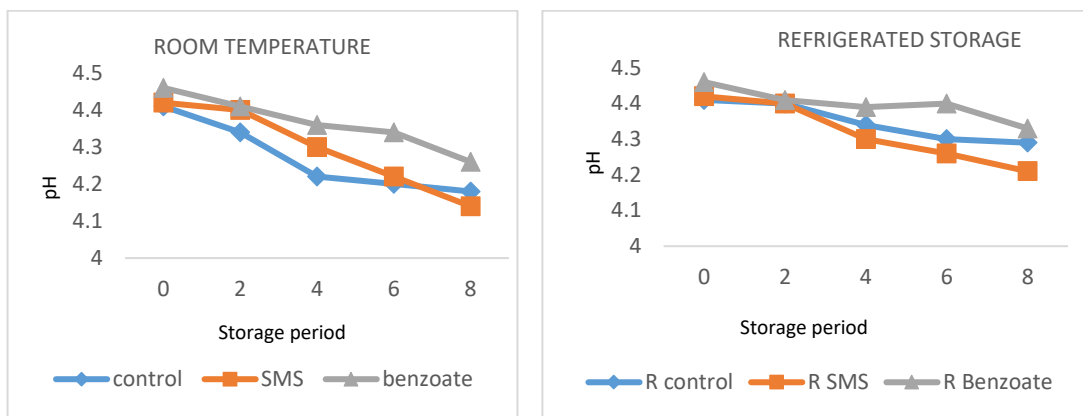
Figure 3. *Effect of SMS and Sodium Benzoate application on pH of energy drink under room temperature and the refrigerated storage*
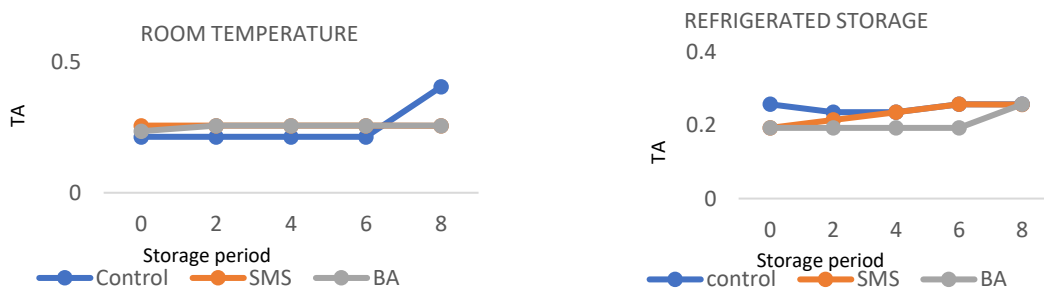
Figure 4. *Effect of SMS and Sodium Benzoate application on TA of energy drink under room temperature and the refrigerated storage*

Total plate counts (TPC) values were recorded in beverages during the storage of eight weeks. The total plate counts were increased in the products at both storage conditions and the high microbial count was observed in the control sample at room temperature,

while preservative added refrigerated samples showed a comparatively low microbial count. Weakening of bacterial growth by lower pH due to addition of SMS and SB and bacterial death due to high temperature used in processing could be the reasons for this low growth of microorganisms in a prepared beverage (Nelugin, 2010). The findings were confirmed with the SLS (729:2010) that the total plate count for Ready serve fruit beverage should 50 per ml in maximum. No Yeast and mold count was observed during storage. Thermal pasteurization for a total heating time of 12 min was able to produce microbiologically stable fruit juices with the retention of quality attributes (Kathiravan et al., 2014).

Mapping of variation in colour of three different products at room temperature and refrigerated conditions condition showed that the minimum variations were observed in SB treatment whereas the variations were minimum at the refrigerated samples when compared to samples at room temperatures. According to Gokhale and Lele (2011) the yellow pigments of beetroot, betaxanthins, are more stable than the betacyanins (red pigments). Zhang et al. (1997) also found a color degradation in the heat pasteurized juice samples.

Based on the estimated median of colour, aroma, taste, appearance and overall acceptability refrigerated SB treated sample was the most preferred sample by the panelists.

Conclusion

The selected formula contained beetroot (40%), watermelon (20%), pomegranate (30%) orange (5%) juices, and king coconut water (5%) by volume with 50 ppm of sodium benzoate as a preservative. It contained 54.74 kcal.g^{-1} energy and 12.37 g of carbohydrate per 100 mL of beverage. The product was able to store at refrigerated conditions (4±2 ℃) for two month period without deteriorating the quality.

References

Ahmad, D., Syed, H.B., Salam, A., Ishfaq, B. (2011). Development of functional and dietetic beverage from bitter gourd. *Internet Journal of Food Safety*, 11(13), 355-360.

AOAC. (2000). Official methods of analysis. Association of Official Analytical Chemist 13th edition. Washington, D.C.

Aranda, M., Morlack, G.E. (2006). Simultaneous Determination of Riboflavin, Pyridoxine, Nicotinamide, Caffeine and Taurine in Energy Drinks by Planar Chromatography-multiple Detection with Confirmation by Electrospray Ionization Mass Spectrometry, *Journal of Chromatography*, A 1131(1-2),253. http://dx.doi.org 60.10.1016/j.chroma.2006.07.018

Bull, M.K., Zerdin, K., Howe, E., Goicoechea, D., Paramanandhan, P., Stockman, R., Sellahewa, J., Szabo, E.A., Johnson, R.L. and Stewart, C.M. (2004). The effect of high pressure processing on the microbial, physical and chemical properties of Valencia and Navel orange juice. *Innovative Food Science and Emerging Technologies*, 5: 135-149.

Chauhan, D.K., Puranik, V., Rai, G.K. (2012). Development of Functional Herbal RTS Beverage. *Scientific reports*, 1,541. https://doi.org :10.4172/. 541.

Crisan, E. V. and Sands, A. Nutritional Value of Edible Mushroom. (1978). In: S. T. Chang and W. A. Hayer, Eds., *Biology and Cultivation of Edible Mushrooms*, Academic Press, New York, pp. 137-168.

Gokhale, S.V., & Lele, S.S. (2011). Dehydration of red beet root (*Beta vulgaris*) by hot air drying: process optimization and mathematical modeling. *Food Science Biotechnology,* 20, 955-964.

Kathiravan, T., Nadanasabapathi, S., & Kumar, R. (2013). Optimization of pulsed electric field processing conditions for passion fruit juice (*Passiflora edulis*) using Response Surface Methodology. *International Journal of Advanced Research* 1(8): 399-411.

Nelugin, S.E., & Mahendran, T. (2010). Preparation of ready to serve (RTS) beverage from Palmyrah (*Borassus flabellifer* L.) fruit pulp. Journal of Agricultural Sciences, 5(2),80-88.

Patil, A.M.S., & Kattimani, K.N.S. (2009). Variability studies in physicochemical parameters in Kokum (*Garcinia indica* Choicy) for syrup preparation. Karnataka *journal of agricultural science*, 22(1), 244-245.

Seifert, S. M., Schaechter, J. L., Hershorin, E. R., & Lipshultz, S. E. (2011). Health effects of energy drinks on children, adolescents and young adults. Pediatrics, 127, 511. http://dx.doi.org/10.1542/peds.2009-3592

SLS. 729:2010, Sri Lanka standard specification for ready to serve fruit drinks (First revision).

Tandon, K., Worobo, R.W., Churey, J.J. & Padilla-Zakour, O.I. (2003). Storage quality of pasteurized and UV treated apple cider. *Journal of Food Processing and Preservation* 27: 21-35.

Zhang, Q. H., Qiu, X., & Sharma, S. K. (1997). Recent developments in pulsed electric field processing in New Technologies Yearbook. Washington, D.C. National Processors Association, pp. 31–42.

Conference Paper No: BF-04

Identification of marker compounds and antioxidant activity of *Terminalia chebula Retz.* fruit pericarps used in selected commercial herbal preparations in Sri Lanka

K.P.C.D. Suraweera[1,2], H.M.R. Amarasekara[2], T.M.S.G. Tennakoon[1] and S.R. Wickramarachchi[2*]

[1]Link Natural Products (Pvt) Ltd., Sri Lanka
[2]Department of Chemistry, University of Kelaniya, Sri Lanka
suranga@kln.ac.lk*

Abstract

Medicinal plants contain phyto-constituents which show pharmacological effects. This study is focused on identification and quantification of marker compounds and determination of the antioxidant activity of *T. chebula* Retz. fruit pericarps used in selected commercial herbal preparations in Sri Lanka. Commercial samples were obtained from Sri Lanka (SL_C) and India (IN_C), separately from three different batches of *T. chebula* stocks from raw material quarantine section at Link Natural Products (Pvt) Ltd. As these commercial samples are a mixture of fruits from wider geographical locations, five samples (SL_A) collected from known locations in Sri Lanka were included for comparison. Methanolic extracts (70 % v/v) were prepared from each sample. Chromatographic profiling was done using thin layer chromatography (TLC) and high-performance liquid chromatography (HPLC). Extracts were assayed for gallic acid content, total tannin content and antioxidant activity. Gallic acid and ellagic acid could be used as marker compounds in quality control of *T. chebula* commercial stocks. All samples had a low IC_{50} value than butylated hydroxytoluene (BHT) standard showing that *T. chebula* fruit pericarps have higher antioxidant activity than BHT. Variations in IC_{50} values were observed within and among SL_A, SL_C and IN_C suggesting that both intrinsic and extrinsic factors may lead to the change in antioxidant potential of the fruits. The mean IC_{50} value of SL_C samples was (6.32 ± 2.09) µg/mL whereas that of IN_C samples was (7.42 ± 0.93) µg/mL suggesting that antioxidant activity was higher in SL_C samples over IN_C samples. A variation in antioxidant activity in SL_A samples was observed, depending on the sampling site.

Keywords

Antioxidants, Gallic acid, Polyphenols, Tannin, *Terminalia chebula*.

Introduction

The demand for the herbal drugs is getting popularized day by day all over the world as they are cheap and natural in origin with less side effects (Naik et al., 2004). Several hundred genera of plants have been used in traditional medicine since ancient times (Gupta, 2012). This study is focused on one such plant species, *Terminalia chebula* Retz, belonging to family Combretaceae, and referred to as 'Aralu' in Sinhala. The plant is native to Asia and found mainly in the dry zone of Sri Lanka (Dassanayake & Fosberg, 1981; Gupta, 2012). The dried fruit pericarp is used in the preparation of many ayurvedic drugs such as Thriphala, Arishta, Asava and Churna. It contains numerous phytochemicals such as tannins, flavonoids, sterols, terpenoids, fixed oils and amino acids. Latest studies have reported that *T. chebula* contain more phenolic compounds compared to the plants studied (Gupta, 2012; Saleem et al., 2002). It also possesses a wide spectrum of pharmacological properties such as antimicrobial, antioxidant, antidiabetic, retinoprotective, immunomodulatory, anti-carcinogenic, anti-arthritic and wound healing. leading to non-toxic therapeutic value of the fruit (Gupta, 2012; Juang et al., 2004; Riaz

et al., 2017). *T. chebula* is a key ingredient in herbal drugs used for the treatment of conditions resulting from oxidative stress caused due to excess reactive oxygen species in cellular environments (Chen et al., 2011; Naik et al., 2004; Naik et al., 2005).

Ayurvedic drug manufacturers in Sri Lanka obtain *T. chebula* dried fruits from both local and Indian suppliers for their herbal preparations. These commercial suppliers obtain fruits from different collectors irrespective of the geographical region or the processing conditions. Hence, the *T. chebula* fruits used in herbal preparation is a mixture of fruits only to be identified as Indian and Sri Lankan origin. Although, many previous studies are reported on the antioxidant and other bioactivities of *T. chebula* fruits from a specific origin, herbal drug manufactures cannot totally rely on those data for their quality control purposes, as their raw materials used in herbal preparations are a mixture of fruits of unknown origin. Hence this study aimed at determining and comparing the antioxidant activity of commercial stocks of *T. chebula*.

Materials and Methods

Materials

Authentic samples (SL_A) of *T. chebula* fresh fruits were collected from the plant itself by onsite visits to five different localities (Bibila, Buththala, Padiyathalawa, Gampaha and Colombo) of Sri Lanka and authenticated against a voucher specimen (Reference Number: LNP/HB/F-COM/TC-01) available at the Herbarium at Link Natural Products Ltd. (LNP). Commercial samples were obtained separately from three different batches of *T. chebula* from Sri Lanka (SL_C) and India (IN_C) at LNP. All solvents and chemicals used were of AR grade and photochemical standards for chromatographic analysis were supplied by Research and development center at Link Natural Products (Pvt) Ltd.

Methods

Dried fruit pericarps of SL_A, SL_C and IN_C samples were ground and sieved through 710 # mesh to make a homogenized coarse powder and were extracted in 70 % v/v methanol. TLC was developed using ethyl formate, toluene, formic acid, water in the ratio of 30:1.5:4:3 (v/v/v/v) as the mobile phase and visualized after spraying with freshly prepared ferric chloride (1% w/v) (Wagner & Bladt, 1996). High performance liquid chromatography (HPLC) was carried out using 1260 Agilent Infinity II HPLC system with reverse phase. Glacial acetic acid (1% v/v) in milli Q water and acetonitrile were used as mobile phase in a gradient mode. The total tannin content of each dried extract was estimated using Folin-Denis assay (Association of Official Analytical Chemists, 1980) with slight modifications. Briefly Folin-Denis reagent (5.00 mL) and saturated Na_2CO_3 solution (10.00 mL) were added respectively into a 100 mL volumetric flask with aqueous stock solution of crude extract (0.01 % w/v, 10.00 mL). The flask was topped up to the 100 mL mark using distilled water. These solutions were gently mixed and incubated in the dark for 30 min at room temperature. Then the absorbances of the resulting solutions were measured at 760 nm with the UV-Visible spectrophotometer (8453 Agilent). The tannin concentration of prepared sample solution was obtained using the regression equation of the standard calibration curve. Total tannin content of *T. chebula* dried fruit pericarps was calculated as a percentage on dry basis. Antioxidant activity was determined using the DPPH radical scavenging assay described by Chatatikun & Chiabchalard (2013) with slight modifications. Briefly methanolic DPPH solutions (0.634 mM, 40 μL) were added to different concentrations of test solution (1.56,

3.13, 6.25, 12.50, 25.00, 50.00, 100.00 μg/mL) in a 96-well plate. These solutions were gently mixed and incubated in the dark for 20 min at room temperature. BHT was used as the standard. Absorbance of the resulting solutions were measured at 517 nm with the microplate reader (Thermo Scientific™ Multiskan™ FC). The % inhibition was calculated and plotted against the test concentrations to obtain the IC_{50} value. The IC_{50} value was calculated using GraphPad Prism 7.00 Statistic Software.

Results and Discussion

1 - Gallic acid
2, 3, 4 - IN_C
5, 6, 7 - SL_C
8 to 12 - SL_A
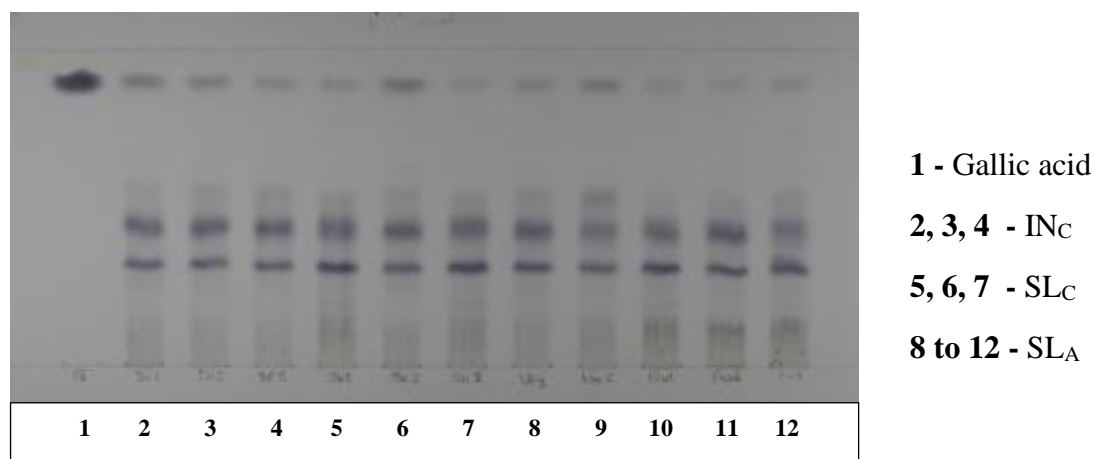
Figure 1. TLC profile of crude extracts of T. chebula after spraying with 1 % aqueous ferric chloride reagent and observed under white light

Polyphenolic compounds in *T. chebula* fruits react with ferric chloride and give blackish blue color spots on TLC plate (Figure 1). Gallic acid standard was used to identify marker compound in crude extracts. All the samples contained gallic acid. TLC fingerprints of SL_A, SL_C and IN_C samples showed a similar pattern with slight variation in the intensity of the corresponding spots.

Presence of gallic acid (GA) and ellagic acids (EA) were shown in HPLC fingerprints of all samples (Figure 2 and 3). Hence these two acids can be used as marker compounds in quality control of *T. chebula* commercial stocks. GA was quantified by determining the area under GA peak. GA and total tannin (TT) content is significantly different (P>0.05) among SL_A depending on the geographical area (Table 1) and in SL_C and IN_C depending on the batch number (Table 2). IN_C showed higher content of GA than SL_C whereas TT content is higher in SL_C than in IN_C (Table 2). GA content can be increased by improper long storage of the *T. chebula* fruits as other complex polyphenolic compounds can be converted into gallic acid during this storage time. Previous studies have reported *T. chebula* with 32% TT content (Chattopadhyay & Bhattacharyya, 2007; Saha & Verma, 2016). But, our results show higher TT contents than this value for all the samples showing our samples are rich in tannins.

Table 1. *GA and TT content of SL_A*

Sample type	GA % (w/w)* (on dry basis)	Total tannin % (w/w)* (on dry basis)
SL_A - Padhiyathalawa	$0.49 \pm 0.01d$	$33.40 \pm 0.17d$
SL_A - Buththala	$0.98 \pm 0.01b$	$43.39 \pm 0.41a$
SL_A - Gampaha	$1.03 \pm 0.02b$	$41.13 \pm 0.61c$
SL_A - Bibila	$0.83 \pm 0.02c$	$42.31 \pm 0.23b$
SL_A - Colombo	$1.86 \pm 0.04a$	$34.12 \pm 0.01d$

Table 2. *GA and TT content of SL_C and IN_C*

Sample type	GA % (w/w)* (On dry basis)	Total tannin % (w/w)* (On dry basis)
SL_{C1}	$1.42 \pm 0.02a$	$51.54 \pm 0.14b$
SL_{C2}	$0.87 \pm 0.11c$	$42.22 \pm 0.25c$
SL_{C3}	$1.10 \pm 0.06b$	$53.67 \pm 0.34a$
IN_{C1}	$2.97 \pm 0.049a^{1}$	$43.57 \pm 0.11a^{1}$
IN_{C2}	$2.18 \pm 0.034b^{1}$	$42.05 \pm 0.54b^{1}$
IN_{C3}	$1.59 \pm 0.003c^{1}$	$42.76 \pm 0.03b^{1}$
SL_C	1.13 ± 0.28	49.14 ± 6.09
IN_C	2.25 ± 0.69	42.79 ± 0.76

Results were analyzed statistically at 95 % level (P>0.05) using ANOVA. Each data point represents mean $\pm$ SD where n=3; SL_C: mean of SL_{C1-3}, IN_C: mean of IN_{C1-3}.
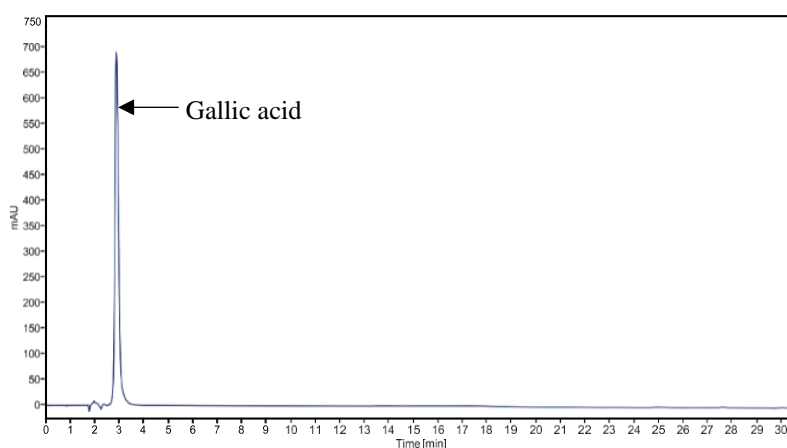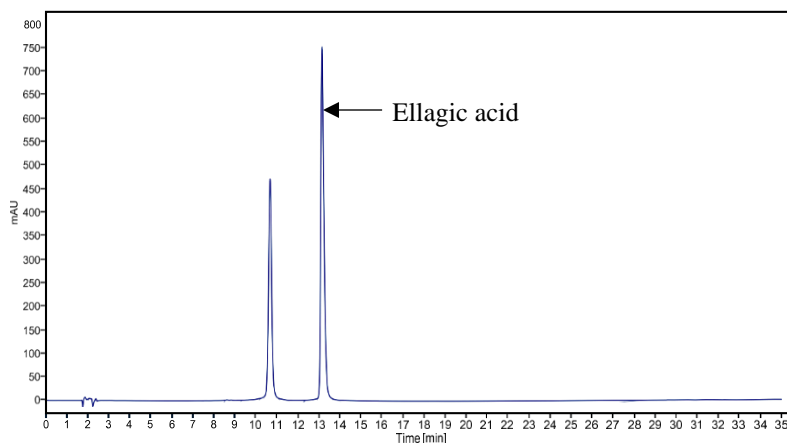
Figure 2. *HPLC fingerprint of GA and EA*
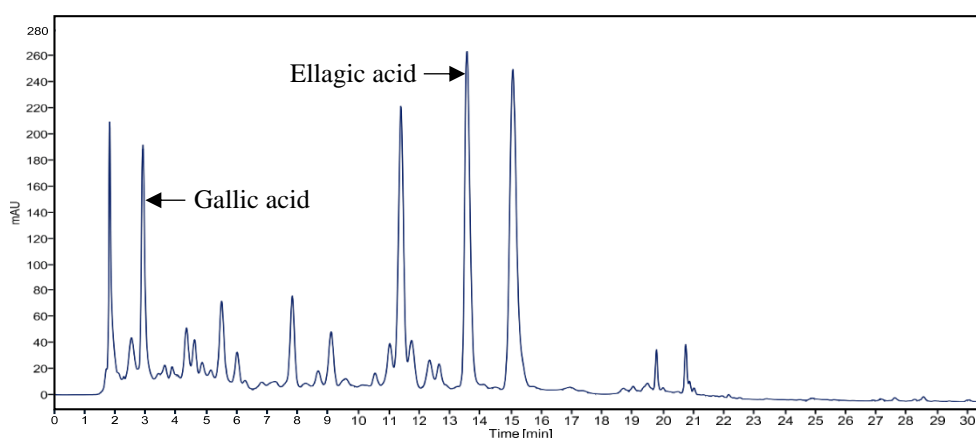
Figure 3. *HPLC fingerprint of IN_{C1}*

Tannins are phenolic compounds which contribute to the antioxidant properties [12]. Hence, the radical scavenging activity of *T. chebula* was tested.

Table 3. *IC_{50} of SL_A, SL_C and IN_C*

Sample	IC_{50} (µg/mL)*	Sample	IC_{50} (µg/mL)*
BHT	39.28 ± 1.68	BHT	39.28 ± 1.68
SL_A - Padhiyathalawa	6.26 ± 0.42	SL_{C1}	8.73 ± 0.53
SL_A - Buththala	9.42 ± 0.66	SL_{C2}	5.18 ± 0.48
SL_A - Gampaha	7.36 ± 0.54	SL_{C3}	5.06 ± 0.49
SL_A - Bibila	8.04 ± 0.68	IN_{C1}	8.11 ± 0.59
SL_A - Colombo	7.45 ± 0.49	IN_{C2}	7.78 ± 0.59
		IN_{C3}	6.36 ± 0.51
		SL_C	6.32 ± 2.09
		IN_C	7.42 ± 0.93

*Each data point represents mean $\pm$ SD where n=3; SL_C: mean of SL_{C1-3}, IN_C: mean of IN_{C1-3}

(a)

(b)   **(c)**
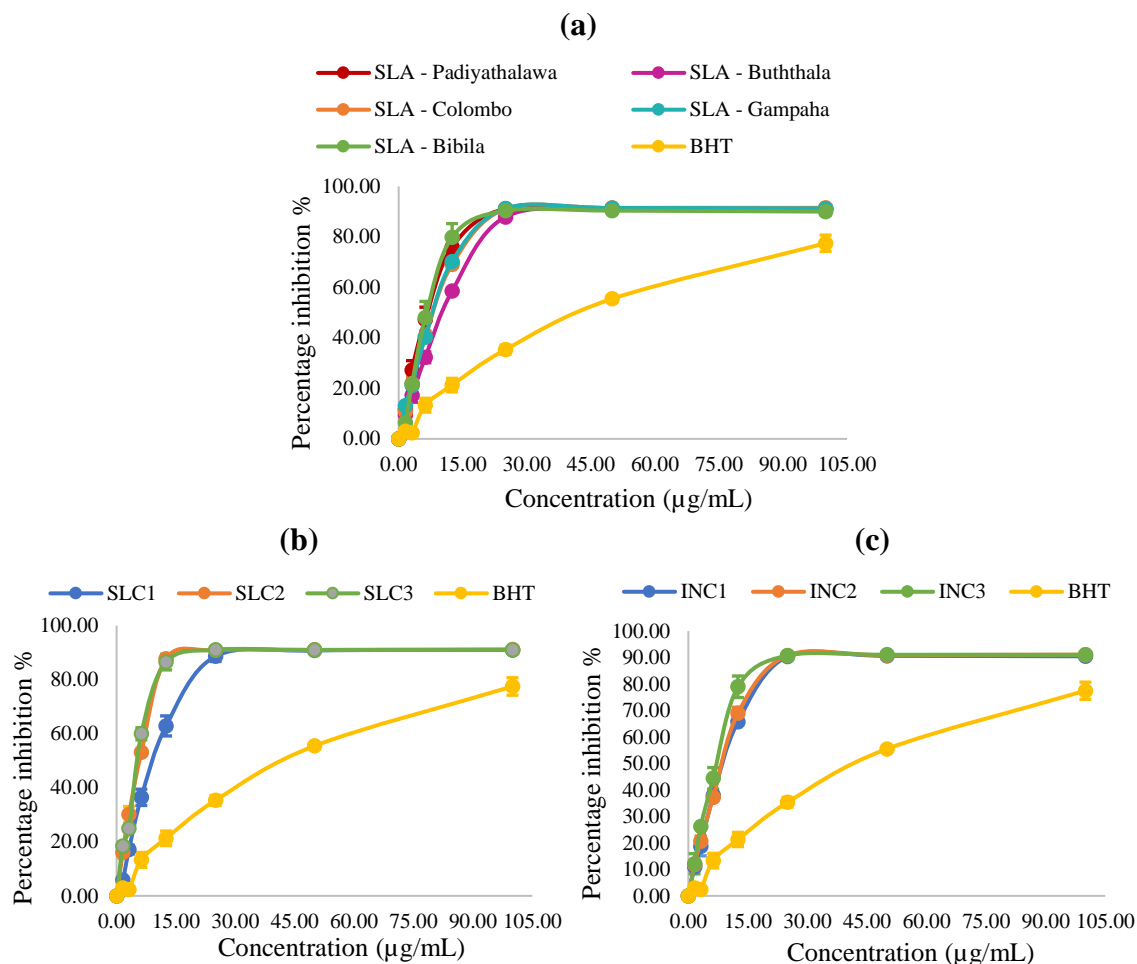
Figure 4. *DPPH radical scavenging activity of (a) SL_A (b) SL_C and (c) IN_C*

All the samples of *T. chebula* showed higher radical scavenging activity than BHT. Slight variations in IC_{50} values were seen among SL_A, SL_C and IN_C samples (Figure 4). The mean IC_{50} value of SL_C samples was lower than the mean IC_{50} value of IN_C samples, showing a higher antioxidant activity in *T. chebula* than in Indian varieties. Previously *T. chebula* fruits showing IC_{50} of 14 ± 0.05 μg/mL is reported (Saha & Verma, 2016). Our results showed lower IC_{50} values for all the samples than this value showing a higher antioxidant activity. Variation of antioxidant activity among themselves and within SL_A, SL_C and IN_C could be attributed to both intrinsic and extrinsic factors. Genetic factors, maturity stage, growth conditions, soil conditions, geographical location, climatic zone (localities in Colombo and Gampaha are in wet zone and Padiyathalawa, Bibila and Buththala are in the dry zone of Sri Lanka), climatic conditions and raw material processing conditions (drying process) affect the ultimate composition of phytoconstituents. In addition, the raw material storage time may also be a contributing factor towards the variations observed in SL_C and IN_C.

Conclusion

Commercial *T. chebula* stocks used in selected herbal preparations are rich in polyphenolic compounds and possess very high antioxidant activity. It may benefit consumers beyond the targeted therapeutic value of these herbal preparations. Commercial samples of Sri Lanka possess higher antioxidant activity than those from India. Gallic acid and ellagic acid could be used as marker compounds in the quality

control of *T. chebula* commercial stocks. However, the study could be expanded to identify and quantify other marker compounds of *T. chebula* dried fruit pericarps. Biological assays are of paramount importance to evaluate the pharmacological properties of medicinal plants. Hence, more biological assays such as anti-microbial, anti-inflammatory, anti-cancer are also recommended to *T. chebula* fruits.

References

Association of Official Analytical Chemists. (1980). *Official method of analysis of the AOAC* (13th ed.). Washington, D.C., 158.

Chatatikun, M., & Chiabchalard A. (2013). Phytochemical screening and free radical scavenging activities of an orange baby carrot and carrot (*Daucus carota* Linn.) root crude extracts. *Journal of Chemical and Pharmaceutical Research*, *5*(4), 97-102.

Chattopadhyay, R. R., & Bhattacharyya, S. K. (2007). Plant review *Terminalia chebula*: an update. *Pharmacognosy Reviews*, *1*(1), 151-156.

Chen, X., Sun, F., Ma, L., Wang, J., Qin, H., & Du, G. (2011). In vitro evaluation on the antioxidant capacity of triethylchebulate, an aglycone from *Terminalia chebula* Retz fruit. *Indian Journal of Pharmacology*, *43*(3), 320-323.

Dassanayake, M. D., & Fosberg, F. R. (1981). *A revised handbook to the flora of Ceylon* (Vol. 2, pp. 38-42). Amerind Publishing Co.

Gupta, P. C. (2012). Biological and pharmacological properties of *Terminalia chebula* Retz. (Haritaki) - an overview. *International Journal of Pharmacy and Pharmaceutical Science*, *4*(3), 62-68.

Juang, L., Sheu, S., & Lin, T. (2004). Determination of hydrolysable tannins in the fruit of *Terminalia chebula* Retz. by high-performance liquid chromatography and capillary electrophoresis. *Journal of Separation Science*, *27*(9), 718-724.

Naik, G. H., Priyadarsini, K. I., Naik, D. B., Gangabhagirathi, R., & Mohan, H. (2004). Studies on the aqueous extract of *Terminalia chebula* as a potent antioxidant and a probable radio protector. *Phytomedicine*, *11*(6), 530-538.

Naik, G. H., Priyadarsini, K. I., Bhagirathi, R. G., Mishra, B., Mishra, K. P., Banavalikar, M. M., & Mohan, H. (2005). In vitro antioxidant studies and free radical reactions of triphala, an ayurvedic formulation and its constituents. *Journal of Phytotherapy Research*, *19*(7), 582-586.

Riaz, M., Khan, O., Sherkheli, M. A., Khan, M. Q., & Rashid, R. (2017). Chemical constituents of *Terminalia chebula*. *Natural Products Indian Journal*, *13*(2), 112.

Saha, S., & Verma, R. J. (2016). Antioxidant activity of polyphenolic extract of Terminalia chebula Retzius fruits. *Journal of Taibah University for Science*, *10*(4), 805-812.

Saleem, A., Husheem, M., Harkonen, P., & Pihlaja, K. (2002). Inhibition of cancer cell growth by crude extract and the phenolics of *Terminalia chebula* Retz. fruit. *Journal of Ethnopharmacology*, *81*(3), 327-336.

Wagner, H., & Bladt, S. (1996). *Plant drug analysis - a thin layer chromatography atlas* (2nd ed.). Germany.

Conference Paper No: BF-05

An ethnobotanical approach to control *Typha angustifolia*: A case study from Sri Lanka

K.P.K. Madushani[1*], M.D. Amarasinghe[1], R.M.C.S. Ratnayake[1] and D.D.G.L. Dahanayaka[2]

[1]Department of Plant and Molecular Biology, University of Kelaniya, Sri Lanka
[2]Department of Zoology, The Open University of Sri Lanka
2017_madushani@kln.ac.lk*

Abstract

Typha is a cosmopolitan genus that is infamous globally for having nuisance plant species. In Sri Lanka, *Typha angustifolia* is distributed in both coastal and inland wetlands, including lagoons, paddy fields, and small reservoirs. Pervasive effects of *Typha* include hindrance to fishing activities, navigation, agriculture, human health, and ecosystem functions, especially provision of habitats for wading birds in coastal lagoons. The present study attempted to formulate an ethnobotanical strategy to control the distribution of *Typha* in Embilikala lagoon in Bundala National Park in Hambantota District in Southern Sri Lanka. *T. angustifolia* edible plant parts were tested for antioxidant activity to promote it as a phytonutrient that boosts the overall health of the body. Hexane, methanol, and aqueous extracts of leaf, leaf base, rhizome, and pollen of *Typha* were analyzed with DPPH and ABTS bioassays for the presence of antioxidants. Leaves were tested for their quality as raw material for making paper using the mould and deckle pouring method and couching technique. Methanol was found to be superior to hexane and deionized water as a solvent for both the assays. Leaf base (99.5±5.3 µg/mL) and rhizome (65.3±0.6 µg/mL) of *T. angustifolia* showed higher radical scavenging activity, and in some instances, higher than that of standard butylated hydroxytoluene (BHT) (119.3±4.5 µg/mL), indicating their potential as sources of bioactive compounds that can reduce free radicals. Contents of heavy metals (Arsenic: 0.338±0.040, Cadmium: 0.628±0.146, Chromium: 63.641±1.30, Lead: 15.657±1.70 ppb) in the rhizomes were below the standard permissible level (100.0 ppb). Pulp made with *Typha* leaves alone and a mixture of *Typha* (95%) and wastepaper (5%) were used successfully to produce writable paper. Findings suggest that *T. angustifolia,* which is widely considered as an invasive plant and marginally utilized currently, has a promising potential to be exploited as food and raw material to introduce new livelihoods to rural communities. This ethnobotanical approach may potentially be used to control the distribution of *T. angustifolia* in wetlands where it is found in invasive proportions.

Keywords

Control, Invasive plants, Sri Lanka, *Typha angustifolia*

Introduction

Typha angustifolia, locally known as "Hambupan", is a cosmopolitan perennial aquatic herb found in wetland ecosystems. It is recorded to be present in at least 56 countries, out of which 15 countries, including Sri Lanka, reckon it as an invasive species (GBIF. Secretariat, 2021). *Typha* is listed as the sixth most invasive plant in Sri Lanka due to its large-scale distribution and threat to the existing ecosystems (MMD&E, 2015). Even though it is a common aquatic plant in dry zone wetlands in Sri Lanka, its' extensive distribution in the coastal lagoons, i.e., Embilikala and Malala lagoons in Bundala National Park, the first Ramsar wetland in the country, has drawn considerable scientific interest.

Prolific production of pollen grains (up to 420 million) and 20,000–700,000 small fruits per inflorescence that are wind-dispersed to more than 1 km distance (Stewart *et al*. 1997) supported by their long viability and rapid germination within 2–20 days qualify *Typha* as a highly invasive plant (van der Valk and Davis 1978). Anthropogenic hydrological changes and eutrophication augment *Typha*'s invasive capacity. Drainage from agricultural fields irrigated by Lunugamvehera reservoir which has been constructed by damming Kirindi Oya is discharged into Embilikala lagoon (4.3 km^2) since 1986 and drainage from Badagiriya reservoir is received by Malala lagoon in Bundala National Park. This has led to reduced water salinity and nutrient enrichment (Matsuno *et al*, 1998; CEA, 1993) in these saline coastal lagoons that have transformed the area into a favorable habitat for *Typha* to colonize.

Nuisance characteristics of *Typha* are not only restricted to invasion and reducing biodiversity, but also blocking canals and covering low-lying agricultural fields. Fishing in Embilikala lagoon is hampered due to the expansion of *Typha* beds that reduces open water surfaces to lay fishing nets. Besides, some villagers are affected by wind-blown *Typha* flowers during the blooming season, causing breathing problems, especially with children. It also has colonized the littoral zones of the lagoons, eliminating the resting and breeding grounds of migratory waterfowl (Suraweera & Dahanayaka, 2017). Dense monocultures of *T. angustifolia* also lowers the scenic beauty of the wetlands, that is reckoned to diminish their value as a tourist attraction.

Although *Typha* is not used in any form in Sri Lanka, young leaves, pollen and rhizomes are reported to be edible and can be used to produce fibre, biofuel, soil stabilizers, weaving and insulating material and paper pulp (Kumar *et al*. 2013). Comparison of nutrient contents in *Typha* with two other types of typical food, *Lasia spinosa* (Kohila) and potatoes, reveal that edible parts of *Typha*, particularly tender leaves and rhizomes, are substantially rich in dietary fiber. It also contains higher amounts of proteins than Kohila, another aquatic plant that contains high amounts of dietary fibre and is consumed as a vegetable. Besides, it contains high amounts of Vitamin C and B6, Na, Ca, and Mg. The absence of fat qualifies *Typha* as healthy food to control weight and obesity as well as non-communicable diseases such as hypertension and diabetes (Costa Fruet *et al*., 2012).

Deliberate water level changes, periodic burning, mechanical/ manual removal of plants and killing them with herbicides are the options available for controlling the distribution of *Typha*. Apart from irregular manual removal, marginal efforts are taken to control rapid distribution of *Typha* in Sri Lanka. We hypothesized that developing methods to utilize *Typha* plant parts as food and raw material to initiate cottage industries may provide a community-based strategy to control the invasive distribution of *T. angustifolia* in wetlands within and outside Bundala National Park. The present study therefore is aimed to investigate the potential of controlling *T. angustifolia* by enhancing their use as food and raw material for cottage industries that can open up new livelihoods for local communities.

Materials and methods

Study area

Bundala wetland complex, i.e., Bundala, Embilikala and Malala lagoons and associated land in Hambantota District, (6°12′50″N 81°13′30″E) on the Southern coast of Sri Lanka

constitute the Bundala National Park. Annual rainfall in this area is less than 1300 mm; therefore, these wetlands are located in the dry climatic zone.

Characterizing *T. angustifolia* as a food

Previous studies (Costa Fruet *et al*., 2012) had shown the nutritional value of *T. angustifolia* and this study focuses on the antioxidant activity of *Typha* and the heavy metal contamination levels that is essential to establish its' potential as a healthy food.

Antioxidant assessment

Hexane, methanol, and aqueous extracts of powdered samples of *Typha* leaves, leaf bases, rhizomes, and pollen (collected from Embilikala lagoon) were prepared, filtered, evaporated and stored at -20 °C for analysis of bioactive properties. Samples were assayed for their antioxidant activity using DPPH (Chatatikun and Chiabchalard, 2013) and ABTS (Piljac *et al*., 2009) assays with BHT and ascorbic acid as controls. Each sample was replicated three times. The absorbance was measured using a Micro-plate Reader (Biotek, USA). The percentage inhibition was calculated using the equation given below.

$$\text{Percentage Inhibition} = \left(\frac{\text{Absorbance of control} - \text{Absorbance of test sample}}{\text{Absorbance of control}} \right) \times 100\%$$

The inhibition rate was calculated and plotted against the test concentrations to obtain the half maximal inhibitory concentration (IC_{50}). The IC_{50} of the extracts were calculated using GraphPad Prism version 8.00 for Windows, GraphPad Software, La Jolla California USA.

Analysis of heavy metal content in edible parts of *T. angustifolia*

Rhizomes of *T. angustifolia* were collected from the Embilikala lagoon, cleaned, chopped into small pieces, and oven-dried at 40 °C for 72 hours. Two grams of powdered material were digested with concentrated nitric acid in a micro-digester and the digestion was topped up with de-ionized water up to 100 ml. An aliquot was then used from the stock digested solution for the analysis of arsenic (As), cadmium (Cd), lead (Pb) and chromium (Cr) using atomic absorption spectrophotometry. The digested samples were atomized in an atomic absorption unit (Shimadzu AA- 6300) and the absorption was measured at their characteristic wavelengths (As: 193.7 nm, Pb: 283.306 nm, Cd: 228.802 nm, Cr: 357.869 nm). Standard series of As, Pb, Cd and Cr solutions were also prepared. Concentrations of the heavy metals of *Typha* samples were calculated from the calibration curves ($R^2 > 0.99$) prepared from the absorbance values of standard series of respective cation solutions.

Paper making with *T. angustifolia* leaves

T. angustifolia plants were collected from Embilikala lagoon and leaf bases and rhizomes were removed after cleaning. The fresh leaves were cut into small pieces (3 x 5 cm) and dried under direct sunlight. One kg of dried leaves was boiled with 200 g of sodium carbonate (Na_2CO_3) and 10L of water at 100 °C for 5 hours. Then, the boiled samples were cleaned under flowing water to remove the chemicals and macerated using an

electric blender. Mould and deckle pouring method and couching techniques were used in the papermaking process (Hiebert, 2006).

Results and Discussion

DPPH radical scavenging activity

The IC_{50} values of extracts of leaf base and rhizome samples were lower than that of the standard BHT (119.3 ± 4.5 μg/mL), nevertheless, the IC_{50} values of leaf and pollen samples were higher than that of BHT (Figure 1 and Table 1). Rhizomes of *T. angustifolia* showed the highest antioxidant activity. Since the crude samples of hexane and aqueous extracts did not dissolve in the DPPH solvent, they were not used for the assay.
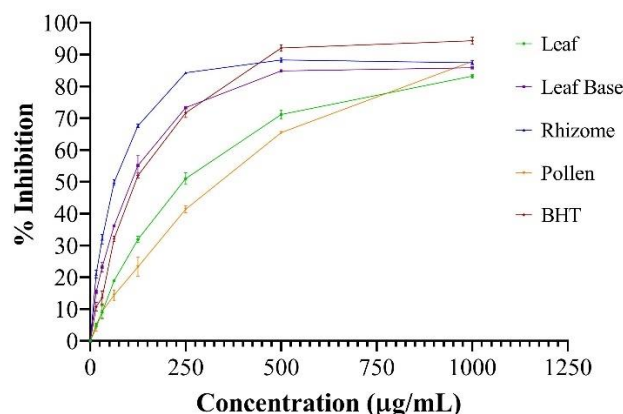
Figure 1. *Antioxidant activities of methanol extracts of leaf, leaf base, rhizome and pollen of T. angustifolia and standard synthetic antioxidant, BHT in the DPPH assay. Each value is expressed as mean ± SD (n=3)*

Table 1. *IC_{50} values of methanol extracts of T. angustifolia plant parts in DPPH assay*

Sample	IC_{50} ($\pm$SD μg/mL)
Leaf	246.3 ± 12.5
Leaf base	99.5 ± 5.3
Rhizome	65.3 ± 0.6
Pollen	324.9 ± 8.9
BHT	119.3 ± 4.5

ABTS radical scavenging activity

Total antioxidant activities of hexane, methanol, and aqueous extracts of *Typha* plant parts (Figure 2 and Table 2) were determined using ABTS assay and compared with the positive controls, BHT and ascorbic acid (Figure 2).

(a)

(b)

(c)
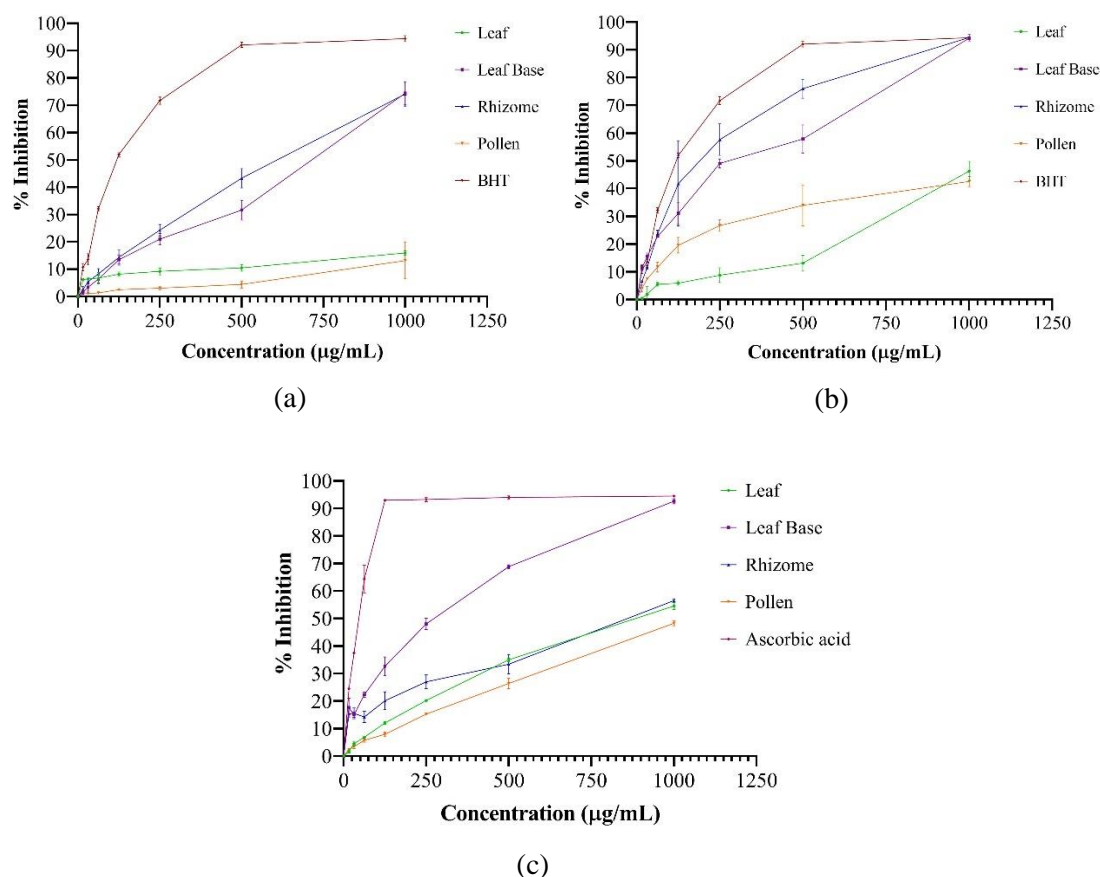
Figure 2. *Antioxidant activities of hexane (a), methanol (b) and aqueous (c) extracts of leaf, leaf base, rhizome, and pollen of T. angustifolia and standard synthetic antioxidant, BHT (a, b) and ascorbic acid (c) in the ABTS assay. Each value is expressed as mean ± SD (n=3)*

The half maximal inhibitory concentration value is the concentration of the sample that can scavenge 50% of free radicals. The IC_{50} value is inversely proportional to the free radical scavenging activity/ antioxidant property of the sample (Table 2).

Table 2. *IC_{50} values of hexane, methanol, and aqueous extracts of T. angustifolia plant parts in ABTS assay*

Sample	IC_{50} (±SD µg/mL)		
	Hexane	**Methanol**	**Aqueous**
Leaf	n.d.	n.d.	847.59±17.37
Leaf base	721.9±22.9	341.36±58.49	263.20±17.74
Rhizome	609.2±53.9	188.90±60.90	807.77±66.56
Pollen	n.d.	n.d.	n.d.
Control	119.3±4.5 (BHT)	119.3±4.5 (BHT)	44.90±1.49 (Ascorbic)

* n.d. - not detected

Results revealed that methanol is the superior solvent for the extraction purpose. All the extracts of plant parts showed higher IC_{50} values than that of positive controls. In comparison of the IC_{50} of the methanol extracts to BHT, the rhizome showed the highest antioxidant activity than other plant parts. Even though hexane extracts of *Typha* edible

parts (leaf base and rhizome) showed higher IC_{50} values than the BHT control, they showed comparable activity with other solvents. *Typha* rhizome showed the highest antioxidant activity than hexane extracts of other parts. All the aqueous extracts of *T. angustifolia* plant parts showed higher IC_{50} values than standard ascorbic acid (44.9 ± 1.4 µg/mL). While *Typha* pollen did not show positive activity, rhizomes are relatively rich in antioxidants. Edible parts of *Typha* plant therefore were revealed to possess significant antioxidant activities that have a tremendous potential to be introduced as a low-cost nutrient source of food. As *Typha* is amply available in these areas, it can potentially be made into preserved foods such as pickles, rhizome floor, dried chips, snacks, and biscuits.

Heavy metals in the edible plant parts of *T. angustifolia*

Presence of As, Cd, Pb and Cr were detected in parts of *Typha* tested, their concentrations however were below the standard permissible levels (Table 3).

Table 3. Heavy metal analysis of T. angustifolia and permissible levels for consumption

Metal	Concentration (±SD ppb) resulted in this test	WHO/FAO CODEX standard (ppb)
Arsenic	0.338±0.040	100.0
Cadmium	0.628±0.146	3.0
Chromium	63.641±1.30	50.0
Lead	15.657±1.70	100.0

***T. angustifolia* as raw material for paper making**

Writable papers were made using pulp made only with *Typha* (100%) and (95%) *Typha* + (5%) wastepaper. These can be successfully produced in different thicknesses; as standard A4 papers (0.1 mm) and shipping boxes (4.8 mm). Further studies are recommended to expand the variety of papers with improved quality. *Typha* leaf material therefore could be used as raw material to initiate new livelihoods based on handmade paper and paper products for the rural communities in Hambantota District, where *T. angustifolia* is distributed in invasive proportions. Continuous use of *Typha* leaves may reduce its' rapid spread in the wetlands of Bundala National Park, the surrounding marshy lands and rice fields.

Conclusion

The findings of this study sufficiently substantiate the potential of edible parts of *Typha angustifolia* (especially the rhizome) to be used as an economical, nutritious source, provided they are harvested from unpolluted areas, particularly with heavy metals. Handmade paper production with *T. Angustifolia* leaves also show promising potential to be developed into a cottage industry in *Typha* infested areas. This ethnobotanical approach supported by institutional facilitation provides a pragmatic green method to control the invasive distribution of *T. angustifolia* in the wetlands of Bundala National Park and elsewhere.

Acknowledgement

References

CEA/Euroconsult. (1993). Bundala National Park Wetland Site Report and Conservation Management Plan. CEA, Colombo, Sri Lanka, pp 103.

Chatatikun, M., & Chiabchalard, A. (2013). Phytochemical screening and free radical scavenging activities of orange baby carrot and carrot (Daucus carota Linn.) root crude extracts. Journal of Chemical and Pharmaceutical Research, 5(4), 97-102.

Fruet, A. C., Seito, L. N., Rall, V. L. M., & Di Stasi, L. C. (2012). Dietary intervention with narrow-leaved cattail rhizome flour (Typha angustifolia L.) prevents intestinal inflammation in the trinitrobenzenesulphonic acid model of rat colitis. BMC complementary and alternative medicine, 12(1), 1-11.

Hiebert, H. (2006). Papermaking with Garden Plants and Common Weeds, Storey Publishing.

Kumar, K., Kumar, D., Teja, V., Venkateswarlu, V., Kumar, M., & Nadendla, R. (2013). A review on Typha angustata. International Journal of Phytopharmacy, 4, 277-81.

Matsuno, Y., van der Hoek, W., & Ranawake, M. (1998). Irrigation water management and the Bundala National Park: Proceedings of the Workshop on Water Quality of the Bundala Lagoons, held at IIMI, in Colombo, Sri Lanka 03 April 1998.

MMD&E.(2015), Invasive Alien Species in Sri Lanka: Training Manual for Managers and Policy Makers (pp. 25).

Piljac-Žegarac, J., Stipčević, T., & Belščak, A. (2009). Antioxidant properties and phenolic content of different floral origin honeys. Journal of ApiProduct and ApiMedical Science, 1(2), 43-50.

Stewart, H., Miao, S. L., Colbert, M., & Carraher, C. E. (1997). Seed germination of two cattail (Typha) species as a function of Everglandes nutrient levels. Wetlands, 17(1), 116-122.

Suraweera, P.A.C.N.B., Dahanayaka, D.D.G.L. (2017) Assessment, monitoring and management of Invasive Alien Species at Bundala National Park (A Ramsar Wetland) in Sri Lanka. Wetlands Sri Lanka 2017, Central Environmental Authority, Sri Lanka (pp.80-85)

Typha angustifolia L. in GBIF Secretariat (2021). GBIF Backbone Taxonomy. Checklist dataset https://doi.org/10.15468/39omei accessed via GBIF.org on 2021-05-18.

Conference Paper No: BF-06

Bioactive properties and metabolite profile of an endolichenic fungus, *Hypoxylon lividipigmentum*

W.R.H. Weerasinghe[1], C.D. Shevkar[2], R.S. De Silva[3], R.N. Attanayake[4], G. Weerakoon[5], A.S. Kate[2], K. Kalia[2] and P.A. Paranagama[1*]

[1]Department of Chemistry, University of Kelaniya, Sri Lanka
[2]National Institute of Pharmaceutical Education and Research, India
[3]College of Chemical Sciences, Institute of Chemistry Ceylon, Sri Lanka
[4]Department of Plant and Molecular Biology, University of Kelaniya, Sri Lanka
[5]Department of Life Sciences, The Natural History Museum, United Kingdom
priyani@kln.ac.lk*

Abstract

Endolichenic fungi (ELF) serve as a novel source of secondary metabolites. *Hypoxylon lividipigmentum* is an ELF isolated from the lichen *Opegrapha medusulina*, collected from mangrove plant *Xylocarpus granatum* from Negombo lagoon, Sri Lanka. The fungus was identified to the species level using morphological and DNA barcoding techniques. Ethyl acetate extract of the fungus was subjected to in vitro assays to determine antioxidant, anti-inflammatory, tyrosinase inhibitory and antibacterial potency. Liquid Chromatography-Mass Spectrometry (LCMS) dereplication was conducted on the crude extract in order to detect the secondary metabolites present. The extract reported a IC_{50} value of 18.34 ± 1.37 µg/ml on par with the positive control BHT, in DPPH radical scavenging assay. It also exhibited moderate anti-inflammatory activity with an IC_{50} value of 81.08 ± 1.05 µg/ml. Tyrosinase inhibitory activity was fairly comparable with an IC_{50} value of 121.20 ± 2.55 µg/ml. Agar well diffusion assay was conducted to determine antibacterial activity against aerobic bacterial species *Escherichia coli, Bacillus subtilis, Staphylococcus aureus* and the anaerobic bacterial species *Streptococcus mutans*. Suppression of growth was shown only against *B. subtilis*. Five major mass peaks were observed during the study of LCMS profile of the extract. After a thorough dereplication process, two masses could be presumed to be from novel scaffolds. Since none of the mass peaks could be dereplicated within the species or genus level, it could be speculated that the chemical profile of *Hypoxylon lividipigmentum* was previously poorly explored in literature thus making it an interesting organism to study further for novel metabolites.

Keywords

Bioactivity, Endolichenic Fungi, *Hypoxylon lividipigmentum*, LCMS dereplication, Lichens

Introduction

Among diverse microorganisms, endolichenic fungi (ELF) play an important role as secondary metabolite producers. Since the first research on isolating secondary metabolites from ELF (Paranagama *et al*., 2007), so far more than 172 compounds have been isolated with various activities such as anticancer, antifungal, antibacterial, antioxidant, anti-inflammatory, UV protectant, antiviral and anti-Alzheimer's disease (Agrawal *et al*., 2020).

ELF associated with the mangrove ecosystem might be adapted to face diverse array of challenges such as high salinity, extreme tides and temperature fluctuations. These fungi should have novel metabolites with significant bioactivities, as evident by the recent study

conducted in the mangrove ecosystem of Puttalam lagoon, Sri Lanka (Maduranga *et al.*, 2018).

Although there have been numerous studies conducted on the phylogenetic and ecological aspects of the fungus *Hypoxylon lividipigmentum* isolated from various sources (Sir *et al.*, 2016), its bioactivity and metabolic profile is scarcely explored in the literature. This study attempts to explore the bioactivities such as antioxidant, anti-inflammatory, tyrosinase inhibitory and anti-bacterial potency of this particular ELF and its metabolite profile using LCMS dereplication. LCMS dereplication method used in this study is a novel and convenient approach as opposed to the conventional bioactivity-guided fractionation, to understand the metabolic profile of the extract before proceeding with further analyses and separation phases (Wolfender *et al.*, 2019).

Methodology

Ethical statement

Permit to collect lichen samples from the mangrove forest in Negombo lagoon was obtained from the Forest Department of Sri Lanka.

Collection of lichen sample and lichen identification

Lichen host was collected on 31st of March, 2018 at the mangrove forest of Negombo lagoon, Sri Lanka from the mangrove plant *Xylocarpus granatum*. The study site was "Kadolkele" area situated at 7.195528 N 79.84389 E GPS coordinates belonging to the lagoon area. The identification of this lichen was carried out using morphological techniques (Maduranga *et al.*, 2018) at Natural History Museum, London.

Isolation and identification of endolichenic fungi

The lichen thallus was surface sterilized, plated on 2% malt extract agar (MEA) supplemented with 0.01% streptomycin and ELF was isolated using the method described in (Maduranga *et al.*, 2018). DNA extraction of the isolated pure culture was carried out using a slightly modified method of CTAB DNA extraction protocol. The nuclear ribosomal internal transcribed spacer region (rDNA- ITS) was amplified, sequenced and identified as described in (Maduranga *et al.*, 2018).

Extraction of secondary metabolites

The ELF was cultured on 5 PDA plates of the size 150×25 mm and incubated at room temperature for a duration of 2 weeks. Extraction was carried out according to the method described in (Maduranga *et al.*, 2018).

Radical scavenging ability by 2, 2-diphenyl-1-picrylhydrazyl (DPPH) method

The radical scavenging ability assay was carried according to the colorimetric method described by (Maduranga *et al.*, 2018), with slight modifications. BHT was used as the positive control and activity was calculated using Equation 1.

$$\% \ Activity \ = \ \frac{A_{control} - A_{sample}}{A_{control}} \ x \ 100\% \qquad \text{Equation 1}$$

Anti-inflammatory assay (HRBC Stabilization method)

The anti-inflammatory assay was conducted using human red blood cells stabilization method which uses the heat induced hemolysis principle (Sakat *et al.*, 2010). Aspirin was used as the positive control and the test was performed in triplicates and the percentage stability was calculated using Equation 1.

Tyrosinase inhibitory assay

Tyrosinase inhibitory assay was carried out in a flat bottom 96-well microtiter plate according to a modified version of (Souza et al., 2012). Kojic acid was used as the positive control and the percentage inhibition was calculated using the Equation 2.

$$\% \ Inhibition \ = \ \frac{(A_{control}-A_{blank})-(A_{sample}-A_{blank})}{(A_{control}-A_{blank})} \ \text{x} \ 100\%$$

Anti-bacterial assay (Agar well diffusion method)

Anti-bacterial assays against aerobic bacterial species *Escherichia coli* (ATCC 25922), *Bacillus subtilis* (ATCC 6051), *Staphylococcus aureus* (ATCC 25923) and the anaerobic bacterial strain *Streptococcus mutans* (ATCC 700610) were conducted using agar well diffusion method (Holder and Boyce 1994). Azithromycin and chlorohexidine were used as positive controls against aerobic and anaerobic strains respectively.

Statistical analysis

IC_{50} values for the bioassays were calculated using the statistical software GraphPad Prism 7.0.4. To statistically determine the significant difference between the extract of *H. lividipigmentum* and positive control, paired t-test was conducted using Wilcoxon matched-pairs signed rank test using 95% confidence level with the same statistical software.

LC-MS dereplication

Chromatographic separation of crude extract was performed on the Agilent (5µm, 4.6×250 mm) C_{18} column and the mobile phase system consisted of 0.1 % Formic acid (A) and Methanol (B) and the gradient was set up as: 0 to 2 min 30% A/70% B, a linear gradient from 2 to 8 min to 5% A/95% B and a linear gradient from 12 to 15 min to again 30% A/70% B. The obtained masses were thoroughly searched in Dictionary of Natural Products (DNP) and SciFinder, using species, genus and fungi level specificity for rationalization of the obtained profiles.

Results and Discussion

Isolation and identification of endolichenic fungi:

The lichen was collected from the mangrove plant *Xylocarpus granatum* and the specimen was identified as *Bactrospora myriadea* using morphological techniques. The obtained ITS sequence matched with *Hypoxylon lividipigmentum* sequence (published record) of KU604567.1 in GenBank with 99.81% homology. The sequence was deposited under the

accession number MT507846 in the GenBank. The isolate showed moderate growth on PDA, covering a 150 mm diameter Petri-dish within two weeks.

Screening for biological activities:

The radical scavenging activity was assessed using the DPPH assay. As shown in the Figure 1(a), the IC_{50} value shown by the extract against DPPH (IC_{50} 18.34±1.37 µg/ml) is less than the value shown by the positive control BHT (IC_{50} 26.22±2.28 µg/ml). Furthermore, paired t-test revealed that the difference is significant with $P < 0.05$ (0.0156). This interestingly displays that the extract contains metabolites which lead to a better antioxidant activity than BHT.

The anti-inflammatory activity shown by the extract (IC_{50} 81.08±1.05 µg/ml) in the HRBC stabilization assay is fairly comparable to the positive control aspirin (IC_{50} 24.17±0.24 µg/ml) with a significant difference of P value (0.0156) as well, confirming its moderate potency.

Inhibition of tyrosinase enzyme is the most convenient way of controlling melanogenesis. Hence, the demand for tyrosinase inhibitors has increased immensely over the past few years. This extract seems to possess quite a similar activity (IC_{50} 121.20±2.55 µg/ml) compared to the commercially available inhibitor Kojic acid (IC_{50} 104.35±2.30 µg/ml) with no significant difference according to statistical analysis (P value 0.0938).

In an era where the antibiotic resistance has become a major issue, emergence of compounds with promising antibacterial activity is vital. The agar well diffusion method carried out to assess the antibacterial activity of the extract with a maximum dose of 5 mg/ml, revealed that the ethyl acetate extract of *H. lividipigmentum* possess antibacterial activity against *B. subtilis* bacterial strain only. This activity statistically has no significant difference (P value 0.2500) (zone diameter 14±0.45 mm) compared to the positive control azithromycin (zone diameter 24±0.24 mm).
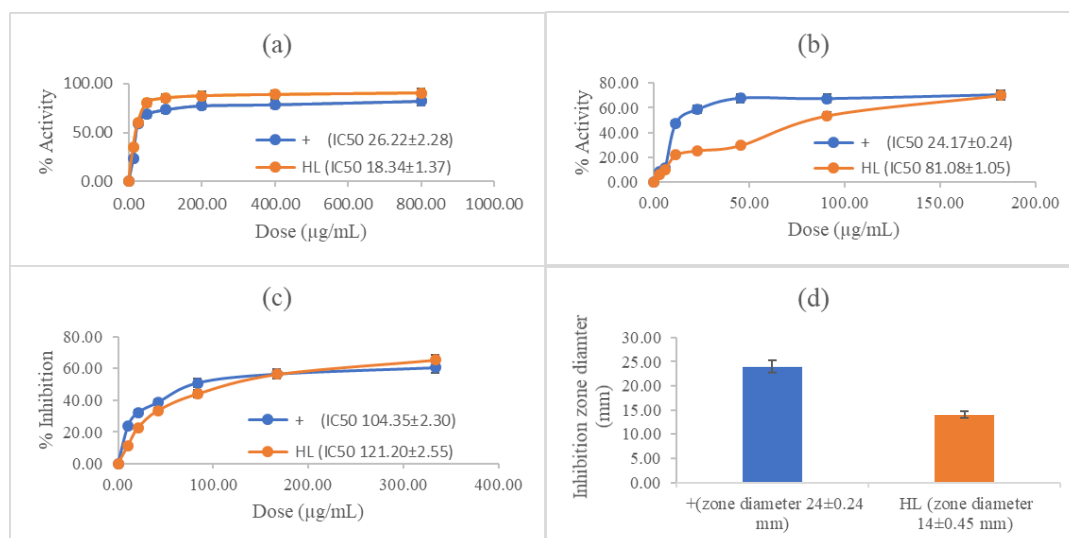

Figure 1. *Activity comparison of in vitro assays; (a) DPPH assay (b) HRBC stabilization assay (c) Tyrosinase inhibitory assay (d) Antibacterial assay against B. subtilis (+: positive control, HL: extract of H. lividipigmentum). Three replicates were used for each assay and error bars represent percentage error.*

It is to be stated that this is the first report of the above mentioned activities for the fungus *H. lividipigmentum* thus far in literature.

LCMS Dereplication

The chromatogram with the cluster of peaks observed at 254 nm is presented in Figure 2. All the proposed structures were confirmed with relevant UV profiles along with the accurate mass defect error below 10 PPM, which is well within the acceptable range.

Integration Peak List

Peak	Start	RT	End	Height	Area	Area %
1	10.074	10.142	10.302	10.45	68.91	5.65
2	10.497	10.548	10.575	5.69	18.04	1.48
3	10.593	10.636	10.705	7.32	28.12	2.31
4	10.722	10.784	10.897	22.87	188.77	15.49
5	10.897	10.943	11.1	14.96	127.06	10.42
6	11.13	11.19	11.352	58.61	444.58	36.48
7	11.352	11.426	11.69	18.85	185.9	15.25
8	11.69	11.791	11.927	19.17	145.95	11.97
9	11.927	12.039	12.767	71.8	1218.84	100
10	12.767	12.842	13.126	5.43	65.55	5.38

Figure 2. *The chromatogram at 254 nm showing cluster of peaks*

Major observed mass peaks for ethyl acetate extract of the fungus were *m/z*: 141.0561, 373.1871, 493.2016, 746.4877 and 919.4281. It is to be stated that none of the mass peaks could be dereplicated at species and genus level specificity. The mass peaks 141.0561, 373.1871, 493.2016 could be dereplicated under the broad filter of fungi, which are presented in the Table 1. No hit in any of the applied filters of species, genus and fungi category could be found for the peaks 919.4281 and 746.4877, suggesting further exploration could be pursued for *H. lividipigmentum* in search of novel scaffolds.

Table 1. *Proposed structures in LC-MS dereplication in fungi category search*

Observed *m/z* [M+H]$^+$	Proposed structures with corresponding accurate mass	Reference
493.2016	Ochrindole C	(De Guzman *et al*., 1994)
141.0561	2,5-Dihydroxybenzenemethanol, Epoformin,	(Cala *et al*., 2018)

26

Isoepiepoformin,
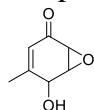
2,3,6-Trihydroxytoluene,
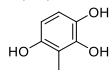
5-Methylpyrogallol,
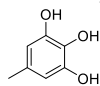
2-Methylene-3-oxocyclopentanecarboxylic acid
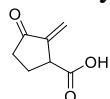
373.1871	Aurantiomide A,	(Tohme *et al.*, 2011)
	Cinatrin B,	
	Jiangolide	
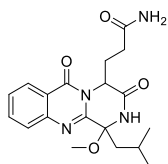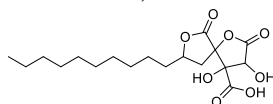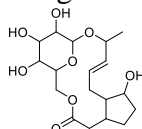
Conclusion

In the present study, *H. lividipimentum* ELF strain, was investigated for its biological activities and metabolic profile. Noteworthy antioxidant, anti-inflammatory, tyrosinase inhibitory and antibacterial activities could be observed from the *in vitro* screenings carried out for the extract. This also becomes the first report of such activities from the fungal strain of *H. lividipigmentum*. However, further studies are required to determine the exact bioactive compounds responsible for these activities. The LCMS dereplication study conducted for the same revealed that it comprises of interesting metabolites reported from literature under the broad fungal category while containing two unknown major compounds. Overall, this fungus seems to be an interesting strain to explore further, in order to uncover novel scaffolds with useful bioactivities.

Acknowledgment

References

Agrawal, S., Deshmukh, S. K., Reddy, M. S., Prasad, R., & Goel, M. (2020). Endolichenic fungi: A hidden source of bioactive metabolites. *South African Journal of Botany*, *134*(2019), 163–186. https://doi.org/10.1016/j.sajb.2019.12.008

Cala, A., Masi, M., Cimmino, A., Molinillo, J. M. G., Macias, F. A., & Evidente, A. (2018). (+)-epi-Epoformin, a Phytotoxic Fungal Cyclohexenepoxide: Structure Activity Relationships. *Molecules*, *23*(7), 1–12. https://doi.org/10.3390/molecules23071529

De Guzman, F. S., Bruss, D. R., Rippentrop, J. M., Gloer, K. B., Gloer, J. B., Wicklow, D. T., & Dowd, P. F. (1994). Ochrindoles A-D: New bis-indolyl benzenoids from the sclerotia of *Aspergillus ochraceus* NRRL 3519. *Journal of Natural Products*, *57*(5), 634–639. https://doi.org/10.1021/np50107a011

Holder, I. A., & Boyce, S. T. (1994). Agar well diffusion assay testing of bacterial susceptibility to various antimicrobials in concentrations non-toxic for human cells in culture. *Burns*, *20*(5), 426–429. https://doi.org/10.1016/0305-4179(94)90035-3

Maduranga, K., Attanayake, R. N., Santhirasegaram, S., Weerakoon, G., & Paranagama, P. A. (2018). Molecular phylogeny and bioprospecting of Endolichenic Fungi (ELF) inhabiting in the lichens collected from a mangrove ecosystem in Sri Lanka. *PLoS ONE*, *13*(8), 1–22. https://doi.org/https://doi.org/ 10.1371/journal.pone.0200711

Paranagama, P. A., Wijeratne, E. M. K., Burns, A. M., Marron, M. T., Gunatilaka, M. K., Arnold, A. E., & Gunatilaka, A. A. L. (2007). Heptaketides from Corynespora sp. inhabiting the Cavern Beard Lichen, *Usnea cavernosa*: First Report of Metabolites of an Endolichenic Fungus. *Journal of Natural Products,* *70*(11), 1700–1705. https://doi.org/10.1021/np070466w

Sakat, S. S., Juvekar, A. R., & Gambhire, M. N. (2010). In-vitro antioxidant and anti-inflammatory activity of methanol extract of *Oxalis corniculata* linn. *International Journal of Pharmacy and Pharmaceutical Sciences*, *2*(1), 146–155.

Sir, E. B., Kuhnert, E., Lambert, C., Hladki, A. I., Romero, A. I., & Stadler, M. (2016). New species and reports of Hypoxylon from Argentina recognized by a polyphasic approach. *Mycological Progress*, *15*(4). https://doi.org/10.1007/s11557-016-1182-z

Souza, P. M., Elias, S. T., Simeoni, L. A., de Paula, J. E., Gomes, S. M., Guerra, E. N. S., Fonseca, Y. M., Silva, E. C., Silveira, D., & Magalhães, P. O. (2012). Plants from Brazilian Cerrado with Potent Tyrosinase Inhibitory Activity. *PLoS ONE*, *7*(11), 1–7. https://doi.org/10.1371/journal.pone.0048589

Tohme, R., Darwiche, N., & Gali-Muhtasib, H. (2011). A journey under the sea: The quest for marine anti-cancer alkaloids. *Molecules*, *16*(11), 9665–9696. https://doi.org/10.3390/molecules16119665

Wolfender, J. L., Nuzillard, J. M., Van Der Hooft, J. J. J., Renault, J. H., & Bertrand, S. (2019). Accelerating Metabolite Identification in Natural Product Research: Toward an Ideal Combination of Liquid Chromatography-High-Resolution Tandem Mass Spectrometry and NMR Profiling, in Silico Databases, and Chemometrics. *Analytical Chemistry*, *91*(1), 704–742. https://doi.org/10.1021/acs.analchem.8b05112

Conference Paper No: PF-07

Thin film cuprous oxide homojunction photoelectrode for water splitting

F.S.B. Kafi, S.A.A.B. Thejasiri, R.P. Wijesundera[*] and W. Siripala

Department of Physics and Electronics, University of Kelaniya, Kelaniya, Sri Lanka
palitha@kln.ac.lk*

Abstract

Employing cuprous oxide (Cu_2O) photoelectrodes in photoelectrochemical cells to generate hydrogen by water splitting is beneficial. Conventionally, it is limited in practice because of the well-known reasons of its inherent corrosiveness and poor conversion efficiencies. In this study, we have investigated the possibility of improving the efficiency of Cu_2O photoelectrode in the form of p-n homojunction together with sulphidation. Initially, the optimum pH values for the n- and p-Cu_2O thin film deposition baths are determined as 6.1 and 13 for Ti/n-Cu_2O/p-Cu_2O in photoelectrochemical cell configuration. Then, at these pH values the duration of n- and p-Cu_2O thin film deposition is optimized by forming Ti/n-Cu_2O/p-Cu_2O photoelectrode. In this study, we found that at 45 minutes of n-Cu_2O and 50 minutes of p-Cu_2O thin film deposition together with sulphidation forms relatively high efficient Ti/n-Cu_2O/p-Cu_2O photoelectrode resulting Solar-To-Hydrogen (STH) conversion efficiency of 0.9%. In addition, current-voltage characteristic of the best Cu_2O homojunction photoelectrode exhibits more negative shift in onset of photocurrent which indicates that photocurrent generation and transportation have improved by the formation of homojunction and further been enhanced by sulphidation.

Keywords

Cuprous oxide, Electrodeposition, Photoelectrode, p-n junction, Water splitting

Introduction

Generation of hydrogen energy by splitting water molecules in photoelectrochemical cell is a clean, environmentally friendly, renewable method of utilizing solar energy to address global energy crisis. Many efforts have been reported to date to harness hydrogen in PEC using different semiconductor materials as photoanodes, photocathodes or both (Nellist et al., 2016). Nevertheless, conversion of solar energy to hydrogen is not easy as reports show that electrochemistry involved in PEC configuration requires qualitative and efficient electrodes to make use of this sustainable energy source viable (Bae et al., 2017; Kafi et al., 2020; Siripala & Kumara, 1990).

Cuprous oxide (Cu_2O) is being investigated over years as one of the most reliable photoelectrode material as it is abundant, economical and pollution free. It is a well-known fact that Cu_2O photoelectrodes display low conversion efficiencies since they suffer from electrochemical corrosion, photocorrosion as well as unstable in PEC configurations. Many reports are available to aim at improving the quality of Cu_2O photoelectrodes (Liu et al., 2014; Siripala & Kumara, 1990; Wick & Tilley, 2015). Annealing, surface passivation, coupling of cuprous oxide to other materials have shown improvements in efficiency as well as stability of Cu_2O in PEC (Azevedo et al., 2014; Bornoz et al., 2014; Kafi et al., 2021).

In comparison to p-type Cu_2O photoelectrodes, studies on improving the stability and performance of n-type Cu_2O in PEC are rarely reported. Unlike p-type photoelectrodes,

in general n-type semiconductors exhibit aggressive photocorrosion in aqueous electrolytes as the thermodynamic oxidation potential lies above the O_2/OH^- redox potential (Wang & Gong, 2015). Further, the existence of high density of surface states together with slow kinetics for oxygen evolution reaction at electrode surface reduces the PEC performance. One possible solution is to modify the surface layer to reduce corrosion/photcorrosion and improve their chemical/photochemical stability when immersed in an electrolyte while allowing sufficient interfacial transfer of photogenerated minority carriers. Our previous reports have revealed that it is possible to improve the PEC water splitting capability of electrodeposited $n-Cu_2O$ thin film electrodes as a result of sulphidation of $n-Cu_2O$ thin film by eliminating electrically active high density of localized surface states (Kafi et al., 2020).

Another strategy to improve the efficiency of $n-Cu_2O$ photoelectrodes in PEC water splitting system is that to combine it with $p-Cu_2O$ thin film to form p-n junction photoelectrode (Wang et al., 2018). It can be expected that this p-n junction with built-in electric field effect between n-type and p-type Cu_2O will separate photogenerated carriers and enhances photocurrent density and photostability (Bai et al., 2019). Additionally, p-n junction photoelectrodes in PEC water splitting systems could increase electron-hole lifetime, efficient electron hole separation and the suppression of electron-hole recombination. Further, our previous studies imply that the sulphidation of Cu_2O thin film surfaces reduces surface reactivity in the sodium acetate aqueous electrolyte (Kafi et al., 2018a; Kafi et al., 2020; Kafi et al., 2021). Therefore, herein, we have investigated the possibility of improving the electrodeposited Cu_2O thin film electrode for watersplitting in PEC by forming p-n junction and modifying the Cu_2O p-n junction surface by sulphidation.

Methodology

$n-Cu_2O$ thin films were potentiostatically electrodeposited on well-cleaned titanium (Ti) substrates at the film deposition bath pH value 6.1. Subsequently, thin films of $p-Cu_2O$ were potentiostatically electrodeposited on these $Ti/n-Cu_2O$ electrodes for bath pH values of 10, 11, 12 and 13. Durations of n- and $p-Cu_2O$ thin film depositions were 60 and 45 minutes respectively (Kafi et al., 2018b). The growth conditions used for the $n-Cu_2O$ and $p-Cu_2O$ thin film deposition are available in our previous reports (Kafi et al., 2018a, 2018b). These $Ti/n-Cu_2O/p-Cu_2O$ thin films were characterized in a PEC which consisted of 0.1 M sodium acetate (CH_3COONa) aqueous solution and determined the best pH combinations of n- and $p-Cu_2O$ film deposition bath for $Ti/n-Cu_2O/p-Cu_2O$ electrode preparation.

At the optimum pH combinations of n- and $p-Cu_2O$ film deposition $Ti/n-Cu_2O/p-Cu_2O$ electrode prepared by varying duration of n- and $p-Cu_2O$ thin film deposition as listed in the Table 1 were characterized in the PEC. Then, these $Ti/n-Cu_2O/p-Cu_2O$ thin film surfaces were exposed to 20 vol% ammonium sulphide (NH_4S) solution for 8 s and once again characterized in the above PEC to determine the effect of sulphidation. The counter and reference electrodes used in the PEC were a 2 cm × 2 cm platinum plate and a Ag/AgCl electrode respectively. Photoresponses and current-voltage (I-V) characterizations were done by using the Keithley multimeter and Gamry series G300 Potentiostat/Galvanostat/ZRA instrument respectively.

Table 1. *Durations of n- and p-Cu$_2$O thin film deposition of Ti/n-Cu$_2$O/p-Cu$_2$O electrodes at respective pH values of film deposition baths 6.1 and 13.0*

Combinations	Duration of thin film deposition (mins)	
	n-Cu$_2$O	**p-Cu$_2$O**
1	60	45
2	45	30
3	45	40
4	45	45
5	45	50
6	45	60

Results and Discussion

Figure 1 represents the photovoltage and photocurrent values obtained for Ti/n-Cu$_2$O/p-Cu$_2$O electrodes prepared by varying the pH values of the p-Cu$_2$O thin film deposition bath. According to Figure 1, it is clear that at the bath pH value 13 of p-Cu$_2$O thin film deposition both photovoltage and photocurrent values of Ti/n-Cu$_2$O/p-Cu$_2$O electrode are high and they are 161 mV and 128 μA cm^{-2} respectively. However, highest voltage is obtained for bath pH value 13 of p-Cu$_2$O thin film deposition.
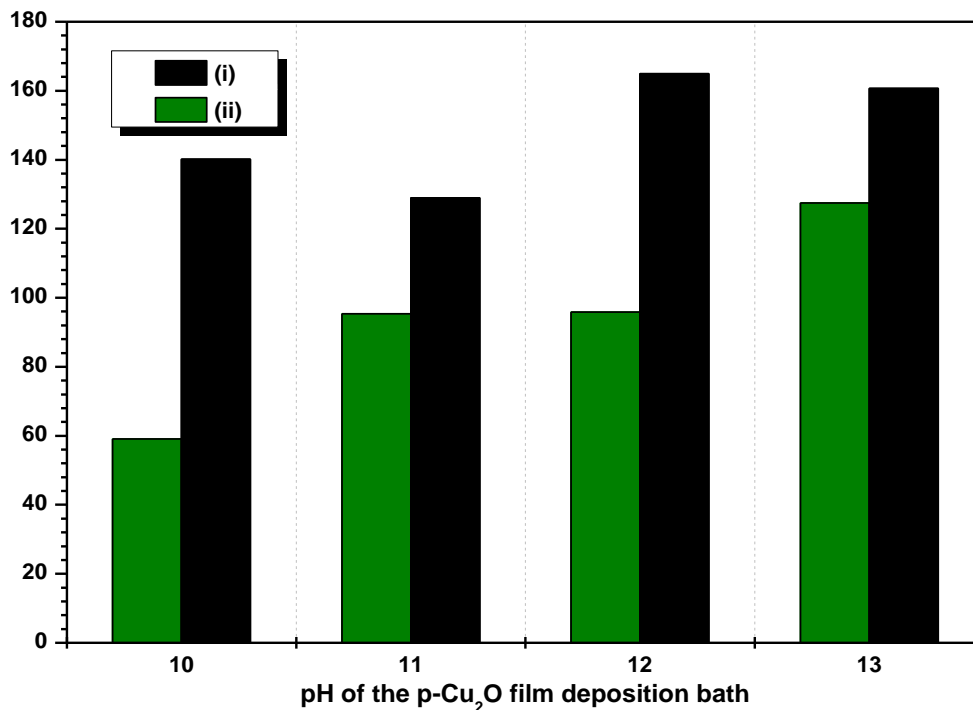
Figure 1. *Values of (i) photovoltage in mV and (ii) photocurrent density in μA cm^{-2} for Ti/n-Cu$_2$O/p-Cu$_2$O electrode in PEC at different pH values of p-Cu$_2$O thin film deposition.*

Additionally, it is noted that varying the durations of n- and p-Cu$_2$O thin films in preparation of Ti/n-Cu$_2$O/p-Cu$_2$O electrodes results in a considerable change in photocurrent value. Conventionally, the bare surfaces of Cu$_2$O in aqueous solutions could produce low photoresponses and thereby solar-to-hydrogen efficiencies (Kafi et al.,

2020). Our previous reports suggest that sulphidation of Cu_2O thin films using ammonium sulphide reduces the surface reactivity and improves the photoactivity of Cu_2O thin film surfaces (Kafi et al., 2018a; Kafi et al., 2020). Figure 2 represents the photocurrent values obtained for ammonium sulphide treated and untreated $Ti/n-Cu_2O/p-Cu_2O$ electrodes prepared for selected n- and $p-Cu_2O$ thin film deposition times listed in Table 1. It is very clear that sulphidation of Cu_2O thin film surfaces has significantly increased the photocurrent values of $Ti/n-Cu_2O/p-Cu_2O$ electrodes in PEC configuration. The combination 5 listed in Table 1 has proven to be the best photoelectrode in PEC configuration and the I-V characteristics of this is presented in Figure 3.
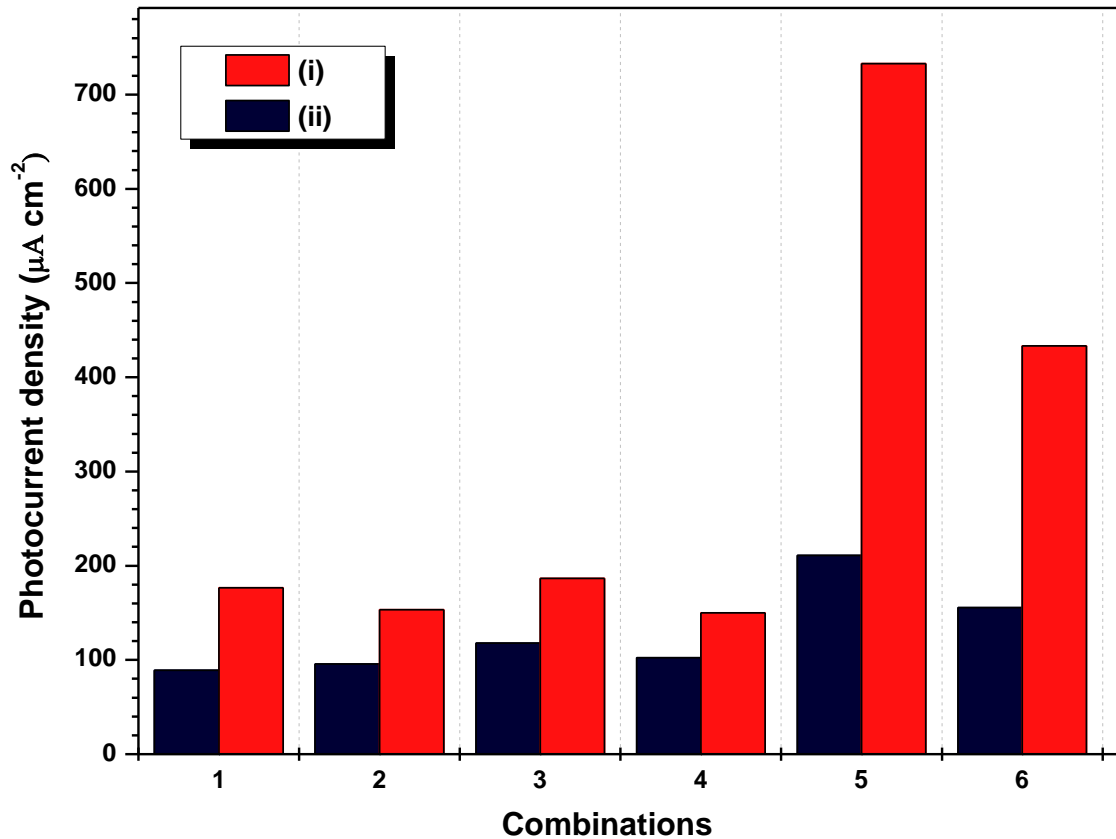
Figure 2. The resulted photocurrent values of $Ti/n-Cu_2O/p-Cu_2O$ electrodes (i) with and (ii) without treating with ammonium sulphide fabricated for different durations of n- and $p-Cu_2O$ thin film deposition as listed in Table 1.

In comparison to our previous work on $n-Cu_2O$ in PEC (Kafi et al., 2020), it is evident that Cu_2O homojunction in the same PEC develops higher built-in-potential. This can be observed by comparing the on-set potential of I-V curves in Figure 3. However, the resulted Cu_2O homojunction in PEC produces relatively low STH conversion efficiency. Further parameterization of the Cu_2O homojunction, modification of photoelectrode configuration as well as PEC configuration could improve the production of hydrogen by splitting water molecules.
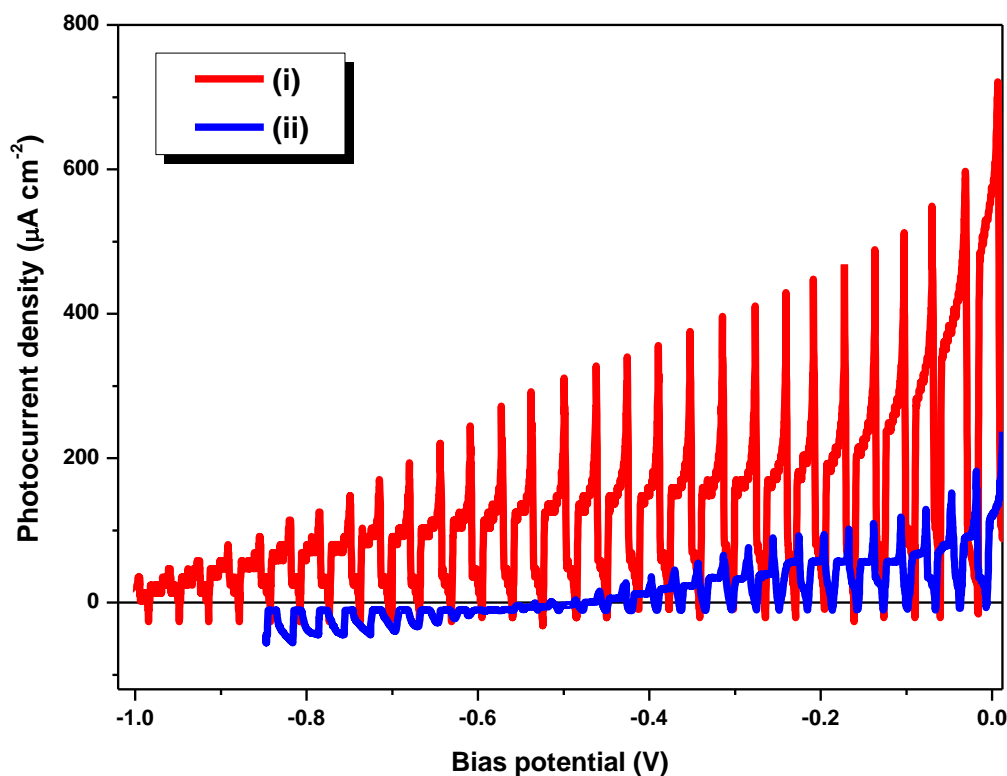
Figure 3. *I-V characteristics of Ti/n-Cu$_2$O/p-Cu$_2$O electrode (i) with and (ii) without treating with ammonium sulphide for the combination 5 considered in Table 1.*

Conclusion

In summary, the study revealed that the PEC water splitting by a Cu$_2$O homojunction depends on both pH and duration of n- and p-Cu$_2$O film deposition. Further, the conversion efficiency of STH has been enhanced by the sulphidation. The best Cu$_2$O homojunction photoelectrode has STH value of 0.9%. In addition, it is notable that the built-in potential is increased in formation of Cu$_2$O homojunction and after the sulphidation of Cu$_2$O homojunction. It can be concluded that further optimization of Cu$_2$O homojunction together with sulphidation could enhance the performance of Cu$_2$O homojunction photoelectrode in PEC water splitting.

Acknowledgment

References

Azevedo, J., Steier, L., Dias, P., Stefik, M., Sousa, C. T., Araújo, J. P., Mendes, A., Graetzel, M., & Tilley, S. D. (2014). On the stability enhancement of cuprous oxide water splitting photocathodes by low temperature steam annealing. *Energy & Environmental Science*, *7*(12), 4044–4052. https://doi.org/10.1039/C4EE02160F

Bae, D., Seger, B., Vesborg, P. C. K., Hansen, O., & Chorkendorff, I. (2017). Strategies for stable water splitting via protected photoelectrodes. *Chemical Society Reviews*, *46*(7), 1933–1954. https://doi.org/10.1039/C6CS00918B

Bai, Y., Zhou, Y., Zhang, J., Chen, X., Zhang, Y., Liu, J., Wang, J., Wang, F., Chen, C., Li, C., Li, R., & Li, C. (2019). Homophase Junction for Promoting Spatial Charge Separation in Photocatalytic Water Splitting. *ACS Catalysis*, *9*(4), 3242–3252. https://doi.org/10.1021/acscatal.8b05050

Bornoz, P., Abdi, F. F., Tilley, S. D., Dam, B., van de Krol, R., Graetzel, M., & Sivula, K. (2014). A Bismuth Vanadate–Cuprous Oxide Tandem Cell for Overall Solar Water Splitting. *The Journal of Physical Chemistry C*, *118*(30), 16959–16966. https://doi.org/10.1021/jp500441h

Kafi, F.S.B., Jayathileka, K. M. D. C., Wijesundera, R. P., & Siripala, W. (2018a). Dependence of interfacial properties of p-Cu_2O/electrolyte and p-Cu_2O/Au junctions on the electrodeposition bath pH of p-Cu_2O films. *Materials Research Express*, *5*(8). https://doi.org/10.1088/2053-1591/aad314

Kafi, F.S.B., Jayathileka, K. M. D. C., Wijesundera, R. P., & Siripala, W. (2018b). Effect of Bath pH on Interfacial Properties of Electrodeposited n-Cu_2O Films. *Physica Status Solidi (B) Basic Research*, *255*(6), 1700541. https://doi.org/10.1002/pssb.201700541

Kafi, F. S. B., Jayathilaka, K. M. D. C., Wijesundera, R. P., & Siripala, W. (2021). Effect of pre-surface treatments on p-Cu_2O/Au Schottky junctions. *Journal of the National Science Foundation of Sri Lanka*, *49*(1), 61–66. https://doi.org/http://doi.org/10.4038/jnsfsr.v49i1.8942

Kafi, F. S. B., Wijesundera, R. P., & Siripala, W. (2020). Enhanced Photoelectrochemical Water Splitting by Surface Modified Electrodeposited n-Cu_2 O Thin Films. *Physica Status Solidi (A)*, 2000330. https://doi.org/10.1002/pssa.202000330

Liu, R., Zheng, Z., Spurgeon, J., & Yang, X. (2014). Enhanced photoelectrochemical water-splitting performance of semiconductors by surface passivation layers. *Energy & Environmental Science*, *7*(8), 2504–2517. https://doi.org/10.1039/C4EE00450G

Minami, T., Nishi, Y., & Miyata, T. (2016). Cu_2O-based solar cells using oxide semiconductors. *Journal of Semiconductors*. https://doi.org/10.1088/1674-4926/37/1/014002

Nellist, M. R., Laskowski, F. A. L., Lin, F., Mills, T. J., & Boettcher, S. W. (2016). Semiconductor–Electrocatalyst Interfaces: Theory, Experiment, and Applications in Photoelectrochemical Water Splitting. *Accounts of Chemical Research*, *49*(4), 733–740. https://doi.org/10.1021/acs.accounts.6b00001

Siripala, W., & Kumara, K. P. (1990). Photovoltaic properties of Cu_2O/Cu_xS heterojunction. *Journal of the National Science Foundation of Sri Lanka*, *18*(2), 109–117. https://doi.org/http://doi.org/10.4038/jnsfsr.v18i2.8197

Wang, T., & Gong, J. (2015). Single-Crystal Semiconductors with Narrow Band Gaps for Solar Water Splitting. *Angewandte Chemie International Edition*, *54*(37), 10718–10732. https://doi.org/https://doi.org/10.1002/anie.201503346

Wang, T., Wei, Y., Chang, X., Li, C., Li, A., Liu, S., Zhang, J., & Gong, J. (2018). Homogeneous Cu_2O p-n junction photocathodes for solar water splitting. *Applied Catalysis B: Environmental*, *226*. https://doi.org/10.1016/j.apcatb.2017.12.022

Wick, R., & Tilley, S. D. (2015). Photovoltaic and Photoelectrochemical Solar Energy Conversion with Cu_2O. *Journal of Physical Chemistry C*, *119*(47). https://doi.org/10.1021/acs.jpcc.5b08397

Conference Paper No: PF-08

Copula-based drought severity-duration-frequency analysis for Anuradhapura and Puttalam in the dry zone of Sri Lanka

W.R.P.M.S.S. Wijesundara[1*] and K. Perera[2]

[1]Computing Center, Faculty of Engineering, University of Peradeniya, Sri Lanka
[2]Department of Engineering Mathematics, Faculty of Engineering, University of Peradeniya, Sri Lanka
sachinisw1515@gmail.com*

Abstract

Drought is a severe problem in many areas of Sri Lanka, where rainfall amounts are low and extremely high due to climatic changes. To reduce the negative consequences of droughts, it is important to understand the drought characteristics (drought duration and drought severity) and their associations. Therefore, to build a drought severity-duration-frequency (SDF) relationship, a probabilistic technique is proposed using rainfall data from 1996 to 2018 in the two districts Anuradhapura and Puttalam in the dry zone of Sri Lanka. Drought characteristics were defined using 3-month standardized precipitation index (SPI) and Copulas are employed to derive the joint distribution function. Occurrences of 41 droughts from both stations were identified. The derived SDF relationship is a function of marginal distribution functions of drought characteristics linked by a copula. Log-normal distribution and Gamma distribution were identified as the best marginal distribution to represent drought duration and drought severity, respectively, using AIC, BIC and Kolmogorov-Smirnov test. Gaussian copula and Frank copula were identified as the best among the other five copulas based on AIC, BIC and Cramer-Von Mises statistics. Both Log-normal distribution and Gamma distribution along with the Gaussian copula and Frank copula combined to derive the joint distribution of Anuradhapura and Puttalam, respectively. Joint return periods in terms of recurrence intervals were calculated and derived the SDF curves. According to the derived SDF curves, drought severity in Puttalam is greater than those in Anuradhapura for a given recurrence interval and drought duration.

Keywords

Copula, Drought, Joint distribution, Marginal distributions, SPI

Introduction

In Sri Lanka, drought is one of the most injurious natural hazards that has islandwide effects. It can cause severe damages to the agriculture, socioeconomic structure of humans, and also the ecosystem. Mainly there are three climatic zones in Sri Lanka as dry, wet, and intermediate which are categorized according to the total annual rainfall received by those climatic regions. The dry zone is the main source that provides both irrigated and rainfed crops for the Sri Lankan food industry. Dryzone receives less than 1,800 mm of rainfall per year throughout both the south-western and north-eastern monsoon seasons. Since there are inadequate irrigation systems and high rainfall fluctuations prevail within the dry zone, areas like Anuradhapura and Puttalam are experienced a prolonged drought stemming from reduced precipitation levels. Anuradhapura is one of the largest crop production areas in Sri Lanka which is frequently affected by droughts. Since Puttalam and Anuradhapura are situated very close to each other in the dry zone it is important to identify the dependence nature of drought

characteristics of those two areas. As it is impossible to evade droughts, drought preparedness can be developed while managing drought impacts to identify the drought severity as it plays a major role in risk management.

Each drought seasons can be categorized by two attributes that correlate to each other: Severity and Duration (Shiau & Shen, 2001). Many indices have been developed for modeling a drought event, such as Palmer Drought Severity Index (Palmer, 1965) and the Standardized Precipitation Index (SPI) (Mckee et al., 1993). Since SPI is simple, spatially invariant, and just requires monthly precipitation data to calculate, (Mckee et al., 1993) drought duration and drought severity derived from SPI used to describe the droughts.

However joint multivariate models of droughts are difficult to develop because different distribution functions are frequently used to fit various drought attributes such as severity and duration. The use of copulas to link different marginal distributions to generate the joint multivariate distribution function alleviates this challenge as it has the advantage of not requiring any assumptions about the variables being independent, normal or having the same type of marginal distributions (Zhang & Singh, 2007b). Most research on multivariate distributions using copulas have been focused on rainfall and floods (Shiau, 2006; Shiau & Modarres, 2009; Zhang & Singh, 2007a, 2007b) which have been used for rainfall frequency analysis, flood frequency analysis and drought frequency analysis. Shiau in 2009 has developed a Copula-based drought severity-duration frequency analysis to assess the simultaneous multi-attributes of droughts occurred in two regions of Iran (Shiau & Modarres, 2009). Dalezios in 2000 developed drought severity-duration frequency (SDF) curves to analyze droughts and wet periods in Greece (Dalezios et al., 2000).

This study aims to derive copula-based drought severity-duration-frequency (SDF) curves for Anuradhapura and Puttalam by identifying the best joint probability distribution function of drought duration and drought severity based on the best mariginal distributions and best Copula. Identified best joint distribution of Anuradhapura and Puttalam will be used to generate the joint return periods of drought events for managing the impacts of droughts.

Methodology

Description of data

Monthly rainfall data for 23 years (1996–2018) were collected from two meteorological stations, Anuradhapura and Puttalam in the dry zone of Sri Lanka.

Defining drought using SPI

SPI values were often estimated over time intervals of 1, 3, 6, 9, and 12 months (Ganguli & Reddy, 2012). SPI on 3-months was employed in this study to identify short-term seasonal drought occurrences. As drought is defined when the values of SPI fall below zero, a period with negative SPI values is considered a drought event while it ends when SPI reaches a value of 0. Drought duration is the continuous negative SPI periods in a drought event. Whereas drought severity is the sum of cumulative SPI periods within a drought event (Shiau & Modarres, 2009).

Modeling the joint cumulative distribution function (JCDF)

Pearson correlation coefficient and Kendall's tau (τ) measure were used to identify the dependence nature of the drought characteristics. Exponential, Gamma, Normal, Lognormal, Weibull and Logistic distributions were fitted and identified the best marginal distribution out of them using Akaike's information criteria (AIC) and Bayesian information criteria (BIC). The Kolmogorov-Smirnov (K-S) test was then employed to confirm the results. Parameters of the distributions were estimated using the maximum likelihood method.

The copula method which allows to study and measure the relationships between random variables is first developed by Sklar (Sklar, 1959) to describe the function that links univariate distribution functions to multivariate distribution function. Tail dependency of drought characteristics can be checked by ranked scatter plots. Five copulas were tested (Gumbel-Hourgaard, Joe, Clayton, Frank, and Gaussian) and identified the best copula using AIC and BIC. Cramer-von Mises S_n statistic was used for further confirmation of the goodness of fit test while the estimation of S_n was done by the methods inverting the tau parameter and parametric bootstrapping (Genest & Rémillard, 2008).

Then generated the Joint Cumulative Distribution Function (JCDF) of drought severity and drought duration using the best fitted marginal distributions and the best copula.

Joint return periods

The joint return period $T_{X,Y}(x, y)$ of a bivariate random variable (X, Y) corresponding to a value (x, y) is given by;

$$T_{X,Y}(x, y) = \left(\frac{1}{1-F_{XY}(x,y)}\right) \tag{1}$$

Where, $F_{XY}(x, y)$ is the joint cumulative distribution function and $F_{XY}(x, y) = P(X \leq x, Y \leq y)$ is the probability of two events $X \leq x, Y \leq y$ (Zhang & Singh, 2007a).

Copula-based drought severity-duration-frequency (SDF) relationship

Since each drought event is treated as a bivariate random variable, joint recurrence intervals can be used to show the relationship between drought severity, drought duration, and frequency (in terms of recurrence interval) (Shiau & Modarres, 2009).

Results and Discussion

During the study period, Anuradhapura has experienced the longest drought duration in 2002 while Puttalam in 2010 & 2012. The most severe droughts in Anuradhapura occurred in 2002 and 2017 and in Puttalam it was in 2008, 2012 and 2017.

The mean annual rainfall for Anuradhapura and Puttalam stations are 117 mm and 97 mm, respectively. The number of droughts that occurred during the study period for both stations is 41. Although it is the same for both stations, the standard deviation of drought duration and severity for Puttalam are larger than those of Anuradhapura. This fact indicates that drought characteristics are highly fluctuating for Puttalam.

Calculated Pearson's correlation coefficients for drought duration and severity of Anuradhapura and Puttalam are 0.876 and 0.844, respectively, while Kendall's tau values

for the drought characteristics of Anuradhapura and Puttalam are 0.770 and 0.768, respectively. Results showed a strong positive relationship. Thus the drought duration and drought severity of each station should be modeled jointly.

Drought duration and drought severity of the two stations can be fitted to Lognormal and Gamma distributions, respectively, as they have low AIC and BIC values while the K-S test result confirmed it further. Parameters of the selected distributions are estimated by the maximum likelihood method and are summarized in Table 1. The critical values for a sample size of 43 (Anuradhapura) and 34 (Puttalam) are 0.00045 and 0.01388 respectively, at the 10% significance level. The maximum deviations between observed data and proposed distributions of drought characteristics for Anuradhapura and Puttalam are also showed in Table 1.

Table 1. *Estimated parameters of the proposed distributions.*

Character	Estimates	Anuradhapura	D max	Puttalam	D max
Duration	meanlog/θ	0.870	0.208	1.078	0.172
	sdlog/α	0.733		0.728	
Severity	shape/α	0.773	0.099	0.873	0.112
	scale/β	0.333		0.269	

Gaussian copula and Frank copula are the best among other copulas to represent two stations as they have low AIC and BIC values and no upper or lower tail dependency. Calculated Cramer-von Mises S_n statistics for the Gaussian copula and Frank copula are 0.028 and 0.022, respectively**.** Inverting Kendall's tau and parametric bootstrapping is used to obtain S_n values. The values of the copula parameters of Anuradhapura and Puttalam are 0.876 and 8.081, respectively.

Then Gaussian copula was used to combine the identified Gamma marginal distribution and Log-normal distribution to create the joint distribution of Anuradhapura while the Frank copula was used to combine the identified Gamma marginal distribution and Log-normal distribution to create the joint distribution of Puttalam.

The developed drought SDF curves for Anuradhapura and Puttalam with selected recurrence intervals generated using equation 1 are sketched in Figure 1. These SDF curves show an increasing pattern in drought severity for the increasing stages of drought duration.

(a)   (b)
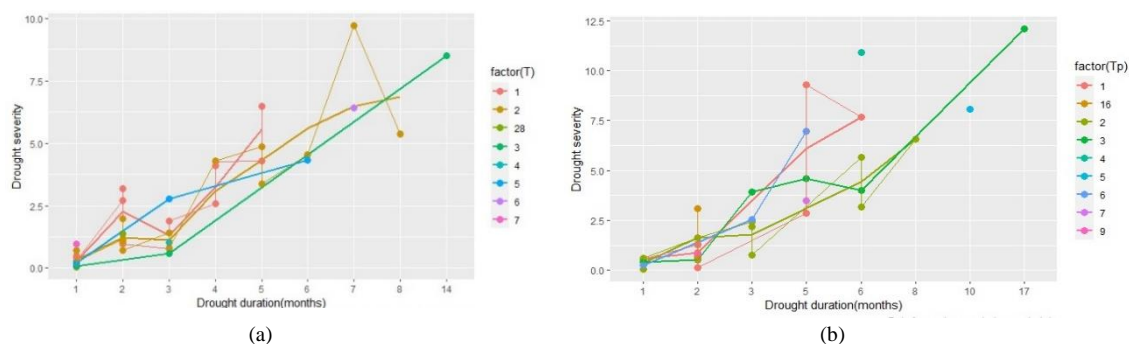
Figure 1. *The drought SDF curves for Anuradhapura (a) and Puttalam (b).*

According to Figure 2, we can identify that drought severity at Puttalam is greater than the value at Anuradhapura for the same duration and recurrence interval. Therefore, more severe droughts can occur in Puttalam than in Anuradhapura.
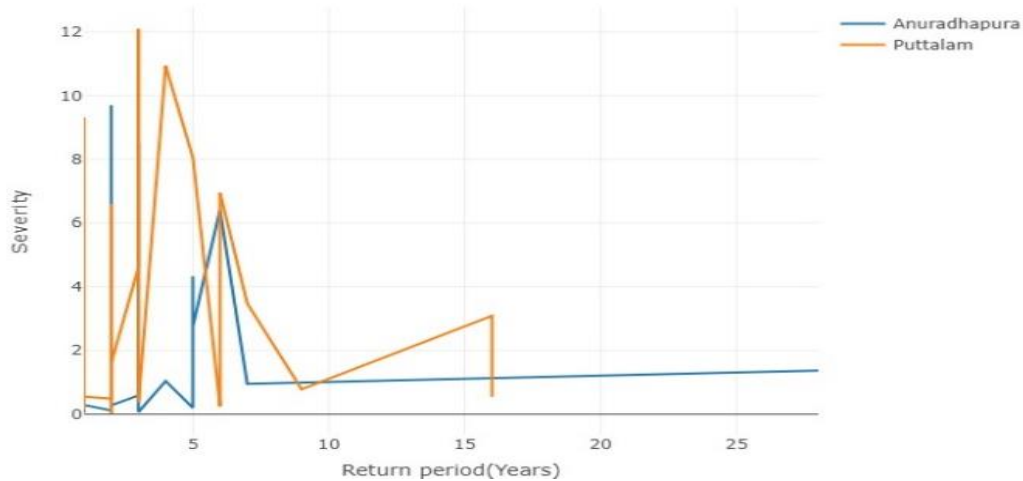
Figure 2. *The drought severity limits with various recurrence intervals for Anuradhapura and Puttalam.*

Conclusion

Understanding drought characteristics is a vital step in developing effective mitigation measures for droughts-related problems. In this study, 3-month SPI series was used and occurrences of 41 drought events from both stations were identified. Anuradhapura region has experienced 2 most severe droughts in 2002 and 2017 while the Puttalam region has experienced 3 most severe droughts in 2008,2012 and 2017. The Kendall's tau correlation and Pearson correlation test results revealed that there is a positive relationship between each drought variable. For both Anuradhapura and Puttalam marginal distributions of drought duration fit to a Log-normal distribution while marginal distributions of drought severity fit to a Gamma distribution quite well among other distributions.

The Gaussian copula and the Frank copula were found to be the best copulas for Anuradhapura and Puttalam, respectively. The Gaussian copula was used to combine the identified Gamma marginal distribution and Log-normal distribution to create the joint distribution of Anuradhapura while the Frank copula was used to combine the identified Gamma marginal distribution and Log-normal distribution to create the joint distribution of Puttalam.

Proposed method is used to create drought SDF curves with various recurrence intervals for the two rain gauge stations in the dry zone of Sri Lanka. These SDF curves show an increasing pattern. That is at most drought severity increases with drought duration, but not at a continuous rate. When comparing the generated drought SDF curves, drought severity at Puttalam is often greater than the value in Anuradhapura for the same period and recurrence interval. Therefore, highly fluctuating rainfall exists in the Puttalam region leads to the occurrences of more severe droughts than those in Anuradhapura. Thus based on the proven results government can develop drought preparedness while managing drought impacts within the dry zone of Sri Lanka.

References

Dalezios, N. R., Loukas, A., Vasiliades, L., & Liakopoulos, E. (2000). Severity-duration-frequency analysis of droughts and wet periods in Greece. *Hydrological Sciences Journal*, *45*(5), 751–769. https://doi.org/10.1080/02626660009492375

Ganguli, P., & Reddy, M. J. (2012). Risk Assessment of Droughts in Gujarat Using Bivariate Copulas. *Water Resources Management*, *26*(11), 3301–3327. https://doi.org/10.1007/s11269-012-0073-6

Genest, C., & Rémillard, B. (2008). Validity of the parametric bootstrap for goodness-of-fit testing in semiparametric models. *Annales de l'Institut Henri Poincaré, Probabilités et Statistiques*, *44*(6), 1096–1127. https://doi.org/10.1214/07-AIHP148

Mckee, T. B., Doesken, N. J., & Kleist, J. (1993). *The relationship of drought frequency and duration to time scales. January*, 17–22.

Palmer, W. C. (1965). Meteorological Drought. In *U.S. Weather Bureau, Res. Pap. No. 45* (p. 58). https://www.ncdc.noaa.gov/temp-and-precip/drought/docs/palmer.pdf

Shiau, J. T. (2006). *Fitting Drought Duration and Severity with Two-Dimensional Copulas*. 795–815. https://doi.org/10.1007/s11269-005-9008-9

Shiau, J. T., & Modarres, R. (2009). *Copula-based drought severity-duration-frequency analysis in Iran. 489*(June), 481–489. https://doi.org/10.1002/met

Shiau, J. T., & Shen, H. W. (2001). R a h d d s. *Water Resources*, *February*, 30–40.

Sklar, M. (1959). Fonctions de Répartition à n Dimensions et Leurs Marges. *Open Access,Publications de l'Institut Statistique de l'Université de Paris*, *229–231*(8).

Zhang, L., & Singh, V. P. (2007a). *Bivariate rainfall frequency distributions using Archimedean copulas*. 93–109. https://doi.org/10.1016/j.jhydrol.2006.06.033

Zhang, L., & Singh, V. P. (2007b). *Gumbel – Hougaard Copula for Trivariate Rainfall Frequency Analysis. August*, 409–419.

Conference Paper No: PF-09

Fourier method for one dimensional parabolic inverse problem with Dirichlet boundary conditions

H.A.K. Amanda[*] and W.P.T. Hansameeu

Department of Mathematics, University of Kelaniya, Sri Lanka
kviamahettiarachchi@gmail.com*

Abstract

The finite difference method, spectral method, and double shifted Lagrange's polynomials have been discussed for the one-dimensional inverse problem of the heat equation with control parameters and the source term in literature. Here, we present, Fourier method for the one-dimensional parabolic inverse problem with Dirichlet boundary conditions. In this study, after analyzing the control parameters, the initial condition and the source term are used to track a temperature distribution at a point in the interval. We validated that desired temperature distribution and measured temperature distribution (or the point evaluation) at an internal point overlap each other for the derived values of control parameters (source term and initial distribution) using the Fourier method. Moreover, we validated the temperature distribution at a point in the domain and tracked the desired harmonic and linear temperature distributions using numerical simulations. Finally, we simplified the above numerical simulations using the COMSOL software and illustrated some figures to the given point.

Keywords

Dirichlet boundary conditions, Fourier method, One dimensional heat equation control, Tracking problem, Point evaluation

Introduction

Heat conduction problems have achieved substantial popularity in science and industrial fields over the last five decades. Industry-related heat conduction research has great significance and is mostly regarded as the inverse problem of the heat conduction equation. Such as, by determining boundary, initial, or the internal data of the medium of heat transferred, a known temperature at the internal or the boundary point of the domain can be controlled. Usually, solving the inverse problem of the heat conduction equation is ill-conditioned and the small perturbation of data will lead to a problem with a huge error.

The inverse problem in (Grysa, 1980) discusses the dependence of the boundary conditions of different types on the prescribed temperature state. Moreover, an example of (Grysa, 1980) illustrates that how to make use of given temperature distribution on the surface to determine the thermal conditions of the heat medium near the sphere surface. (Dehghan, 2003) discusses a numerical approach for the one-dimensional parabolic inverse problem with control parameters. It presents several finite difference formulas for the inverse problem of finding a source parameter in the diffusion equation. Though the most usual way of generating a finite difference scheme is the use of Taylor's series, the method developed here is based on the modified equivalent partial differential equations. A direct computation technique for the inverse problem of finding a source term control parameter, using the spectral method can be found in (M Dehghan, 2006) Moreover there

the function u(x,t) of two independent variables $0 \leq x \leq l$ and $0 \leq t \leq T$ has been expanded in terms of double shifted Lagrange's Polynomials. In (Ivanchov, Inverse Problem for General One Dimensional Parabolic Equation, 1998) the boundary integral method for solving one-dimensional homogeneous heat conduction equation has been discussed while (Ivanchov, One Dimensional Heat Conduction Equation for Inverse Problem, pp.60-66 2011) the existence and the uniqueness of the solutions of the one-dimensional inverse problem of the heat equation with time-dependent leading coefficient have been discussed. (Kanca, 2013) investigates the inverse problem of finding a time-dependent diffusion coefficient in a parabolic equation with the periodic boundary and integral overdetermination conditions. However, (Zhang & Guo, 2015)shows the numerical method is proposed to solve the inverse problem based on a Fourier expansion. Moreover, the articles (Hussein, Lesnic, & Ivanchov, 2014), (Negero & Tufa, 2014) and (Ivanchov, Inverse problems for Parabolic Equations, 2003) have been discussed on several sides of inverse problems for the parabolic equation. The novelty of our work is we use the Fourier method to construct the control parameters, initial condition, and the source term.

Consider the following uncontrolled heat equation with homogeneous Dirichlet boundary conditions in a finite-dimensional interval:

$$u_t(x,t) - u_{xx}(x,t) = 0 \qquad 0 \leq x \leq l \tag{1}$$
$$u(0,t) = u(l,t) = 0 \quad t \geq 0 \tag{2}$$
$$u(x,0) = \phi(x) \quad 0 \leq x \leq l \tag{3}$$

Find control parameters, initial temperature $g(x)$ and the heat source $f(x,t)$ such that point evaluation $u(x_0,t)$ tracks the desired signal $F(t)\epsilon\mathbb{C}[0,T]$ satisfying the system:

$$u_t(x,t) - \alpha u_{xx}(x,t) = f(x,t) \quad 0 < x < l, t > 0 \tag{4}$$
$$u(0,t) = u(l,t) = 0 \quad t \geq 0 \tag{5}$$
$$u(x,0) = g(x) \qquad 0 \leq x \leq l \tag{6}$$

Hence F(t) is a known function. In this research, we construct the control parameters, the initial condition, and source term so that the point evaluation at an internal point in the domain will track a known function. Finally, we validate our findings using the finite difference solver COMSOL as it provides better solution accuracy, consistency and easy meshing more efficiently and effectively.

Methodology

Consider the Fourier series representations of u(x,t) , f(x,t) and g(x) as follows.

Since u(x,t) which solves Equation(4) depends on both time and space, it can be represented as a Fourier sine series, $\quad u(x,t) = \sum_{n=1}^{\infty} a_n(t)\sin\left(\frac{n\pi x}{l}\right)$ (7)

Notice that the u satisfy the boundary conditions in Eq.(5). Then the coefficient $a_n(t)$ is given by $\quad a_n(t) = \frac{2}{l}\int_0^l u(x,t)\sin\left(\frac{n\pi x}{l}\right)dx.$

We represented the right-hand side f(x,t) and the initial function g(x) in the same way as,
$f(x,t) = \sum_{n=1}^{\infty} c_n(t)\sin\left(\frac{n\pi x}{l}\right) \qquad ; \qquad c_n(t) = \frac{2}{l}\int_0^l f(x,t)\sin\left(\frac{n\pi x}{l}\right)dx.$ (8)

$$g(x) = \sum_{n=1}^{\infty} b_n \sin\left(\frac{n\pi x}{l}\right). \tag{9}$$

We setup the IVP for $a_n(t)$:

First, we can differentiate Eq.(7) with respect to t and x. Then we can derive the following equations to u_t, u_x, u_{xx} .

$$u_t(x,t) = \sum_{n=1}^{\infty} a'_n(t) \sin\left(\frac{n\pi x}{l}\right). \tag{10}$$

$$u_x = a_n(t) \sum_{n=1}^{\infty} \cos\left(\frac{n\pi x}{l}\right)\left(\frac{n\pi}{l}\right).$$

$$u_{xx} = -a_n(t) \sum_{n=1}^{\infty} \sin\left(\frac{n\pi x}{l}\right)\left(\frac{n\pi}{l}\right)^2. \tag{11}$$

Plugging Equations (11), (10), (9), and (8) in Partial Differential Eq. (4), we can derive

$$\sum_{n=1}^{\infty} a'_n(t) \sin\left(\frac{n\pi x}{l}\right) + a_n(t) \sum_{n=1}^{\infty} \sin\left(\frac{n\pi x}{l}\right)\left(\frac{n\pi}{l}\right)^2 = \sum_{n=1}^{\infty} c_n(t) \sin\left(\frac{n\pi x}{l}\right). \tag{12}$$

The above equation implies, $\quad c_n(t) = a'_n(t) + a_n(t)\left(\frac{n\pi}{l}\right)^2 \quad, \quad n = 1,2,3 \dots \dots$

According to the initial condition in Eq.(6), $u(x,0) = g(x)$. Thus we can derive the following,

$$\sum_{n=1}^{\infty} a_n(0) \sin\left(\frac{n\pi x}{l}\right) = \sum_{n=1}^{\infty} b_n \sin\left(\frac{n\pi x}{l}\right),$$

$$b_n = a_n(0) \tag{13}$$

Then we solve the IVP Equation(13) and find $c_n(t)$ and b_n. Let $F(t) \in \mathbb{C}(\mathbb{R}, \mathbb{R})$ for all $t > 0$ be the reference signal to be tracked at the point $x = x_0$. Where $0 < x_0 < l$. Next, we derive Equations for $c_n(t)$ and b_n in terms of $F(t)$. Let F(t) be the temperature distribution (reference signal) to be tracked at $x = x_0$. Then,

$$a_n(t) = \frac{2}{l} \int_0^l u(x_0,t) \sin\left(\frac{n\pi x_0}{l}\right) dx \quad ; \quad a_n(t) = \frac{2}{l} \int_0^l F(t) \sin\left(\frac{n\pi x_0}{l}\right) dx$$

Finally, we have $\quad a_n(t) = 2\sin\left(\frac{n\pi x_0}{l}\right) F(t) \tag{14}$

Differentiating the above $a_n(t)$ w.r.t. t and plugging $a_n(t)$ and $a'_n(t)$ in IVP in Eq.(13)

$$c_n(t) = 2 \sin\left(\frac{n\pi x_0}{l}\right) F'(t) + 2\left(\frac{n\pi}{l}\right)^2 \sin\left(\frac{n\pi x_0}{l}\right) F(t). \tag{15}$$

$$b_n = a_n(0) = 2 \sin\left(\frac{n\pi x_0}{l}\right) F(0), \quad n = 1,2,3 \dots \dots \tag{16}$$

Next, we prove the existence of one value for n. The orthogonal decomposition of f(x,t) can be written as $f(x,t) = c_1\varphi_1 + c_2\varphi_2 + \cdots$

where, $\quad c_m = \frac{<\varphi_m, f>}{<\varphi_m, \varphi_m>} \quad ; \quad \varphi_m = \sin\left(\frac{m\pi x}{l}\right).$

Hence $\quad f(x,t) = \sum_{n=1}^{\infty} c_n \varphi_n = \sum_{n=1}^{\infty} \frac{<\varphi_n, f>}{<\varphi_n, \varphi_n>} \varphi_n.$

___

Since $< \varphi_n, \varphi_m > = \int_0^l \sin\left(\frac{n\pi x}{l}\right) \sin\left(\frac{m\pi x}{l}\right) dx = 0 \quad \forall x \quad n \neq m$

We have, $\quad < c_1 \varphi_1 - f, \varphi_1 > = 0 \, , \, \forall x$

Finally, the above equation implies $f(x,t) = c_1(t) \sin\left(\frac{\pi x}{l}\right)$.

Example 1: Tracking F(t)=sin(t) at $x = x_0$.

Using the Eq.(15) Eq.(16) for b_n and c_n in the previous section,

$$c_1(t) = 2\sin\left(\frac{\pi x_0}{l}\right)\cos(t) + 2\left(\frac{\pi}{l}\right)^2 \sin\left(\frac{\pi x_0}{l}\right)\sin(t). \tag{17}$$
$$b_1 = 0 \tag{18}$$
$$f(x,t) = \sum_{n=1}^{\infty}\left[2\sin\left(\frac{\pi x_0}{l}\right)\cos(t) + 2\left(\frac{\pi}{l}\right)^2 \sin\left(\frac{\pi x_0}{l}\right)\sin(t)\right]\sin\left(\frac{\pi x}{l}\right). \tag{19}$$
$$g(x) = 0. \tag{20}$$

Example 2: Tracking F(t)=cos(t) at $x = x_0$.

Substituting Eq.(15),Eq.(16) we can obtain c_n and b_n for this case,

$$c_1(t) = -2\sin\left(\frac{\pi x_0}{l}\right)\sin(t) + 2\left(\frac{\pi}{l}\right)^2 \sin\left(\frac{\pi x_0}{l}\right)\cos(t). \tag{21}$$
$$b_1 = 2\sin\left(\frac{\pi x_0}{l}\right). \tag{22}$$
$$f(x,t) = \sum_{n=1}^{\infty}\left[-2\sin\left(\frac{\pi x_0}{l}\right)\sin(t) + 2\left(\frac{\pi}{l}\right)^2 \sin\left(\frac{\pi x_0}{l}\right)\cos(t)\right]\sin\left(\frac{\pi x}{l}\right). \tag{23}$$
$$g(x) = \sum_{n=1}^{\infty} 2\sin\left(\frac{\pi x_0}{l}\right)\sin\left(\frac{\pi x}{l}\right). \tag{24}$$

Example 3: Tracking F(t)=4t at $x = x_0$,

Then using the derived equations for b_n and c_n,

$$c_1(t) = 2\sin\left(\frac{\pi x_0}{l}\right)4 + 2\left(\frac{\pi}{l}\right)^2 \sin\left(\frac{\pi x_0}{l}\right)4t. \tag{25}$$
$$b_1 = 0 \tag{26}$$
$$f(x,t) = \sum_{n=1}^{\infty} 8\left[\sin\left(\frac{\pi x_0}{l}\right) + \left(\frac{\pi}{l}\right)^2 \sin\left(\frac{\pi x_0}{l}\right)t\right]\sin\left(\frac{\pi x}{l}\right). \tag{27}$$
$$g(x) = 0. \tag{28}$$

Results and Discussion

We set F(t)=sin(t) and solve

$$u_t(x,t) - u_{xx}(x,t) = 2\sin\left(\frac{\pi x_0}{l}\right)\sin\left(\frac{\pi x}{l}\right)\left[\cos(t) + \sin(t)\left(\frac{\pi}{l}\right)^2\right].$$
$$u(x,0) = 0. \qquad u(0,t) = u(l,t) = 0$$

On $x \in [0,1]$ in COMSOL.Then we tracked the temperature distribution at the point x=0.75. The measured output is the point evaluation at x=0.75. The figure1 illustrates the desired temperature distribution and the measured output at x=0.75 in one figure. The

figure1 shows that the desired temperature and the measured output overlap each other for the derived control parameters.

Figure 3. *The graph of sin(t) and measured output at x=0.75.*

Next, we consider F(t)=cos(t) and solve the following system.

$$u_t(x,t) - u_{xx}(x,t) = 2\sin\left(\frac{\pi x_0}{l}\right)\sin\left(\frac{\pi x}{l}\right)\left[\cos(t)\left(\frac{\pi}{l}\right)^2 - \sin(t)\right].$$

$$u(x,0) = 2\sin\left(\frac{\pi x_0}{l}\right)\sin\left(\frac{\pi x}{l}\right). \qquad u(0,t) = u(l,t) = 0.$$

On $x\epsilon[0,1]$ in COMSOL.Then we tracked measured output(point evaluation) at x=0.75. The figure 2 shows desired temperature distribution and the measured output at x=0.75 in one figure. The desired temperature and the measured output overlap each other for the derived control parameters as shown in figure2.
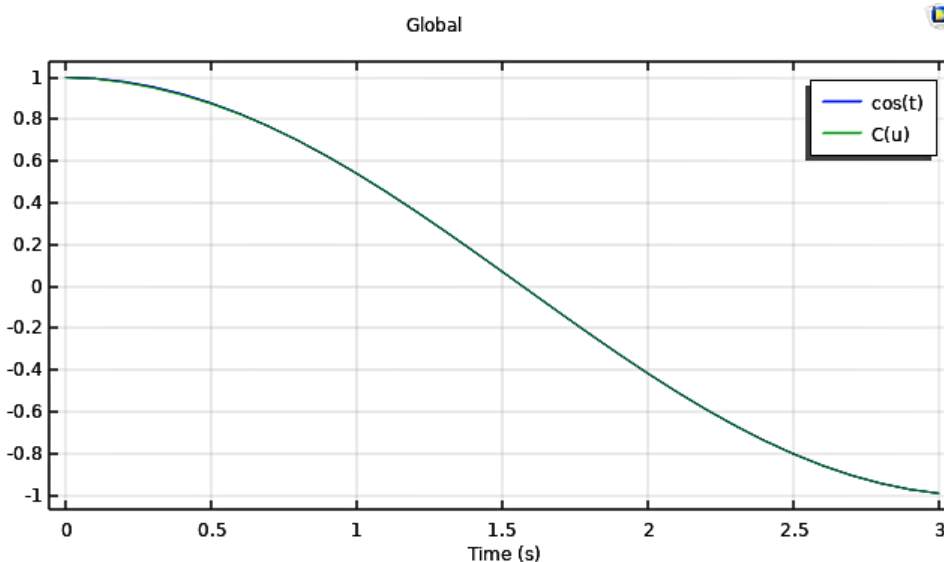
Figure 4. *The graph of cos(t) and the measured output at x=0.75.*

Considering F(t)=4t we solve,

$$u_t(x,t) - u_{xx}(x,t) = 8\sin\left(\frac{\pi x_0}{l}\right)\sin\left(\frac{\pi x}{l}\right)\left[1 + t\left(\frac{\pi}{l}\right)^2\right].$$
$$u(x,0) = 0. \qquad\qquad u(0,t) = u(l,t) = 0.$$

On $x\epsilon[0,1]$ in COMSOL. The measured output is the point evaluation at x=0.25. The figure3 illustrates desired temperature distribution and the measured output at x=0.25 in one figure. The figure3 clearly shows that the desired temperature and the measured output overlap each other for the derived control parameters.
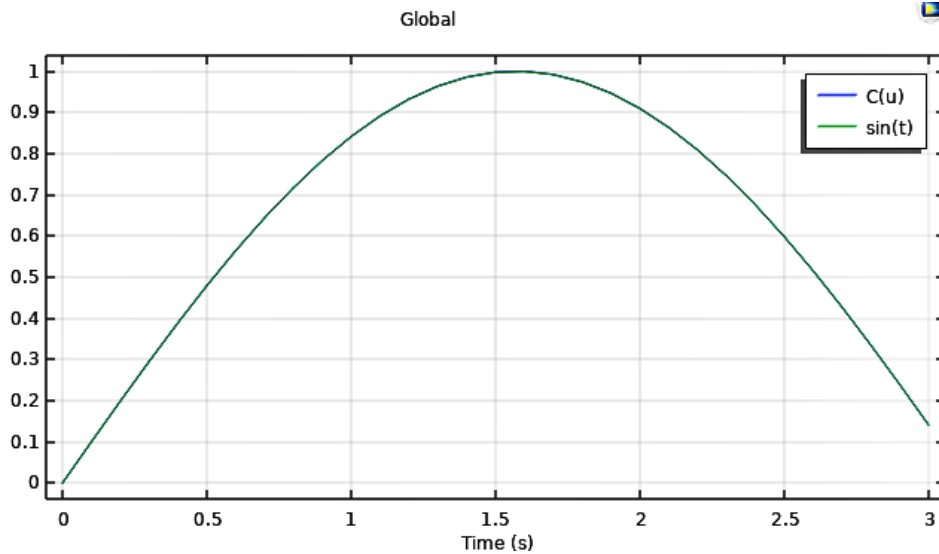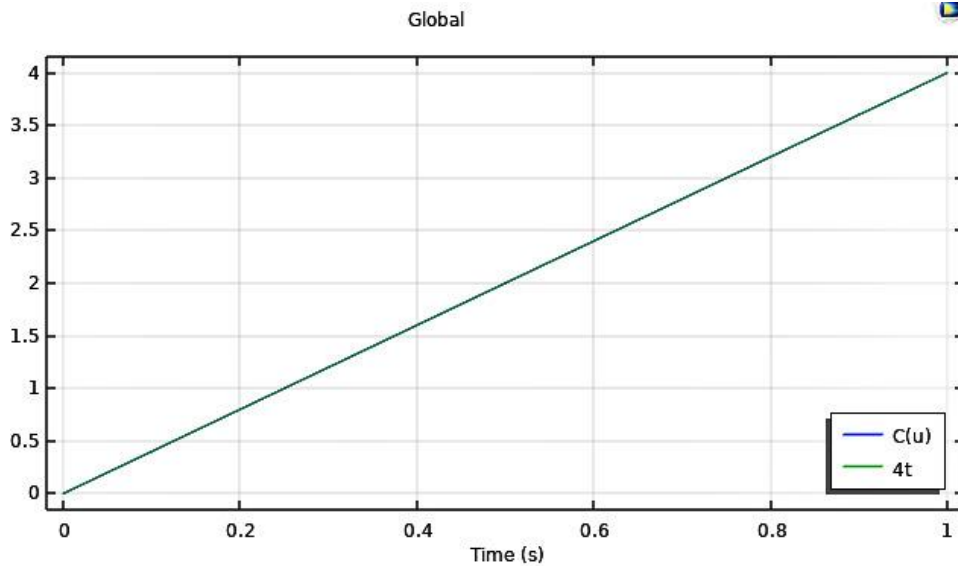

Figure 5. *The graph of 4t and the measured output at x=0.25.*

Conclusion

In this research work, we have considered the Fourier method for solving the one-dimensional parabolic inverse problem with Dirichlet boundary conditions where we first derived an ordinary differential equation for the Fourier coefficients. Then we expressed unknowns in our research problem, source term, and initial data in terms of those Fourier coefficients. Finally, we solved the heat equation on the one-dimension domain with the derived source term and the initial data. Furthermore, we validated that temperature distribution at internal points on the domain (x=0.25,x=0.75) tracked the harmonic and linear temperature distributions, using numerical simulations in COMSOL with the derived control parameters (source term and initial condition).

References

Dehghan, M. (2003). Numerical Solution of One-dimensional Parabolic Inverse Problem. *Journal of Applied Mathematics and Computaion*, pp.333-344.

Grysa, K. (1980). On Certain Inverse Problem of Temperature and Thermal Stress Fields. In *Acta Mechanica* (pp. Volume 36,pp 169-185).

Hussein, M., Lesnic, D., & Ivanchov, M. (2014). Simultaneous determination of time-dependent coefficients in the heat equation. *Computers & Mathematics with Applications*, volume 67;1065-1091.

Ivanchov, M. (1998). Inverse Problem for General One Dimensional Parabolic Equation. *Seberian Matematical Journal, 39*.

Ivanchov, M. (2003). Inverse problems for Parabolic Equations. *VNTL*.

Ivanchov, M. (pp.60-66 2011). One Dimensional Heat Conduction Equation for Inverse Problem. *International Conference of Information Computing and Applications.*

Kanca, F. (2013). Inverse Coefficient Problem of the Parabolic Equation with Periodic Boundary and Integral Overdetermination Condtions. *Abstract and Applied Analysis*, p.7.

M Dehghan. (2006). A Tau Method for One Dimensional Parabolic Inverse Problem Subject to Temperature Over specification. *Journal of Computers and Mathematics, 52*, pp.933-940.

Negero, & Tufa, N. (2014). Fourier Transform Methods for Partial Differentail Equations. *International Journal of Partial Differential Equations and Applications* , 44-57.

Zhang, D., & Guo, Y. (2015). Fourier method for solving the multi-frequency inverse source problem for the Helmholtz equation. pp. volume 31,Number 3.

Conference Paper No: PF-10

The Holt-Winters' method for forecasting water discharge in Attanagalu Oya

M.L.P. Anuruddhika[1*], L.P.N.D. Premarathna[1], K.K.K.R. Perera[1], W.P.T. Hansameenu[1] and V.P.A. Weerasinghe[2]

[1]Department of Mathematics, University of Kelaniya, Sri Lanka
[2]Department of Zoology and Environmental Management, University of Kelaniya, Sri Lanka
prasadianuruddhika@gmail.com*

Abstract

Forecasting river water discharge is significant in developing flood and agriculture management plans. Annual flood events damage properties, agricultural field, and infrastructures, etc. can be observed in Attanagalu Oya catchment area in Sri Lanka. Therefore, the aim of this study is to forecast water discharge rates (m^3/s) at the Dunamale gauging station of Attanagalu Oya using Holt-Winter's method. Holt-Winter's method was chosen because of its' ability to model trend and seasonal fluctuations, less data requirements and simplicity. Time series models were fitted using the Holt-Winter's method to daily water discharge rates for the period of 2015 –2019 and water discharge was forecasted for the year 2020. The accuracy of the fitted time series models was tested using root mean squares error (RMSE) and mean absolute error (MAE) values. Results showed that the additive Holt-Winters' method is more appropriate for future forecasting which gave the minimum RMSE and MAE values. Forecasted results will be useful to identify future flood events in advanced to take necessary actions to mitigate damages.

Keywords

Attanagalu Oya, Flood, Holt Winters' Methods, Time Series Analysis, Water Discharge

Introduction

Time series analysis is widely used in hydrological and meteorological applications. Time series is a series of data points that are measured over a regular time interval and most of the series can be decomposed into three main components, namely trend, seasonality, and random. The trend exists when there is a long term up or down in the data. Seasonal variations are fluctuations in a time series that occur at regular short intervals such as daily, weekly, monthly, quarterly, etc. Seasonality may be caused by various factors such as weather, seasons etc. Random components do not comply with any of the above components and they are uncontrollable and unpredictable. Most of the water discharge rates contain above three components due to climatic variations such as rainfall, temperature and humidity.

Time series forecasting methods predict the future occurrences based on historical data. Even though many time series forecasting methods are available in literature, the choice of the method depends on the nature of the data series. Traditional time series methods like naive method, drift method, simple exponential smoothing method, Holt-Winters' method, and ARIMA method are successfully used to model univariate time series. Real-world data has many seasonality and trends. When forecasting data in such cases, it is required to handle both seasonality and trends. Holt-Winters' method can handle many seasonality and trends using triple exponential smoothing. This method is popular, because it is simple and requires low data-storage. Holt-Winters' method has two variations namely, additive and multiplicative. An appropriate variation is selected

according to the nature of the seasonal and trend component. Additive method is selected when the seasonal variation of the time series is roughly constant over time and multiplicative method is selected when the seasonal variations are changing proportional to the level of the series (Kalekar, 2004).

Literature showed that Holt-Winters' method has been used widely for forecasting in different fields. Szmit, M., and Szmit, A. (2011) have used the Holt-Winters' method to analyze network traffic data. Veiga *et al.* (2014) have used Holt-Winters' method and ARIMA method for forecasting food retail and they have shown that better forecasting was obtained from the Holt-Winters' method. Puah *et al.* (2016) have examined the rainfall patterns using additive Holt-Winters' method. Dantas *et al.* (2017) have also used the Holt-Winters' method for forecasting air transportation demand.

Further, forecasting river water discharge is applicable in various water resource applications, such as flood forecasting, drought management, operation of water supply utilities and building mathematical models for future predictions. According to the literature, Tamagnone *et al.* (2019) have analyzed water discharge of the Sirba river in western Africa to identify the river behavior and developed a flood mitigation procedure. Pelletier and Turcotte (1997) have used water discharge for drought hazard assessment. Trepanier *et al.* (1996) have used the time series analysis of water discharge for controlling the upstream migration of adult salmonids to their spawning areas. Wang *et al.* (2006) have explained a connection between decreasing water discharges, global weather patterns and anthropogenic impacts in the drainage basin using datasets of river water discharge, water consumption and regional precipitation. Albostan and Onoz (2015) have used water discharge pattern to investigate whether all stations of river basin exhibit chaotic behavior. Accordingly, forecasting of water discharge can be applied in different applications in flood and agriculture management activities. Therefore, the study aims to forecast water discharge rates (m³/s) at the Dunamale gauging station of Attanagalu Oya for year 2020 using the Holt-Winters' method.

Methodology

Study area

Attanagalu Oya, which is situated in Gampaha district, was selected for the study. Total catchment area of the Attanagalu Oya is about $727 km^2$ and the basin has an elevation of about 30m MSL (mean sea level) at its highest according to Wijesekara and Perera (2012).

Data collection

Daily water discharge rates (m³/s) for the period of 1ˢᵗ January 2015 – 31ˢᵗ December 2019 at the Dunamale gauging station in Attanagalu Oya were used for the analysis and required data were collected from the Department of Irrigation. Statistical analysis was carried out using R statistical software.

Holt-Winters' method

Augmented Dickey-Fuller (ADF) test was used to determine the stationarity of the time series. This test can handle more complex models than other tests. *adf.test( )* function in R was used to check stationary of the time series and when series is stationary, p-value (out-put of *adf.test( )*) is less than or similar to 0.05. Then, both additive and multiplicative

Holt-Winters' methods were fitted to the time series and predict the daily water discharge rates for the period of 1st January 2020 – 31st December 2020. *HoltWinters()* function in R was used to fit the both models and Table 1 shows the model equations. Holt-Winters' method has three smoothing factors, namely alpha (α) : data smoothing factor, beta (β) : trend smoothing factor and gamma (γ) : seasonal change smoothing factor. Adequacy of the methods were examined by calculating RMSE (Equation 1) and MAE (Equation 2) values for the period of 2015-2019. The best fitted method shows the minimum RMSE and MAE values (Szmit, M., and Szmit, A., 2011).

Table 1. *Model equations of additive and multiplicative Holt-Winters method (Lima, S. et al., 2019)*

Additive Holt-Winters' method	Multiplicative Holt-Winters' method
$S_t = \alpha(X_t - C_{t-L}) + (1 - \alpha)(S_{t-1} + B_{t-1})$	$S_t = \alpha \dfrac{X_t}{C_{t-L}} + (1 - \alpha)(S_{t-1} + B_{t-1})$
$B_t = \beta(S_t - S_{t-1}) + (1 - \beta)B_{t-1}$	$B_t = \beta(S_t - S_{t-1}) + (1 - \beta)B_{t-1}$
$C_t = \gamma(X_t - S_t) + (1 - \gamma)C_{t-L}$	$C_t = \gamma \dfrac{X_t}{S_t} + (1 - \gamma)C_{t-L}$
$F_{t+m} = S_t + mB_t + C_{t-L+h}$	$F_{t+m} = (S_t + mB_t)C_{t-L+h}$

S_t is the smoothed observation at time t, X_t is the observed data at time t, α is the data smoothing factor i.e. $0 \le \alpha \le 1$, β is the trend smoothing factor i.e. $0 \le \beta \le 1$, γ is the seasonal change smoothing factor i.e. $0 \le \gamma \le 1$, B_t is trend factor at time t, C_t is seasonal index at time t, F_{t+m} is the forecast at m periods ahead of time t, L is the length of the seasonality, m is the number of forecast ahead, t is time period and $h = \big((m - 1) mod\ L\big) + 1$.

$$RMSE = \sqrt{\frac{1}{n}\sum_{t=1}^{n} |e_t{}^2|} \qquad\qquad (1)$$

$$MAE = \frac{\sum_{t=1}^{n}|e_t|}{n} \qquad\qquad (2)$$

where e_t is the error at time *t and n* is the number of observations.

Results and Discussion

Time series was prepared using daily water discharge rates (m^3/s) of the period of 1st January 2015 – 31st December 2019. There were no any missing values observed. Figure 1 shows the seasonal and trend components of the water discharge time series and ADF test (p value = 0.01) stated that the time series is stationary. The trend is not specifically increasing or decreasing (Figure 1B) and complex consistent seasonal pattern and two peaks can be observed in each year (Figure 1C).
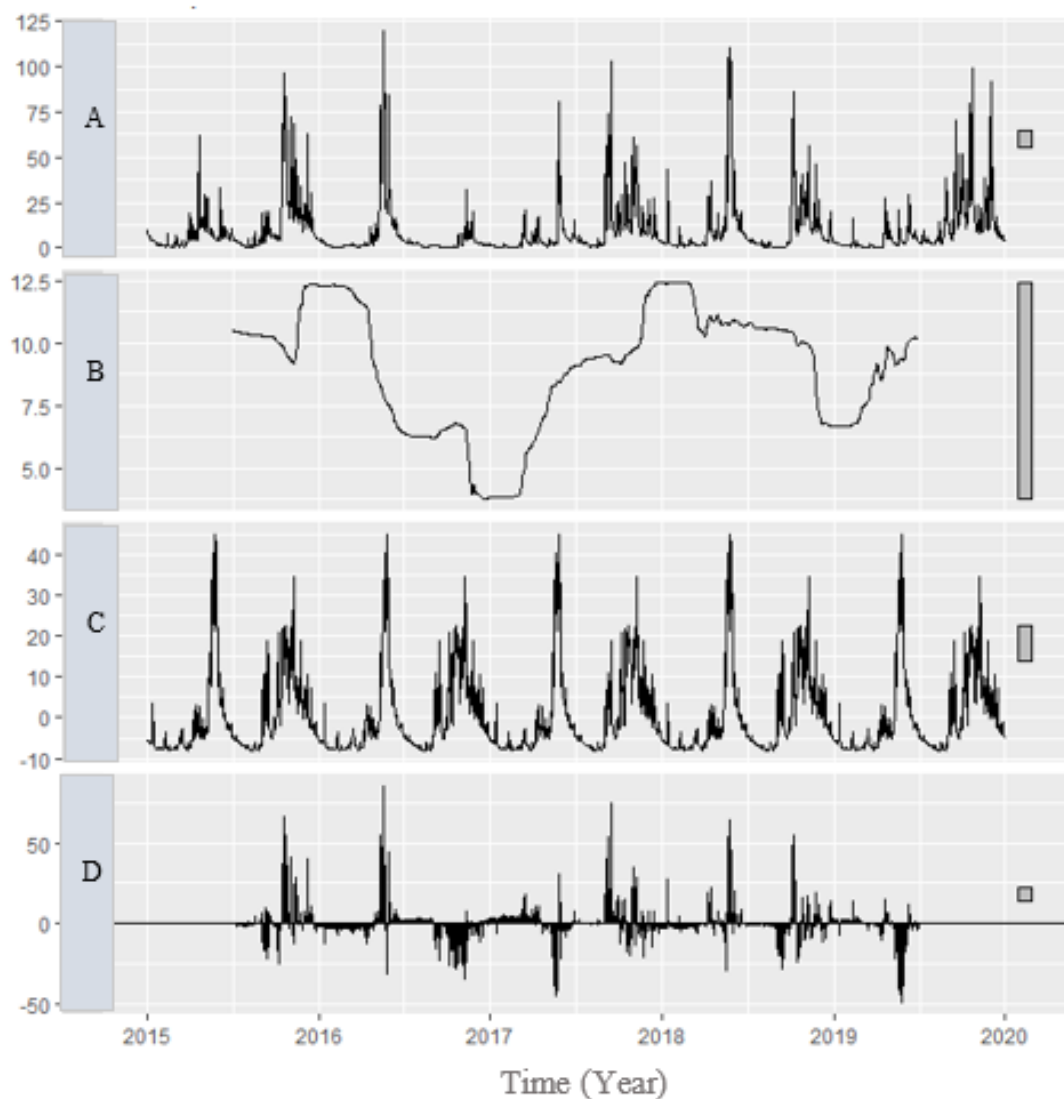
Figure 1. *Decomposition of time series of water discharge for the period of 2015-2019, A: Data, B: Trend, C: Seasonal variation, D: Remainder.*

Table 2. *Error values and smoothing parameters of the additive and multiplicative Holt-Winters' method for the period of 2015-2019.*

Method	RMSE	MAE
Additive method		
α : 0.7665214	11.70029	5.472673
β : 0		
γ : 1		
Multiplicative method		
α : 0.2947401	23.58825	8.165856
β : 0.1034771		
γ : 0.09994384		

Table 2 shows the optimal smoothing parameters (α, β, γ) and error values (RMSE and MAE) of both fitted additive and multiplicative Holt-Winters' method. For additive Holt-Winters' method, $\alpha = 0.7665214$ indicates that the forecasts are more responsive to more recent observations, $\beta = 0$ indicates that the initial trend component is the trend component for all periods and $\gamma = 1$ indicates that seasonality at each time period is estimated as the difference between the corresponding level and trend components at each time period. For multiplicative Holt-Winters' method, all smoothing parameters α, β and γ are closed to 0, that indicates forecasts are more response to older values of each components. The results show that the forecasted errors have approximately constant variance over time, and normally distributed with mean zero for both additive and multiplicative methods. Therefore, both methods are suitable for forecasting water discharge rates. But according to the error values (Table 2), the additive Holt-Winters' method has the minimum RMSE and MAE values, which implies the additive Holt-Winters' method is much better than the multiplicative Holt-Winters' method.

Figure 2 shows the forecasted data of the additive method. Predicted values are shown in blue line and prediction intervals are shown in gray. Two peaks were identified in the forecasted data. The highest water discharge rate was observed as 115.09 m^3 in May 2020. The second period which has increment of water discharge was observed in mid of October, 2020.

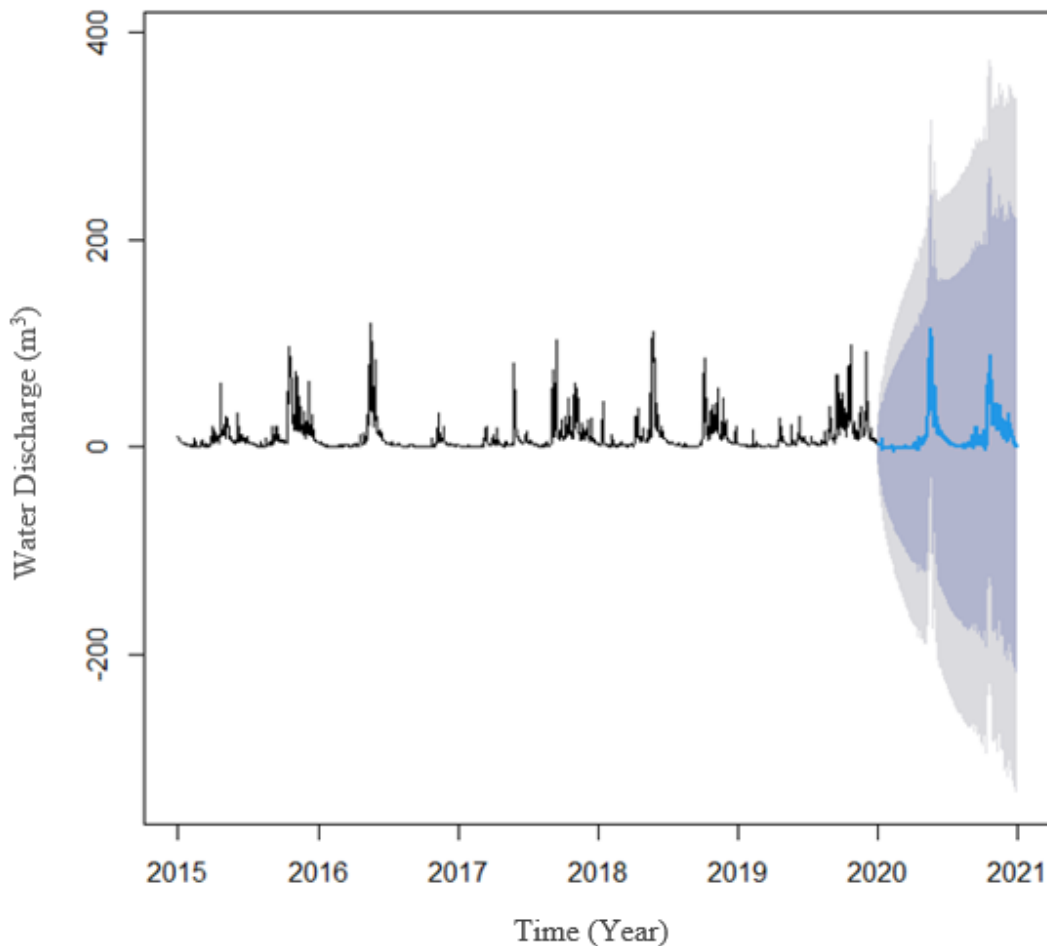***Figure 2.*** *Forecasted water discharge data for 2020 using additive Holt-Winters' method.*

Conclusion

The water discharge is an important factor for identifying flood incidents and flood inundation areas. It is worth to observe variations in water discharge series changes in future to have better agricultural management procedure such as crop selection, identifying suitable harvesting time. Based on the results, the additive Holt-Winters' method is more appropriate than the multiplicative Holt-Winters' method for forecasting water discharge. The forecasted values will be useful to identify the future flood events and to measure the intensity of flood. Moreover, it will also helpful to farmers and residencies of Attanagalu Oya basin to take precautionary steps to mitigate flood damages. Further, this study will be extended to simulate future flood prone areas of Attanagalu Oya basin using Hydrologic Engineering Center's Hydrologic Modelling System (HEC-HMS) and Hydrologic Engineering Center's River Analysis System (HEC-RAS).

Acknowledgment

References

Albostan, A., and Onoz, B. (2015). Implementation of chaotic analysis on river discharge time series. *Energy and Power Engineering,* 7(03), 81. https://doi.org/10.4236/epe.2015.73008.

Charles C. H. (1957). Forecasting seasonals and trends by exponentially weighted moving averages. *International Journal of Forecasting.* 20(1), 5-10. https://doi.org/10.1016/j.ijforecast.2003.09.015.

Chatfield, C. (1978). The Holt-winters forecasting procedure. *Journal of the Royal Statistical Society: Series C (Applied Statistics),* 27(3), 264-279. https://doi.org/10.2307/2347162.

Dantas, T. M., Oliveira, F. L. C., & Repolho, H. M. V. (2017). Air transportation demand forecast through Bagging Holt Winters methods. *Journal of Air Transport Management*, 59, 116-123. https://doi.org/10.1016/j.jairtraman.2016.12.006.

Dikkubura, H.K.S., and Weerasinghe, V.P.A. (2016). Rainfall-Runoff-Inundation (RRI) model for flood analysis in Attanagalu Oya basin, Sri Lanka. *International Symposium of ICT for Sustainable Development.*

Kalekar, P.S. (2004). Time series forecasting using holt-winters exponential smoothing. *Kanwal Rekhi school of information Technology*, 4329008(13),1-13. https://doi.org/10.1063/1.5137999.

Lima, S., Gonçalves, A. M., & Costa, M. (2019). Time series forecasting using Holt-Winters exponential smoothing: An application to economic data. *In AIP Conference Proceedings. AIP Publishing LLC.* 2186(1), 090003.

Pelletier, J.D., and Turcotte, D.L., (1997). Long-range persistence in climatological and hydrological time series: analysis, modeling and application to drought hazard assessment. *Journal of hydrology,* 203(1-4), 198-208. https://doi.org/10.1016/S0022-1694(97)00102-9.

Puah, Y. J., Huang, Y. F., Chua, K. C., & Lee, T. S. (2016). River catchment rainfall series analysis using additive Holt–Winters method. *Journal of Earth System Science*, 125(2), 269-283. http://dx.doi.org/10.1007/s12040-016-0661-6

Pushpakumara, T.D.C., and Isuru, T.V.A. (2018). Flood modeling and analyzing of Attanagalu Oya river basin using geographic information system. *International Journal of Advanced Remote Sensing and GIS*, 7(1), 2712-2718. https://doi.org/10.23953/cloud.ijarsg.366.

Szmit, M., and Szmit, A. (2011). Use of holt-winters method in the analysis of network traffic: case study. *International Conference on Computer Networks*, 224-231. http://dx.doi.org/10.1007/978-3-642-21771-5_24.

Tamagnone, P., Massazza, G., Pezzoli, A., and Rosso, M. (2019). Hydrology of the Sirba river: Updating and analysis of discharge time series. *Water*, 11(1),156. https://doi.org/10.3390/w11010156.

Thushari, N.H., and Manawadu, L. (2008). Flood monitoring in Gampaha district using SAR data as a case study in the lower basin in Attanagalu Oya (river).

Trepanier, S., Rodriguez, M.A., and Magnan, P. (1996). Spawning migrations in landlocked Atlantic salmon: time series modelling of river discharge and water temperature effects. *Journal of Fish Biology*, 925-936. https://doi.org/10.1111/j.1095-8649.1996.tb01487.x.

Veiga, C.P.D., Veiga, C.R.P.D, and Catapan, A.,Tortato, U., and Silva, W.V.D. (2014). Demand forecasting in food retail: A comparison between the Holt-Winters and ARIMA models. *WSEAS transactions on business and economics*, 11(1), 608-614. https://doi.org/10.17559/TV-20160615204011.

Wang, H., Yang, Z., Saito, Y., Liu, J.P., and Sun. X. (2006). Interannual and seasonal variation of the Huanghe (Yellow River) water discharge over the past 50 years: connections to impacts from ENSO events and dams. *Global and Planetary Change*, 50(3-4), 212-225. https://doi.org/10.1016/j.gloplacha.2006.01.005.

Wijesekara, N.T.S., and Perera, L.R. H. (2012). Key issues of data and data checking for hydrological analysis- case study of rainfall data in Attanagalu Oya basin of Sri Lanka. *Engineer Journal of the Institution of Engineer, Sri Lanka*,45(2). http://dx.doi.org/10.4038/engineer.v45i2.6936.

Winters, Peter R. (1960) Forecasting sales by exponentially weighted moving averages. *Management science*, 6(3), 324–342. https://doi.org/10.1287/mnsc.6.3.324.

Conference Paper No: PF-11

Time series modeling and forecasting of total primary energy consumption in Sri Lanka

P.A.D.S.P. Caldera[*], N.N.D. Malshika, S.H.A.S. Nikapitiya, U.S.C.B. Udugedara and N.V. Chandrasekara

[1]Department of Statistics and Computer Science, University of Kelaniya, Sri Lanka
sandunicaldera97@gmail.com*

Abstract

Primary energy is the energy that is harvested directly from natural resources. Forecasting total primary energy consumption in Sri Lanka is significant as primary energy consumption worldwide is expected to continue increasing. This study aimed to model and forecast total primary energy consumption in Sri Lanka, which has not yet been analysed using Time Series Analysis. For this purpose, the annual data of total primary energy consumption in Sri Lanka from 1960 to 2019 in terawatt-hours was extracted from the world wide web and analysed with Auto-Regressive Integrated Moving-Average (ARIMA) model. The stationary of the series was tested using the Kwiatkowski–Phillips–Schmidt–Shin (KPSS) test, Phillips-Perron (PP) test, and Augmented Dickey-Fuller (ADF) test. The study revealed the ARIMA(4,2,1) model as a best-fitting model, which gave the minimum value of Akaike Information Criterion (AIC). Total primary energy consumption from 2008 to 2019 was forecasted using ARIMA(4,2,1) model as it satisfied the model diagnostics, which are ARCH test, autocorrelation function, and normality of residuals. With Mean Absolute Error (MAE) of 5.0283 and Root Mean Squared Error (RMSE) of 5.9216, the results illustrate that ARIMA(4,2,1) model captures the trend in total primary energy consumption accurately. Based on the results, the study suggests ARIMA(4,2,1) is more convenient in determining the trends and the patterns of the future in total primary energy consumption in Sri Lanka.

Keywords

ARIMA model, Energy consumption, Forecasting, Sri Lanka, Time series modeling

Introduction

Primary energy consumption is that the direct use or supply at the source of energy that has not been converted or transformed. Energy consumption in the world has been increasing over the years, that has been mainly due to the ever-increasing world population and the need to meet the energy needs of industries that are ever-expanding their capacity. Sri Lanka's primary energy supply mostly comes from oil and coal. The country imports crude oil and refined products with Liquefied Petroleum Gas (LPG) and coal. These global resources in Sri Lanka are used mainly for lighting, cooking in households, rail, road, air, and sea in transports, boilers in power generation. Forecasting is the process of making predictions of the future by gathering and analysing the past and the current data. Time series modeling is used widely in the process of forecasting (Fernando et al., 2017; Ozturk & Ozturk, 2018; Tian et al., 2019). Analysing and forecasting how the total primary energy consumption in Sri Lanka changes over time is very important as the government holds a strong interest in lowering energy usage. Total primary energy consumption in Sri Lanka has not yet been analysed and forecasted using time series modeling. Observing the past primary energy consumption patterns in Sri Lanka, the main goal of this study is to analyse and forecast it using Time Series Analysis.

This is further elaborated by identifying and analysing trends and patterns of the series, determining the relevant candidate models, and selecting the best fit time series model to forecast total primary energy consumption in Sri Lanka.

In 2012, two researchers Yasmeen and Sharif analyzed the monthly electricity consumption in Pakistan from January 1990 to December 2011 and obtained the forecast. The study concludes that ARIMA(3,1,2) model is the most appropriate model for forecasting the electricity consumption of Pakistan. Their results revealed that, electricity consumption is continuously increasing over time, and they have suggested that the government of Pakistan must take effective steps to increase the electricity production through different energy sources to restore the economic status of the country by meeting the demand for electricity in the country.

A study on forecasting hydroelectricity consumption in Pakistan based on the historical data of the past 53 years using Auto-Regressive Integrated Moving-Average (ARIMA) modeling was done by Jamil in 2020. Up to the year 2030, the hydroelectricity consumption was predicted, based on the developed forecasting equation. To validate the reliability of the forecasted data, the results were compared with the actual values and the results showed a good fit with minimum error.

Peiris and Kumarasinghe have presented a forecasting study of total annual tea production in Sri Lanka and major tea growing areas. They have fitted time series models by the Box and Jenkins ARIMA model approach, tested for stationary by the Augmented Dickey-Fuller test, and applied differencing techniques to make the series stationary. Model diagnostics were performed using the Ljung Box test and autocorrelation function of residuals. The ARIMA(2,2,1) model was identified as the most appropriate model for the total annual tea production. Their study concluded that, the total tea production increases in Sri Lanka by 2020, compared to the average production from 2011 to 2015.

This article is organized as follows: In the introduction, the background, objective, and significance of this study are specified, and a brief literature review is included; the methods used in this study are introduced in the methodology section; in Results and Discussion, total primary energy consumption in Sri Lanka is analyzed, predicted with ARIMA model and the results are compared; finally, the conclusions of this study are made in the Conclusion. References concludes the article.

Methodology

Initially, the dataset was divided into two subsets, as one contains the latest 20% data in the dataset and the other contains the remaining 80%. Next, an exploratory data analysis was performed for the sub dataset contains 80% data of total primary energy consumption in Sri Lanka, and forecasting was done on the latest 20%, using the selected model.
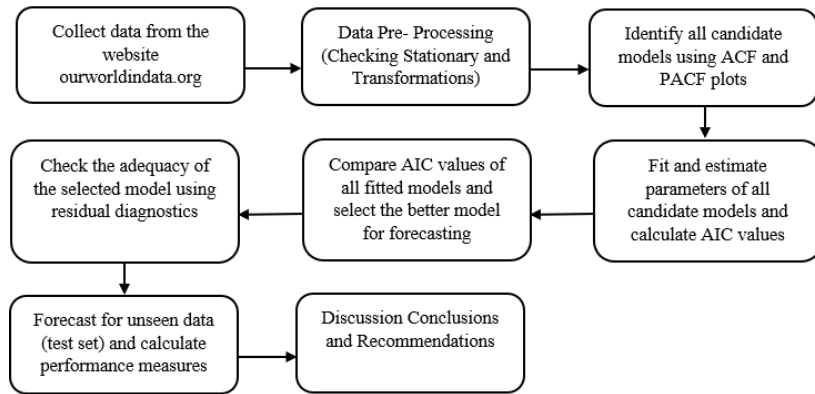
A. Step by step Methodology

Figure 1. *Step by step procedure followed in the study.*

In this study, time-series analysis was used to model the time-dependent structure of total primary energy consumption in Sri Lanka. Figure 1 illustrates the step-by-step methodology employed in the study.

B. Theories

Time series: A time series is a set of observations x_t, each one being recorded at a specific time t.

The three statistical tests used to assess the stationarity of the time series, namely, Kwiatkowski–Phillips–Schmidt–Shin (KPSS) test, Phillips-Perron (PP) test and Augmented Dickey-Fuller (ADF) test, have the following null hypothesis and alternative hypothesis.

ADF test   - H_0: The series is not stationary. H_1: The series is stationary.

PP test   - H_0: The series is not stationary. H_1: The series is stationary.

KPSS test   - H_0: The series is stationary. H_1: The series is not stationary.

In both ADF and PP tests, if the p value is less than 0.05, then H_0 will be rejected. In KPSS test, if the Test Statistic < Critical value at 5% level, then H_0 will be rejected.

Moving Average process of order q, MA(q) : $y_t = \mu + \varepsilon_t - \theta_1 \varepsilon_{t-1} - \cdots - \theta_q \varepsilon_{t-q}$ (1)

Auto Regressive process of order p, AR(p) : $y_t = \delta + \emptyset_1 y_{t-1} + \cdots + \emptyset_p y_{t-p} + \varepsilon_t$ (2)

where ε_t is white noise.

A mixed Autoregressive/ Moving Average process containing p AR terms and q MA terms is said to be an ARMA process of order (p, q), which is given by,

$$y_t = \delta + \emptyset_1 y_{t-1} + \cdots + \emptyset_p y_{t-p} + \varepsilon_t - \theta_1 \varepsilon_{t-1} - \cdots - \theta_q \varepsilon_{t-q} \qquad (3)$$

ARIMA Model is one of the most successful time series forecasting techniques. According to Box-Jenkins (1976), a non-seasonal ARIMA model is denoted by ARIMA (p, d, q). This model is a combination of Auto-Regressive (AR) and Moving Average (MA), where the number of AR terms, the number of non-seasonal differences needed for

stationarity, and the number of MA terms are denoted by p, d, and q, respectively. The ARIMA is the generalization form of the ARMA approach.

The residual diagnostics: i.e., the heteroscedasticity, autocorrelation, and the normality of residuals, are tested using the ARCH test, Ljung–Box Q test, and the Jarque-Bera test, respectively. Those residual diagnostics have the following null and alternative hypotheses regarding the residuals.

Heteroscedasticity - H_0: There is no heteroscedasticity. H_1: There is heteroscedasticity.

Autocorrelation   - H_0: There is no autocorrelation. H_1: There is autocorrelation.

Normality   - H_0: Normally distributed. H_1: Not normally distributed.

For all three tests, if the p value is less than 0.05 (at 5% level of significance) then H_0 will be rejected.

Results and Discussion
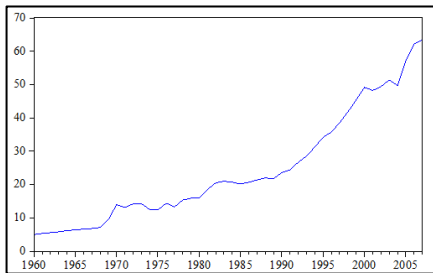
Figure 2. *Time Series plot of total primary energy consumption in Sri Lanka.*

This section illustrates the results of the analysis and the discussion. The time series plot which was generated with observations from 1960 to 2007 illustrates in Figure 2 and it exhibits an upward trend. It seems that the mean function of the series, $E[X_t]$ increases with time. Therefore, it can be concluded that the series is not stationary. Then stationary conditions of primary energy consumption were measured using three Unit Root tests. The tests with their estimated results are presented in Table 1.

Table 1. *The results of Stationary tests.*

Total primary energy consumption	Statistical test		Stationarity at 5% level of significance
Level data	ADF PP KPSS	p-value: 1.0000 p-value: 1.0000 Test statistic: 0.84803 Critical value at 5%: 0.463	Not stationary
First differenced data	ADF PP KPSS	p-value: 0.0000 p-value: 0.0000 Test statistic: 0.60337 Critical value at 5%: 0.463	Not stationary
Second differenced data	ADF PP KPSS	p-value: 0.0001 p-value: 0.0000 Test statistic: 0.03728 Critical value at 5%: 0.463	Stationary

All three tests imply that the original series of total primary energy consumption in Sri Lanka is not stationary at a 0.05 level of significance. Thus, to make the series stationary by reducing the trend component, the first differenced data were considered. According to the results shown in Table 1, the first differenced data of primary energy consumption were not stationary. Therefore, the second differenced data were considered.
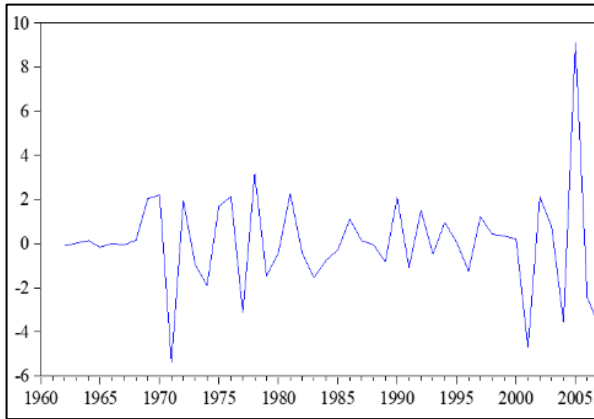
Figure 3. *Time Series plot of second differenced data of the series.*
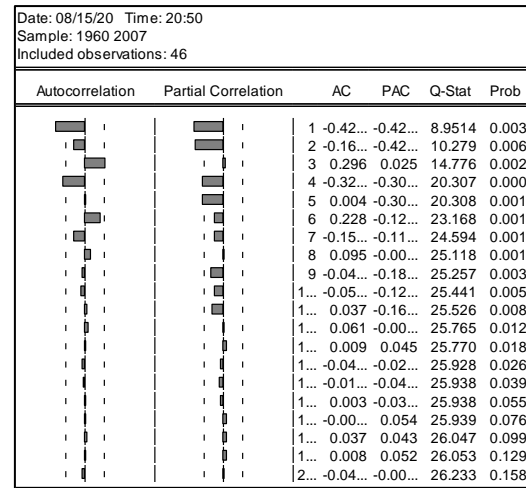
Figure 4. *Correlogram of the stationary series.*

As exhibits in Figure 3, the series of the second differenced data fluctuate around a horizontal line. It indicates, the series seems to be stationary. By the results in Table 1, all three tests imply that the second differenced data of Primary energy consumption were stationary under the 0.05 level of significance.

Figure 4 shows the ACF and PACF plots of the stationary series. ACF cuts off at lags 1, 3, 4 and PACF cuts off at lags 1, 2, 4, 5. According to the cut-off lags, MA, AR, and ARIMA candidate models were suggested and fitted. Table 2 contains the candidate models with their respective AIC values.

Table 2. *Candidate models with AIC values.*

Model	AIC	Model	AIC
AR(1)	4.4147	ARIMA(2,2,1)	4.181
AR(2)	4.1751	ARIMA(2,2,3)	4.0492
AR(4)	4.1529	ARIMA(2,2,4)	4.0624
AR(5)	4.0689	**ARIMA(4,2,1)**	**3.9975**
MA(1)	4.0277	ARIMA(4,2,3)	4.0705
MA(3)	4.0914	ARIMA(4,2,4)	4.1144
MA(4)	4.114	ARIMA(5,2,1)	4.1414
ARIMA(1,2,1)	4.0705	ARIMA(5,2,3)	4.181
ARIMA(1,2,3)	4.1144	ARIMA(5,2,4)	4.0492
ARIMA(1,2,4)	4.1414		

```
Dependent Variable: D(PRIMARY_ENERGY_CONSUMPTI,2)
Method: ARMA Maximum Likelihood (OPG - BHHH)
Date: 08/16/20  Time: 10:05
Sample: 1962 2007
Included observations: 46
Failure to improve objective (non-zero gradients) after 427 iterations
Coefficient covariance computed using outer product of gradients
```

Variable	Coefficient	Std. Error	t-Statistic	Prob.
C	0.055729	0.014413	3.866622	0.0004
AR(1)	0.085938	0.127494	0.674055	0.5043
AR(2)	-0.067162	0.196886	-0.341121	0.7348
AR(3)	0.234006	0.177363	1.319363	0.1947
AR(4)	-0.470917	0.187446	-2.512279	0.0162
MA(1)	-0.999989	3077.206	-0.000325	0.9997
SIGMASQ	2.091331	468.8527	0.004461	0.9965

R-squared	0.601353	Mean dependent var	0.019566
Adjusted R-squared	0.540022	S.D. dependent var	2.315739
S.E. of regression	1.570572	Akaike info criterion	3.997485
Sum squared resid	96.20121	Schwarz criterion	4.275756
Log likelihood	-84.94215	Hannan-Quinn criter.	4.101727
F-statistic	9.805142	Durbin-Watson stat	2.029529
Prob(F-statistic)	0.000001		

Inverted AR Roots	.59-.51i	.59+.51i	-.55+.68i	-.55-.68i
Inverted MA Roots	1.00		

Figure 5. *ARIMA(4,2,1) model.*

According to Table 2, ARIMA(4,2,1) model was chosen as a better model to forecast the series of total primary energy consumption of Sri Lanka, which exhibits a minimum AIC of 3.9975 among all candidate models.

In the fitted ARIMA(4,2,1) model, the coefficients of AR(1), AR(2), AR(3), MA(1) were insignificant. Thus, corresponding model equation is represented in the Equation 4:

$$y_t = 0.0557 - 0.4709y_{t-4} + \varepsilon_t \qquad (4)$$

Figure 5 illustrates the coefficients, probabilities, and standard errors of parameters of the ARIMA(4,2,1) model. As the next phase of the study, the adequacy of the ARIMA(4,2,1) model was checked as follows.

Table 3. *Results of residual diagnostic tests.*

Tests	ARCH test: (Heteroskedasticity)	Ljung–Box Q test: (Autocorrelation)	Jarque-Bera test: (Normality)
p-value	0.2150	All the p-values > 0.05	0.2582

As shown in Table 3, since the p-values for each test were greater than 0.05, study concluded that homoscedasticity in the residuals and the residuals are independently, normally distributed. Hence, all three assumptions were satisfied by the model ARIMA(4,2,1) and the model was used for forecasting total primary energy consumption in Sri Lanka from 2008 to 2019.
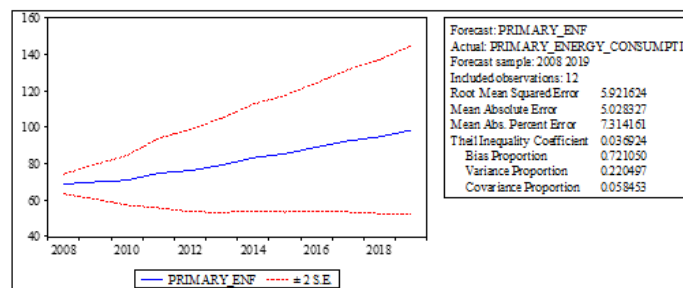

Figure 6. *Forecasted data from 2008 to 2019 using ARIMA(4,2,1) model.*

Figure 6 exhibits that Mean Absolute Error (MAE) is 5.0283 and Root Mean Squared Error (RMSE) is 5.9216 of the forecasted series using ARIMA(4,2,1) model. Since RMSE and MAE were considerably low, ARIMA(4,2,1) model could be used for forecasting total primary energy consumption in Sri Lanka.
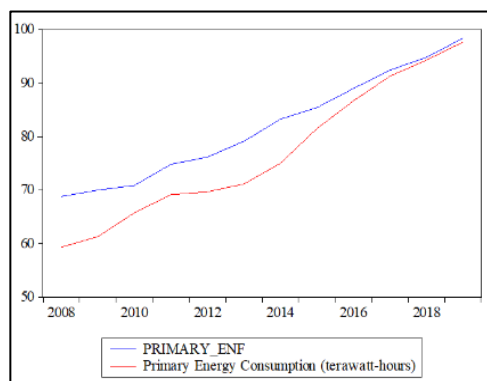
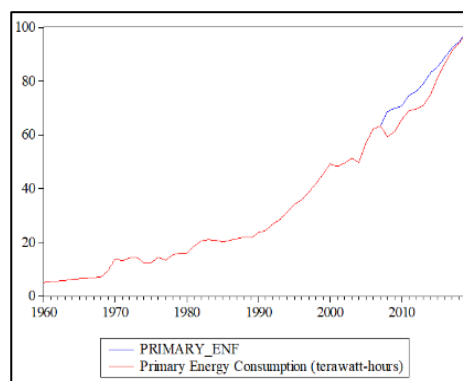**Figure 7.** *Actual values vs forecasted values from 2008-2019.*

Figure 8. *Total primary energy consumption in Sri Lanka from 1960 to 2019 with forecasted series from 2008 to 2019.*

As displayed in Figure 7, the differences between values of actual and forecasted data from 2008 to 2019 were considerably low. Figure 8 demonstrates the trend of the fitted values is generally consistent with that of the actual values. These findings suggested that ARIMA(4,2,1) model can capture the future movements of total primary energy consumption in Sri Lanka. Hence, the forecast using the model ARIMA(4,2,1) can help the decision-makers to know the volume and trend of the future primary energy consumption to better schedule and plan the operations of the supply system. Since this study is a univariate time series forecasting, it can further be improved by applying multivariate time series models.

Conclusion

This study takes up the modeling and forecasting of total primary energy consumption in Sri Lanka using Time Series Analysis. After applying the tests of stationary and the data was stationary at the second difference. Subsequently, the suggested models are identified using cut-off lags of ACF and PACF plots and fitted. Using minimum AIC criteria ARIMA(4,2,1) model was selected as a better model among all the candidate models. Since all the performed residual diagnostics were satisfied by the ARIMA(4,2,1) model, total primary energy consumption in Sri Lanka from 2008-2019 is forecasted using it. The forecasted series captures the increasing trend and patterns of the actual series more accurately with considerably low forecasted errors: an MAE of 5.0283 and an RMSE of 5.9216. Thus, the study concludes that ARIMA(4,2,1) model is the most appropriate model for forecasting total primary energy consumption in Sri Lanka. As the forecasted values show an increasing trend of total primary energy consumption in Sri Lanka, it suggests that the government must go for alternative energy sources that will not run out instead of using non-renewable primary energy resources to meet the demand for primary energy in the country.

References

Fernando, J. L. L. S., Gunawardana, J. R. N. A., Perera, K. A. I. T., Perera, M. L. D. M., Shashikala, M. A. G., Jayasundara, D. D. M., & Rathnayaka, R. M. (2017). Time Series Modelling approach for forecasting Electricity Demand in Sri Lanka.

Montgomery, D. C., Jennings, C. L., & Kulahci, M. (2015). Introduction to time series analysis and forecasting. John Wiley & Sons.

Ozturk, S., & Ozturk, F. (2018). Forecasting energy consumption of Turkey by Arima model. Journal of Asian Scientific Research, 8(2), 52.

Rahman, A., & Ahmar, A. S. (2017, September). Forecasting of primary energy consumption data in the United States: A comparison between ARIMA and Holter-Winters models. In AIP Conference Proceedings (Vol. 1885, No. 1, p. 020163). AIP Publishing LLC.

Ritchie, H., & Roser, M. (2020). Energy. Published online at OurWorldInData. org. https://ourworldindata.org/energy.

Tian, C. W., Wang, H., & Luo, X. M. (2019). Time-series modelling and forecasting of hand, foot and mouth disease cases in China from 2008 to 2018. Epidemiology & Infection, 147.

Conference Paper No: SF-03

Human in the loop design for intelligent interactive systems: A systematic review

N. Arambepola[*] and L. Munasinghe

Software Engineering Teaching Unit, Faculty of Science, University of Kelaniya, Sri Lanka
nimasha_2019@kln.ac.lk*

Abstract

It is undeniable that modern computers are incredibly fast and accurate. However, computers cannot 'think' (act intelligently) as humans unless it is trained to learn from the past knowledge. Despite their intelligence, humans are comparatively slow in computational tasks. However, the combination of the computational capacity of computers and human intelligence could produce powerful systems beyond the imagination. This concept is called Human-in-the-Loop (HITL) where both human and machine intelligence support the creation of Machine Learning (ML) models. HITL design is an emerging technology which is used in many domains such as autonomous vehicle technology, health systems and interactive system implementations. In this research, we systematically reviewed past research of HITL systems with the objectives of identifying key benefits and limitations of the HITL design. This systematic review was conducted by analyzing 68 research papers published in top-ranked journals and conferences during the past decade. Moreover, the papers were selected using keyword-based searching and references of the most cited HITL research papers. The PRISMA model was used to exclude irrelevant papers, and keyword-based clustering was used to identify the frequent keywords in the selected papers. Although the HITL design often improves the performance of intelligent interactive systems, there are certain drawbacks of this concept when compared to fully manual or fully automated systems such as making decisions with emotional bias and being unable to take actions when demanded. Thus, we comprehensively discuss the approaches proposed by the recent researchers to overcome some of the issues of the existing HITL designs.

Keywords

Human-in-the-loop design, Human intelligence, Intelligent interactive systems, Machine learning, Keyword-based clustering

Introduction

This is the era of Artificial Intelligence (AI) which is the fastest-growing research domain that aims to produce smart solutions to real-world problems. Automated systems such as autonomous cars and intelligent robots are becoming common and essential technologies in day-to-day life. However, some of the recent researchers have investigated the effectiveness of the AI-based systems which includes a part for humans instead of completely automating a system by removing human involvement from the task (Bhardwaj et al., 2014). This concept is called Human-in-the-Loop (HITL) and the main objective of this approach is to provide efficient, intelligent automation for system improvements through human feedback (Holzinger, Valdez and Ziefle, 2016). Here, humans are directly involved in the training, tuning and testing of the ML algorithms. When using a completely automated ML model, there is a certain possibility of having inaccurate results. In HITL design, the general human population can contribute to correct the inaccuracies in machine predictions. HITL systems use supervised ML and active learning together to produce the output. Here, supervised ML is used for the future

predictions through training the algorithms using labelled data. Active learning is used to make the algorithm more accurate and efficient by managing the data (Holzinger, 2016).

Novel technologies have been introduced by investigating the possibility of substituting ML algorithms and optimizing system performance through human experience. For instance, interactive ML techniques have been introduced with novel concepts to improve existing models in different domains. The use of human cognition in the random AI design process is the key benefit to produce outcome design according to human's preferences. It is a common truth that today, people do not have time for choosing their essential daily items. Therefore, AI-based recommender systems have been introduced to make their selections more efficient and easier (Sun et al., 2019). They are commonly used in different domains and fields such as hotels and restaurants, health, fashion, movies, news, and online courses to assist users to discover products with less effort and time. For example, the applicability of the HITL concept for visual analytic tasks was studied by recognizing existing work processes and fitting analytics according to the user feedback (Endert et al., 2014). Nevertheless, most of the existing recommender systems are fully automated systems. There is a huge potential to improve these systems in a more effective way through user-centric design by injecting a human, meaning that a particular domain expert into the system. Thus, we set the main objectives of this literature review as:

1. To identify different domains where HITL design concept can be utilized effectively.
2. To describe how HITL design concept applies in ML based interactive systems.
3. To determine the key benefits and limitations of using HITL for AI-based systems.
4. To explain the approaches that has been proposed to enhance HITL design concept in AI-based systems.

The rest of the paper is organized as follows. In the following section, we describe the flow of our review process with the methodology used. Then, we present the results of our findings with the analysis and the discussion. Finally, we conclude this paper with the future directions of the research.

Methodology

The review design of this work has three main stages. In the first stage, we retrieved research papers and articles from different sources. In the second stage, the contents of each paper were analyzed based on the extracted keywords. Finally, the results were presented as a comprehensive summary.

The most appropriate research papers for this comprehensive literature review were chosen using the Preferred Reporting Items for Systematic Reviews and Meta-Analyses (PRISMA) model as shown in figure 1. Here, we collected a total number of 68 research papers and articles related to the fields of intelligent interactive systems, AI and ML applications, and recommender systems that used the HITL design concept. Papers were collected through context keyword searching and choosing the most relevant research papers using the reference section of selected papers that have published in top-ranked journals and conferences during the past decade. The ResearchGate and IEEE Xplore are the main sources used but not limited, to collect research papers. For example, we retrieved papers from Google Scholar. Among the selected papers, 4 duplicate papers and

10 irrelevant research papers were excluded during the identification and screening stages. The remaining 54 papers were eligible for the review but had to exclude 2 papers due to the fact that they are out of the research scope. Then the keyword-based clustering which is an unsupervised ML technique was applied for further analysis. There were five main clusters, after grouping the extracted keywords that are collected from the abstracts of the selected papers and articles. The identified main keywords are machine learning, interactive design, recommender systems, design concepts, Human-in-the-Loop and artificial intelligence.
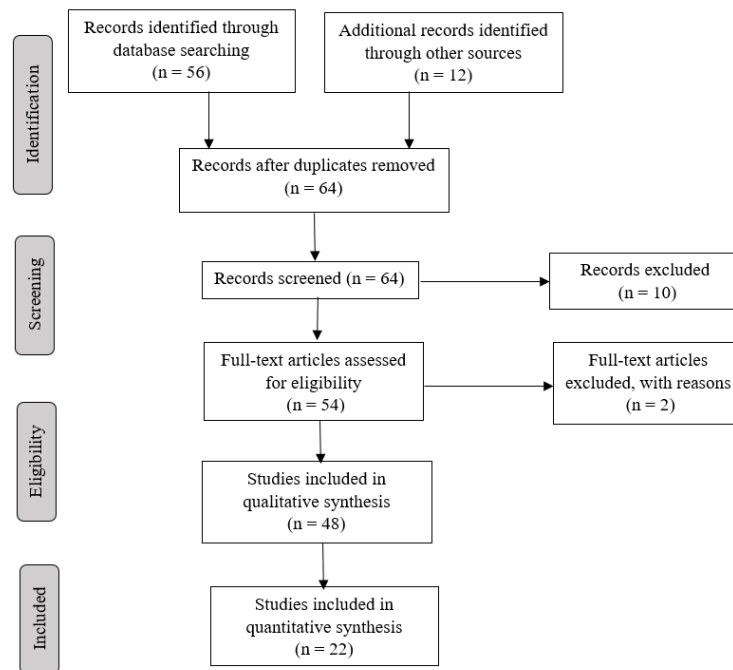
Figure 1. The approach used to select research papers.

In the overall review, the HITL design concept which can be used in different software systems was systematically analyzed by examining findings, advantages, limitations of each individual study to provide the knowledge comparatively. The different domains gain significant advantages from using this HITL design concept. Yet, there are certain limitations pertain to this concept, and researchers in the past decade have presented different views to overcome these limitations. Those points were comparatively discussed, and the results were summarized in the next section.

Results and Discussion

According to the literature review, the areas in table 1 are widely used HITL concept. Decision making is very critical in the Healthcare field. Therefore, completely automated systems can be a risk when communicating with patients and their sensitive data. Thus, the Doctor-in-the-loop concept comes into play, and doctors work as expert humans in the domain.

***Table 1.** Different areas that use HITL design concept*

Area	Papers from the literature
Health	(Holzinger et al. 2016), (McKinney et al.)
Recommender systems	(Bhardwaj et al. 2014), (Sun et al. 2019), (Holzinger et al. 2016), (Goecks 2020)
Interactive systems	(Emmanouilidis et al. 2019), (Wang et al. 2019a), (Zanzotto 2019), (Wang et al. 2019b), (Goecks 2020), (Endert et al. 2014)

In ML, the HITL design concept comes into play in different scenarios. Following are the identified main cases:

- When there is a lack of data available to train and test the ML model at present
  - In these cases, humans can be used to collect a sufficient amount of data.
  - Humans can make much better judgments in the early stages.
- When there are class imbalances
  - Humans can resolve class imbalance problem if there is any and retrain the ML model.
- When the cost of errors is very high in an ML algorithm.

The key benefits that can be obtained by applying the HITL design concept into intelligent interactive systems can be categorized as shown in table 2. It reveals the importance of the HITL concept when designing sophisticated automated systems, especially for the systems which must frequently interact with general users such as multi-agent systems (Dorri et al., 2018). An example for a successful HITL application is Google's search engine which designed using HITL learning. Thus, it provides better service with the access of more users (Johnson, n.d.). Yet, past researchers have proven that the HITL approach is more applicable in the medical domain because medical experts have a high ability in predicting patients' status where medical datasets and ML system along cannot be achieved (Maadi et al., 2021).

***Table 2.** Key benefits of HITL design concept*

Benefits	Description/ Use case
Avoiding bias	Most of the ML models are biased because of the biased data. Biased data can be identified as early as possible having a person-in-the-loop.
Increase the amount of rare and limited data	ML models require a large amount of data sets to train and test models accurately. When there is limited amount of data in some areas, humans can be used to collect more data. For example, Facebook keeps HITL for monitoring users and tracking their actions.
Improve efficiency in systems	Recent research has shown that HITL design concept performs better for some cases. For example, it saves time and results are more accurate than AI or human doctors on their own.

Increase safety of humans	Improve the safety through autonomous vehicles to have lesser accidents. In there, professional gamers can be used to simulate actual driving conditions. In addition, humans use to ensure the safety, when manufacturing critical component for field which required high safety level such as aircraft.
Create employment opportunities	Even though the advancement of AI technologies causes the elimination of current jobs, it also generates new jobs, especially in labelling data for ML. Furthermore, it will increase the accuracy of algorithms (Grønsund & Aanestad, 2020).
Subject expert includes in the loop	When a subject expert is generating and preparing data, the system provides more accurate and appropriate results. For example, Doctor-in-the-loop is a commonly use novel paradigm (Holzinger et al. 2016).
Transparent decision making	When replacing human with a robot to provide services for public, it is better to implement the system with HITL design so that people are more familiar with the system rather than a completely automated AI system.

Despites its advantages, it is worth to examine the limitations of this approach. For example, human emotional decisions make bad choices. In addition, human involvement causes to invite human mistakes, and this is considered a form of data poisoning (Carley & Price, 2021). For example, common human errors such as mislabeling critical data which are used to train ML algorithms would incorrectly produce outputs. It decreases the performance of algorithms. A few of the other limitations are what it can be slow down the AI systems because of taking too much time to make decisions and failed to take immediate actions when needed. Even though HITL design improves the efficiency when compared with fully manual systems, in some cases it can be slow down the system when compared with fully automated systems. The explainable ML model is another concern that still does not has a clear definition (Lipton, 2018). In there, the HITL ML concept is used for making decisions mainly in two ways. One way is, making decisions through a specialized professional in the domain (Zanzotto, 2019). For example, a domain specialist doctor can work as an adviser for the Doctor-in-the-loop system in the medical field (Holzinger, Valdez and Ziefle, 2016). On the other hand, machines make decisions based on the knowledge extracted from data. In there, data are produced by people who are not specialized knowledgeable workers. In both cases, these AI-based systems keep the HITL design concept in a direct or indirect way.

Nevertheless, Zanzotto has identified a huge disadvantage of this approach, and its main victim is the knowledgeable person who works as the adviser for those AI systems (Zanzotto, 2019). The concerns are that the stolen knowledge will produce never-ending revenue, not for the real owner of the knowledge but the company it owns. Because it is a one-time knowledge acquiring process from the knowledgeable person. This will become a huge threat for the AI field as it can cause to reduce the skilled workers who are willing to share their exhausting knowledge to implement AI systems. To tackle this issue, a fairer paradigm named Human-in-the-loop Artificial Intelligence (HitAI) has proposed to repay the decisions of AI systems' revenues to real knowledge owners by tracking each interaction with the automated AI system (Zanzotto, 2019). This will be a turning point towards implementing AI-based systems with the HITL design concept. However, the ethical challenges related to HITL design are yet to be addressed. For

instance, security and privacy are important concerns that may violate through the applications of this concept such as social networking and surveillance applications as they directly communicate with people's sensitive data in their daily lives (Nunes et al., 2015). In future, this research can be extended to comparatively study HITL and Human out of the Loop systems by implementing ML models focusing on human cognitive factors. Even though the HITL design concept is being applied for different areas, it is yet to discover the effectiveness of this concept in the e-Learning and educating fields. This will be a successful step towards increasing human cognition through the combination of emerging technologies such as ML, gamification and HITL design approach.

Conclusion

Even though a considerable number of industries are practicing HITL ML, it is still a relatively new area of AI. Therefore, this research focused on studying how HITL design has been utilized in different AI systems, and their key benefits and limitations through a systematic literature review. Moreover, the approaches proposed by past researchers to overcome some of those disadvantages and limitations were discussed. This systematic analysis was conducted by collecting altogether 68 research papers from different sources. The results of this study can be utilized to effectively expand this design concept for future AI systems and to explore enhancement to overcome the limitations identified in the existing HITL intelligent interactive systems.

References

Bhardwaj, A., Jagadeesh, V., Di, W., Piramuthu, R., & Churchill, E. (2014). Enhancing Visual Fashion Recommendations with Users in the Loop. *ArXiv:1405.4013 [Cs]*. https://arxiv.org/abs/1405.4013

Enabling the human in the loop: Linked data and knowledge in industrial cyber-physical systems. (2019). *Annual Reviews in Control*, *47*, 249–265. https://doi.org/10.1016/j.arcontrol.2019.03.004

Endert, A., Hossain, M. S., Ramakrishnan, N., North, C., Fiaux, P., & Andrews, C. (2014). The human is the loop: new directions for visual analytics. *Journal of Intelligent Information Systems*, *43*(3), 411–435. https://doi.org/10.1007/s10844-014-0304-9

Goecks, V. G. (2020). Human-in-the-Loop Methods for Data-Driven and Reinforcement Learning Systems. *ArXiv:2008.13221 [Cs, Stat]*. https://arxiv.org/abs/2008.13221

Holzinger, A. (2016). Interactive machine learning for health informatics: when do we need the human-in-the-loop? *Brain Informatics*, *3*(2), 119–131. https://doi.org/10.1007/s40708-016-0042-6

Holzinger, A., Valdez, A. C., & Ziefle, M. (2016). Towards Interactive Recommender Systems with the Doctor-in-the-Loop. In *Mensch & Computer Workshopband*. https://doi.org/10.18420/muc2016-ws11-0001

Lipton, Z. C. (2018). The mythos of model interpretability. *Communications of the ACM*, *61*(10), 36–43. https://doi.org/10.1145/3233231

McKinney, S. M., Sieniek, M., Godbole, V., Godwin, J., Antropova, N., Ashrafian, H., Back, T., Chesus, M., Corrado, G. C., Darzi, A., Etemadi, M., Garcia-Vicente, F., Gilbert,

F. J., Halling-Brown, M., Hassabis, D., Jansen, S., Karthikesalingam, A., Kelly, C. J., King, D., & Ledsam, J. R. (2020). International evaluation of an AI system for breast cancer screening. *Nature*, *577*(7788), 89–94. https://doi.org/10.1038/s41586-019-1799-6

Sun, W., Khenissi, S., Nasraoui, O., & Shafto, P. (2019). Debiasing the Human-Recommender System Feedback Loop in Collaborative Filtering. *Companion Proceedings of the 2019 World Wide Web Conference*. https://doi.org/10.1145/3308560.3317303

Todd, D. (2020, January 10). *Douglas Todd: Robots replacing Canadian visa officers, Ottawa report says*. Vancouversun. https://vancouversun.com/opinion/columnists/douglas-todd-robots-replacing-canadian-visa-officers-ottawa-report-says#:~:text=from%20our%20team.-

Wang, P., Peng, D., Li, L., Chen, L., Wu, C., Wang, X., Childs, P., & Guo, Y. (2019). Human-in-the-Loop Design with Machine Learning. *Proceedings of the Design Society: International Conference on Engineering Design*, *1*(1), 2577–2586. https://doi.org/10.1017/dsi.2019.264

Zanzotto, F. M. (2019). Viewpoint: Human-in-the-loop Artificial Intelligence. *Journal of Artificial Intelligence Research*, *64*, 243–252. https://doi.org/10.1613/jair.1.11345

Grønsund, T., & Aanestad, M. (2020). Augmenting the algorithm: Emerging human-in-the-loop work configurations. *The Journal of Strategic Information Systems*, *29*(2), 101614. https://doi.org/10.1016/j.jsis.2020.101614

Carley, S. S., & Price, S. R. (2021). Analyzing a human-in-the-loop's decisions for the detection of data poisoning. Proc. SPIE 11746, Artificial Intelligence and Machine Learning for Multi-Domain Operations Applications III, 1174616. https://doi.org/10.1117/12.2586260

Nunes, D. S., Zhang, P., & Sá Silva, J. (2015). A Survey on Human-in-the-Loop Applications Towards an Internet of All. *IEEE Communications Surveys Tutorials*, *17*(2), 944–965. https://doi.org/10.1109/COMST.2015.2398816

Johnson, J. (n.d.). *What Is Human in The Loop (HITL) Machine Learning?* BMC Blogs. Retrieved August 20, 2021, from https://www.bmc.com/blogs/hitl-human-in-the-loop/

Maadi, M., Akbarzadeh Khorshidi, H., & Aickelin, U. (2021). A Review on Human–AI Interaction in Machine Learning and Insights for Medical Applications. *International Journal of Environmental Research and Public Health*, *18*(4), 2121. https://doi.org/10.3390/ijerph18042121

Dorri, A., Kanhere, S. S., & Jurdak, R. (2018). Multi-Agent Systems: A Survey. *IEEE Access*, *6*, 28573–28593. https://doi.org/10.1109/access.2018.2831228

Conference Paper No: MF-02

Effect of application process and physical properties of penetrant material to the sensitivity of liquid penetrant inspection

D.S.K.L. Fernando[1*] and M.W.S. Perera[2]

[1]Faculty of Science, University of Peradeniya, Sri Lanka
[2]National Center for Non Destructive Testing, Sri Lanka Atomic Energy Board, Sri Lanka
klf.shelly@gmail.com*

Abstract

Liquid Penetrant Testing is one of the most popular and widely used NDT method in a wide range of industries such as oil & gas, power generation, aerospace, marine and automotive. It can be used to detect open to surface defects on all non-porous materials. Solvent removable visible dye penetrant testing is employed in this project. Reliability of using dye penetrants that have elapsed their manufacturer-recommended usable time for liquid penetrant testing, is presented in this paper. There are two main parts in this study; comparing the sensitivity of dye penetrants by varying inspection techniques, and comparing the physical properties of penetrant materials. Four color contrast dye penetrant samples, with different chemical aging, were selected to perform the tests. For the first part, penetrant testing was performed on two selected welding discontinuities by varying dwell time and the number of developer layers with the aid of selected dye penetrant samples. For the second part, the density and viscosity of each dye penetrants were measured. According to the results, sensitivity and detectability of solvent removable visible dye penetrant decreases with the chemical aging. However, with increased dwell time and a minimal number of developer layers, it can be used to detect volumetric defects. With chemical aging, density does not change significantly but viscosity can be changed with different thermal and environmental influences.

Keywords

Color contrast dye penetrant, Liquid penetrant testing, Non-destructive testing, Penetrant dwell time, Sensitivity

Introduction

Some phenomena like a fine surface crack on a flight of an airplane wing, landing gears or engine fan blades could lead to catastrophic failures, even to the loss of human lives. In order to prevent such undesirable circumstances, regular quality assurance inspections and maintenance procedures have been established in many industries. To carry out this task, Non-Destructive Testing (NDT) is a leading technique that has been used over the last few decades.

NDT is a physical inspection and analysis technique which used to evaluate the properties of a material, component, or system without causing any damage to the tested object.

Liquid Penetrant Testing (PT) is one of the most popular and widely used NDT method in the industry, since it is a relatively low cost and effective method with high accuracy. It requires minimal training compared to other NDT methods. PT can be used to detect cracks, fractures, porosity, and any other surface opening defects and applicable to all non-porous materials. Welding inspection is one of the most common applications of PT in the local industry.

PT mechanism is based on the physical principle of capillary action. First, dye penetrant is applied on the surface of the specimen. Then this fluid penetrates into surface-breaking discontinuities with the aid of capillary action. After adequate penetration time (this time is known as "Dwell Time") excess penetrant is removed from the surface and a developer is applied. It draws back the penetrant trapped in discontinuities and provides visible indications of discontinuities which are invisible to the naked eye.

Although PT is widely used in the local industry, there are no local penetrant material manufacturers. Hence, these penetrant materials are imported from the international market and stored for some time in local warehouses before distributing among users. Also, these chemicals are not freely available in the local market so, the procurement process will also take another short time. These issues cause to elapse of the date, that the manufacturer stated as "Best Before" after a short period received by the end-users. Then, such penetrant materials are discarded without use. This is a huge material and economical waste. In addition to that, discarding these materials could have an adverse impact on the environment due to their high penetrability and toxicity. These materials can penetrate into the water through the soil and results in serious threats to the ecosystem.

In this paper, the reliability of using color contrast dye penetrants that have elapsed their manufacturer-recommended usable time is presented. This consists two main parts,

- Comparing sensitivity of dye penetrants by varying inspection technique (dwell time, number of developer layers)
- Comparing physical properties of dye penetrants (viscosity, density)

Methodology

In this study, penetrant testing was performed according to the international standard of American Society of Mechanical Engineers (ASME) boiler and pressure vessel code, section V, article 6. As given in the below table, four color contrast dye penetrant samples from the same product, the same manufacturer and the same country of origin but with different chemical aging were used in this study. In addition to that, for the first part of the study intact developers and cleaner/solvent removers were used from the same penetrant family.

Table 1. Details of used penetrant materials

Penetrant Material	Product Specification	Batch Number	Manufacture Date	Use Best Before
Dye Penetrant Sample 1	Type II-Visible Penetrant	120106	19th Jan 2012	Jan 2015
Dye Penetrant Sample 2	Type II-Visible Penetrant	151103	05th Nov 2015	Nov 2018
Dye Penetrant Sample 3	Type II-Visible Penetrant	160803	10th Aug 2016	Aug 2019
Dye Penetrant Sample 4	Type II-Visible Penetrant	180701	03rd Jul 2018	Jul 2021
Cleaner	Solvent Remover	191108	23rd Oct 2019	Oct 2022
Developer	Non-aqueous Type II	190E03	14th Jun 2019	Jun 2022

Part I*:* In this part, two surface breakings of welded joints are investigated by performing PT. For this, two test blocks with artificially made flaws given in below table were used.

Table 2. *Details of artificially made flaws*

Flow Number	Test Block	Discontinuity Description	Start of flaw to Reference Edge	Total flaw Length	Flaw Type
1	Flawtech RT-2839	Toe Crack in Butt weld	64mm	13mm	Surface Breaking
2	Flawtech MT-7719	Lack of Fusion in Fillet weld	33mm	8mm	Surface Breaking

First, the surfaces of the two test blocks were cleaned using a wire brush to remove rust. Then the test blocks were dipped in a hydrophilic emulsifier for 5 min and then cleaned with water for 2 min. This is an extra step to clean inside the flaws additionally to general cleaning using solvent remover in the pre-clean step. Then, the test blocks were completely dried by keeping them under sunlight for 10 min. In the pre-cleaning step, the test blocks were cleaned using solvent remover/cleaner. It was applied to the surface by spraying and then wiped using a lint-free cloth. After completion of pre-cleaning, a thin uniform layer of sample 1 visible dye penetrant was applied to the test blocks by spraying, such that the dye layer covers the inspection area. To achieve the objective of the study, PT was performed by varying dwell times. As per the standard methodology given in the ASME Code, minimum dwell time is 5 min. As a rule of thumb, applicable range of the dwell time is considered 5min to 20 min. Therefore, in this study, dwell time was chosen to be 5 min, 10 min, 15 min, and 20 min. After the dwell time, excess penetrant was removed by wiped using a lint free cloth and then wiped using a lint free cloth dampened with solvent remover. Once the part is dried by normal evaporation, as soon as possible a non-aqueous Type II developer was applied by spraying. For each chosen dwell time, the developer was applied by varying the number of developer layers. As per the standard methodology given in the ASME code, it has to apply minimum no of thin transparent developer layers one after one under visual examination. In this study, number of developer layers was chosen to be 1, 2, and 3. After 10 s of developing time, results were recorded.

For all the above-mentioned dwell times and number of developer layer variations, surface preparation and pre-clean processes were repeated totally 12 times. The same procedure was repeated for sample 2, sample 3 & sample 4. At the end of every penetrant test, detected indication lengths of each flaw were measured by using calibrated steel ruler and results were recorded as photographs in JPEG format. Then, weighting factors from 0 (No indication) to 5 (Very clear and bright indication) were assigned to data points by considering their indication lengths and acuity of color brightness in order to observe the obtained results comparatively. Then the data set was analyzed.

Part II: In this part, the physical properties; density, and viscosity of four visible penetrant samples were observed.

A pycnometer was used to determine the density of four visible penetrant samples. First, the pycnometer was cleaned with distilled water and dried completely. Then the weight of the empty pycnometer was measured using the electronic balance. Next, the pycnometer was filled with distilled water and the weight was measured. After that

pycnometer was dried completely and filled with sample 1, then the weight was measured. Again, pycnometer was cleaned and dried completely.

This same procedure was repeated for sample 2, sample 3 and sample 4. Room temperature was recorded. Finally, density of each sample at the corresponding was calculated using below equation [2].

$$\rho_L = \frac{m_L}{m_{H_2O}} \rho_{H_2O} \qquad (1)$$

$V = Volume\ of\ the\ Pycnometer,\ m_{H_2O} = Mass\ of\ water,\ m_L = Mass\ of\ liquid,$
$\rho_{H_2O} = Density\ of\ water,\ \rho_L = Density\ of\ liquid$

Ubbelohde viscometer was used to determine the viscosity of the dye samples. First, the viscometer was cleaned using distilled water and then dried completely. After that, sample 1 was poured into the vertically fixed viscometer until it reaches the upper line of the reservoir. Then using a rubber suction valve, the sample was introduced to the measuring bulb through the capillary tube. Then the sample was allowed to travel back through the capillary tube to the reservoir, and the time taken by the sample to pass through two calibrated marks was measured. Finally, the viscometer was cleaned and dried.

The same procedure was repeated for sample 2, sample 3, and sample 4. Room temperature was measured. Finally, using the obtained results and the viscometer constant, the viscosity of each sample at the corresponding temperature was calculated. For a given glass capillary viscometer, the driving force is the hydrostatic pressure of the liquid column in the form of the mean pressure height. Considering the laminar flow within the capillary, Hagen-Poiseuille Law gives that,

$$\nu = \frac{\pi R^4 h g}{8LV} t \qquad (2)$$

In addition to the flow time, equation 2 contains only constants and geometric details. So, for a given viscometer, that constant part can be summarized into one characteristic magnitude. Which is known as "Viscometer Constant" (K). This value is a determined value for each individual viscometer according to its type and size. So, the viscosity of a liquid can be calculate using the below equation. [1]

$$\nu = Kt \qquad (3)$$

Results and Discussion

Weighted results were analyzed based on three variables; different dye penetrant samples, different number of developer layers & different dwell times.

The Figs. 1 and 2 show the results regarding the different dye penetrant samples on both test blocks. According to the results, each dye penetrant sample gives considerable fair results when it is used on test block 2, but there is a clear difference in the results from test block 1. For both test blocks, sample 4 gives the best results and sample 1 shows less detectability compared to others. When the defect is tight (very narrow opening), dye penetrants that elapsed their usable time tends to refrain penetrate into the flaw. Therefore, sample 1, 2 & 3 gives fewer defect detections compared to sample 4 when they are applied on block 1.
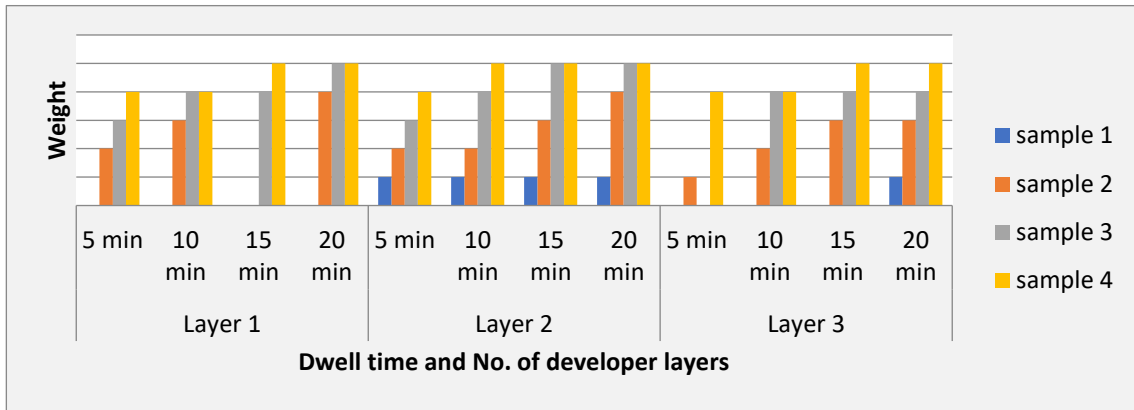
Figure 1. Results for four dye penetrant samples from Flaw 1 of the test block 1.

When considering the number of applied developer layers, double layers indicate high detectability of flaws in both test blocks than single developer layer or triple developer layers. The developer extracts the entrapped penetrant in the flaw and gives indications. When a single layer of developer is applied, it is not sufficient to bring back the entrapped penetrant back to the surface. Therefore, it gives less defect detection. When triple layers of developer are applied, thickness of the developer layer is considerably large and tends to mask the defects. Double layers' developer is sufficient and effective. But, when the defect width is larger, number of developer layers does not affect much on results.
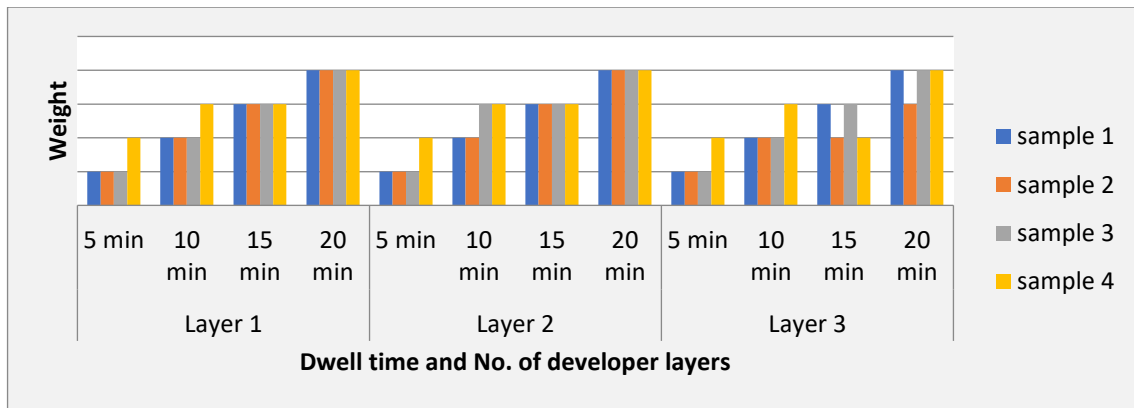

Figure 2. Results for four dye penetrant samples from Flaw 2 of test block 2.

An increase in dwell time has enhanced the defect detection capability in both test blocks. Dwell time is an important factor of PT because it allows the penetrant to be drawn into the defect. As per the both standard methodology given in the ASME Code and manufacturer's recommendations minimum dwell time is 5min, these experimental results indicate that the penetrant material getting aged, it is required to increase the dwell time respectively.

In the second part of this study, the density and viscosity of four dye penetrant samples were analyzed. When the density variation is considered, samples 1 and 2 have a density of 0.83×10^3 kg/m^3, and samples 3 and 4 have a density of 0.82×10^3 kg/m^3 at 31˚C. Both values are approximately close to the valve given in the manufacturer's specification (0.85×10^3 kg/m^3). In this experiment, densities of dye penetrants were measured to monitor the quality of the dye penetrants; In order to check whether these dye penetrant samples have been contaminated with the time. Contamination of a penetrant by another

liquid or any other means will change the surface tension and hence its penetration ability. Test results indicate that the dye penetrant samples were not contaminated.

According to the manufacture's specification viscosity of the solvent removable visible dye penetrant is $3.80 \times 82 \times 10^{-6}$ m^2/s at 38°C. The viscosity of penetrant sample 1, 2, 3 and 4 is found 2.15×10^{-6} m^2/s, 1.93×10^{-6} m^2/s, 1.82×10^{-6} m^2/s and 1.8×10^{-6} m^2/s respectively (at 31°C). Although viscosity is decreasing with the increment of temperature, there is a possibility that exposure to heat can lead to increased viscosity. This means, increased heat or temperature can be caused to evaporate the volatile content in the dye penetrant and it results in high viscous dye penetrants [3]. Dye penetrant samples used in this project were stored in a normal storeroom without controlled temperature conditions prior to the experimental use. So, they had been exposed to different temperature and heat conditions over time and it can cause to change the volatile content, viscosity and the penetrability of the penetrant with their chemical ageing. Sample 1 has the largest time gap between its usable times, so it has exposed to heat than the other three samples; which explains its high viscosity compared to the three other samples. Improved storage conditions with controlled temperature can have positive impacts on the quality of dye penetrants.

Conclusion

The sensitivity and detectability of the penetrant will decrease with penetrant chemical aging, but considering flaw size and type, dye penetrants which have elapsed their usable time can be used utilizing increased dwell time and minimal number of developer layers. With the chemical aging of penetrant, density does not change significantly but viscosity can be changed with different thermal conditions and environmental impacts of storage facility.

Acknowledgment

References

B. Larson, (2002), Study of the Factors Affecting the Sensitivity of Liquid Penetrant Inspections: Review of Literature Published from 1970 to 1998.

D. S. Viswanath, T. K. Gosh, D. H. L. Prasad, N. V. K. Dutt, and K. Y. Rani, (2007), Viscosity of Liquids; Theory, Estimation, Experiment, and Data.

[1] J. Wike, H. Kryk, and J. Hartmann, Theory and Praxis of Capillary Viscometer.

[2] M. Gülüm and A. Bilgin, (2018), pp 289, Energetic & Environmental Dimensions.

[3] A. G. Sherwin, and W. O. Holden, (1979), pp. 52-56, 61. Heat Assisted Fluorescent Penetrant Inspection, Materials Evaluation.

Conference Paper No: MF-03

Perceived value analysis of motorcycles in Sri Lanka

P.A.L. Chanika[1*], A.M.C.H. Attanayake[1] and M.D.N. Gunaratne[2]

[1]Department of Statistics & Computer Science, University of Kelaniya, Sri Lanka
[2]Agriculture Sector Modernization Project, Sri Lanka
laknichanika1213@gmail.com*

Abstract

The motorcycle is the vehicle with highest demand in Sri Lanka. Motorcycle usage in Sri Lanka is expanding rapidly over the years primarily due to its affordable price range. Customer perception refers to the customer's opinion of the service/product and evaluates through perceived value analysis. It is important to know the relationship between the price of motorcycles and customer perceived value of motorcycles for decision-makers in the automotive industry. The objectives of this study are to identify the attributes which are most important in formulating the customer perception towards motorcycle prices, identify the relationship between the price and customer perception of the motorcycles and calculate the perceived value for each motorcycle model under consideration. A total of 1117 customers were used to generate data with respect to 21 motorcycle models. Non- probability sampling techniques were appliedin the market survey, that gathered data on customer opinion on attributes such as brand, appearance, features, fuel efficiency, resale value, after-sale services, and suitability for road. were identified as the important attributes in formulating the customer perception towards motorcycle prices. Perceived value for each Commuter Standard, Commuter Deluxe, Sports Classic and Sports Premium motorcycle models were calculated by using the weightage of each attribute and rank of motorcycles. According to the Pearson correlation coefficient, there is a positive relationship between the actual price and the perceived value of motorcycles. Therefore, this analysis helps to understand purchasing decisions of customers and industry players can use this information for adjusting their pricing strategies against the market competition.

Keywords

Customer perception, Perceived value analysis, Prices of motorcycles

Introduction

The motorcycle is the best-selling vehicle in Sri Lanka according to the data of the Ministry of Transport, Sri Lanka. (Ministry of Transport) Sri Lankan automobile companies import a diverse range of motorcycles from different countries. Competition between motorcycle companies would be beneficial to customers themselves on one hand. In the automobile industry of Sri Lanka, customers have access to a wide variety of product choices at different prices and qualities. Therefore, the knowledge of customer's opinions on motorcycles is important in attracting new customers, retaining existing customers as well as maintaining the survival of the automobile companies.

Customer perception refers to the customer's opinion of the service/products. This explains the customer's feeling about the service/product including direct and indirect experiences of the customer. Companies can recognize common user-specific problems and attract customers by analyzing consumer perceptions. Customers' total appraisal of the product is based on impressions of what is received and what is given, and this is known as perceived value (Zeithmal, 1988). Customer value can be defined as a

customer's perception and evaluation of product attributes, attribute performances, and use consequences that help the customer to achieve their objectives (Woodruff, 1997). According to Jansri, 2018 scholars should focus further on consumer behavior when studying on perceived value. Perceived value is a vital aspect of marketing and it can be used for the long-term success of businesses. Simply, the perceived value shows the interaction between the customer and the product.

Sri Lankan consumers pay their attention to some of the attributes before buying a motorcycle. Especially the Motorcycle brand, style and also accessories of the motorcycle are affected to the customer perception (Weerasiri & Mendis, 2015). The manufacturing country of the motorcycle is another main factor according to the views of subject expertise in automotive industries.

The main objectives of this study are to identify the attributes which are most important in formulating the customer perception towards motorcycle prices, identify the relationship between the price and customer perception of the motorcycles and calculate the perceived value for each motorcycle model. Calculating the perceived value for each motorcycle brand and analyzing perceived value will be most important because it is useful for the decision-makers of the automotive industry in Sri Lanka.

Many researchers have studied customer perception. Weerasiri & Mendis, (2015) examined the factors which affect the purchasing decision for Indian two-wheelers in the Sri Lankan market. The researcher employed six variables namely price, technology, and design, product awareness, spare parts availability, after-sales services, and economic conditions. According to the correlation analysis of this study, it was revealed that there is a significant relationship between each independent variable namely price, technology, and design, economic condition, product-related awareness, after-sales services, spare parts, and consumer buying intention towards the Indian two-wheelers. According to the results of this research, there was a strong, positive, linear relationship between those variables and the consumer preference towards the Indian two-wheelers.

Dr.Khoso, Dr.Kazi, Dr.Ahamedai, & Memon, (2016) have examined the factors which affect customer preference/purchase decision for motorcycle brands in Hyderabad. They have used a survey method and a questionnaire was used to collect the primary data about the customer preference for motorcycle brands. They have employed quantitative methods for collecting data on factors that influence an individual's decision to purchase a particular brand of motorcycle. The researchers identified the internal factors such as family, personal consciousness of brand (brand perception), friends and peer advice, word of mouth, occupation and previous experience, and external factors such as price affordability, quality, mileage, maintenance cost, style are affected to the customer preference for motorcycle brands.

Ramana & Dr. Subbaiah, (2013) conducted a study on consumer's perception towards the purchase decision of two-wheeler motorcycles in Nellore District, Andhra Pradesh. They have examined the factors which affect customer perception. The main objectives of the research were identifying the relationship between the current brand of the motorcycle being used by respondents and demographic characteristics of consumers and analyzing the factors/attributes influencing the purchase decision of motorcycle users while making the purchase decision. The researchers analyzed the data by using percentages, factor analysis, and ANOVA. The conclusion of this research is producers and marketers should pay more attention to those factors which connect to the buyer and influence their

purchase decision, consumers give importance to the style, promotional offers, price, capacity of engine, maneuverability, fuel economy, service availability, maintenance cost, brand ambassador.

Although several studies have conducted perceived value analysis on motorcycles an updated analysis of the area is important in the Sri Lankan context.

Methodology

One thousand one hundred and seventeen samples were used for this research representing 21 motorcycle models. Through a market survey, Brand, Appearance, Features, Fuel Efficiency, Resale Value, After-Sale Services, and Suitability for Road of motorcycles were identified as the important attributes in perceived value analysis, and ranks of each factor were obtained (as 1 being the most important) 21 number of motorcycles which are most demanded models in Sri Lankan automotive market were chosen, which were divided into four categories namely commuter standard, commuter deluxe, sports classic, and sports premium after discussing with a subject matter specialist. For each motorcycle category, the variable weights were revealed using customer perception data. Commonly factor analysis is used to reduce a large number of variables into fewer numbers of factors. In this study, factor analysis was used to extrapolate the weightage of each variable. The principal component technique was used for the factor analysis as the extraction method. The perceived value for each motorcycle was calculated by using the weightage and percentage of rating across the competition. The following equation was used to calculate the perceived values.

$$\sum_{i=1}^{n} Weightage_i(Motorcycles\ Rating\ as\ a\ Percentage_i)$$

Where, $i = 1,..,n$

n is the number of attributes/features we used. The rating across competition of motorcycles for each variable is defined by the subject expertise of the automotive industry in Sri Lanka. The Person correlation was used to determine the relationship between actual motorcycle prices and perceived values.

Results and Discussion

The results of factor analysis were shown in Table1.

Table 1. *Weightage of variables.*

Variables	Weightage			
	Commuter Standard	**Commuter Deluxe**	**Sports Classic**	**Sports Premium**
Appearance	2%	2%	11%	4%
Features	6%	13%	1%	3%
Fuel Efficiency	10%	11%	11%	13%
Resale Value	11%	16%	15%	13%
Engine Power	37%	9%	17%	42%
After Sales Service	18%	18%	20%	20%
Suitability for Roads	16%	31%	25%	5%

Table 1 shows that the weightage of the factors for each Motorcycle Category. The highest weight percentage belongs to the Engine Power than the other factors for Commuter Standard and Sports Premium motorcycle categories (37% and 42%). Commuter Deluxe and Sports Classic motorcycles have the highest weight percentage for Suitability for Roads (31% and 25%). According to Table 1, 2% of the minimum weight percentage belongs to the Appearance for Commuter Standard and Commuter Deluxe motorcycles. Sports Classic motorcycles and Sports Premium motorcycles have the minimum weightage for Features.

The perceived value for each motorcycle was calculated according to each motorcycle category.

Table 2. *Perceived Values and Actual Prices of Motorcycles.*

	Model	Perceived Value	Actual Price (LKR)
Commuter Standard	Honda Dream CD 110	19.76%	241900
	Bajaj CT 100	20.80%	265950
	Hero HF Deluxe ES	19.88%	245000
	TVS Metro ES	17.39%	238900
	Bajaj Platina	22.18%	249950
Commuter Deluxe	Bajaj Discover 110	24.89%	258950
	Hero Splendor I smart	13.91%	235000
	Hero Passion Pro	21.89%	264500
	Honda Shine	24.36%	282900
	Honda CB Twister	14.96%	248900
Sports Classic	TVS Apache 150	18.46%	358900
	TVS Apache 180	19.67%	413500
	Bajaj Pulsar 135	15.73%	307950
	Bajaj Pulsar 150	31.54%	371950
	Bajaj Pulsar 180	37.32%	410950
Sport Premium	Bajaj Avenger	15.65%	429950
	Yamaha FZ S-V2	21.86%	452900
	Suzuki Gixxer	15.47%	443900
	Honda CB Hornet	14.10%	399900
	Hero Hunk	12.15%	385000
	Bajaj Pulsar 200	20.77%	488950

Table 2 illustrates that the calculated perceived value of motorcycles and their actual prices. The motorcycles are categorized into four categories and the highest perceived value belongs to Bajaj Discover 110 motorcycle.
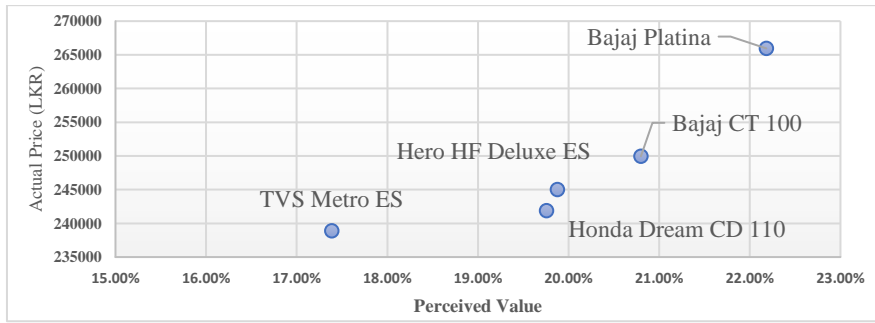
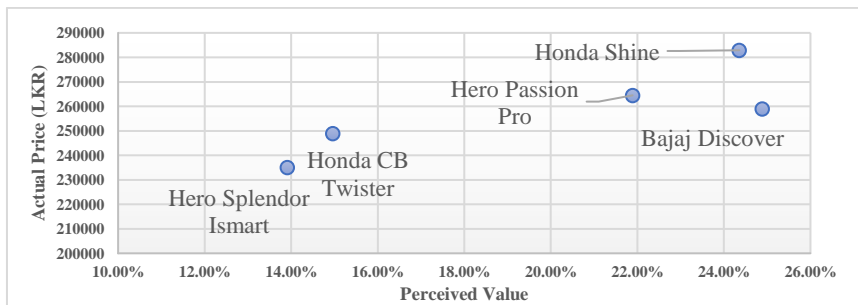***Figure 1.*** *Graph of Perceived Value Vs Actual Price for Commuter Standard Motorcycles.*

Figure 2. *Graph of Perceived Value Vs Actual Price for Commuter Deluxe Motorcycles.*
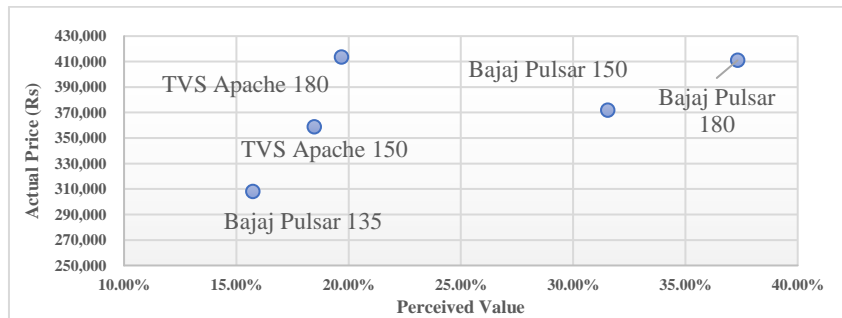

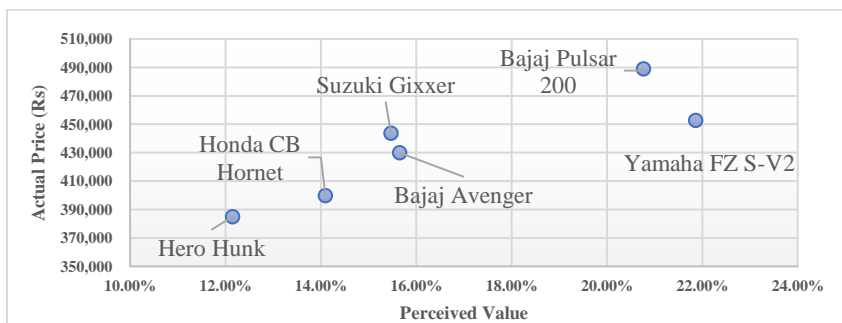***Figure 3.*** *Graph of Perceived Value Vs Actual Price for Sports Classic Motorcycles.*

Figure 4. *Graph of Perceived Value Vs Actual Price for Spots Premium Motorcycles.*

Figure 1, Figure 2, Figure 3, and Figure 4 shows that the motorcycle's perceived value increasing, then the actual price also generally increasing for all motorcycle categories.

Table 3. *Pearson correlation coefficient between perceived value and the actual price for each motorcycle category.*

Motorcycle Category	Pearson Correlation Coefficient
Commuter Standard	0.6
Commuter Deluxe	0.8
Sports Classic	0.6
Sports Premium	0.9

According to the Pearson correlation coefficient Commuter, Standard, and Sport Classic motorcycle's actual prices have a moderate positive relationship with the perceived value. Commuter Deluxe and Sports Premium motorcycle's actual price have a fairly positive relationship with the perceived value of each motorcycle.

Conclusion

The relationship between the price of motorcycles and customer perceived value of motorcycles is important for decision-makers in the automotive industry. The objectives of this study are to identify the attributes which are most important in formulating the customer perception towards motorcycle prices, identify the relationship between the price and customer perception of the motorcycles and calculate the perceived value for each motorcycle model in the study. Through a market survey, Brand, Appearance, Features, Fuel Efficiency, Resale Value, After-Sale Services, and Suitability for Road were identified as the important attributes in formulating the customer perception towards motorcycle prices. Factor Analysis was used to assign a weight for each attribute of each motorcycle category and the Principal Component analysis was used to obtain the weight using the Extraction sums of squared loadings for each attribute. The highest weights for the Commuter standard and Sports premium categories were assigned for the attribute of 'Engine power' which were 37% and 42% respectively. It is for Commuter deluxe and Sports classic were 31% and 25% respectively by recording the attribute 'Suitability for roads'. Perceived value for each Commuter Standard, Commuter Deluxe, Sports Classic and Sports Premium motorcycle models were calculated by using the weightage of each attribute and rank of motorcycles. The Pearson correlation coefficient is calculated between the actual price and perceived value for each motorcycle category. The correlation coefficients were 0.6, 0.8, 0.6, and 0.9 for Commuter Standard, Commuter Deluxe, Sports Classic, and Sports Premium categories respectively. There is a moderate positive relationship between the actual price and perceived value of the Commuter standard and Sports classic motorcycles and a fairly strong positive relationship between the Commuter deluxe and Sports premium motorcycles.

All the objectives of the study are accomplished and this analysis helps to make purchasing decisions of customers and industry players can use the results of this study to adjust their pricing strategies against the market competition. Further, the authors strongly believe that this study will provide a guide for further studies on perceived values analysis of motorcycles.

References

(n.d.). Retrieved from Ministry of Transport: https://www.transport.gov.lk/web/index.php?option=com_content&view=article&id=26&Itemid=146&lang=en#vehicle-population

Dr.Khoso, A., Dr.Kazi, A., Dr.Ahamedai, M., & Memon, M. (2016). Assessment of factors affecting the customer Preferences / Purchase decision for motorcycle brands: An analysis of the motorcycle users of Hyderabad. *International Journal of Multidisciplinary Research and Development*, 239-247.

Jansri, W. (2018). Consumer Perceived Value: A Systematic Review of the Research. *International Journal of Management and Applied Science*, 20-25.

Ramana, D., & Dr.Subbaiah, P. (2013). A Study on Consumer's Perception towards the Purchase Decision of Two Wheeler Motorcycles in Nellore District, Andhra Pradesh. *International Journal of Research in Commerce, IT and Management*, 9-14.

Weerasiri, R., & Mendis, A. (2015). Factors Affecting Purchase Decision for Indian Two Wheelers in Sri Lankan Market. *Kelaniya Journal of Management, 4*(2), 10-22.

Woodruff, R. (1997). Customer value: The next source for competitive advantage. *Journal of the Academy of Marketing Science*, 139-153.

Zeithmal, V. (1988). Consumer perceptions of price, quality, and value: a means-end model and synthesis of evidence. *The Journal of Marketing*, 2-22.

Conference Paper No: MF-04

Applicability of modified queueing model with encouraged arrivals for economic recession

J.A.S. Dinushan[*] and C.K. Walgampaya

Department of Engineering Mathematics, University of Peradeniya, Sri Lanka
sanoj.j@eng.pdn.ac.lk*

Abstract

Businesses often offer lucrative deals and discounts so that customers' encouragement to engage with those firms are developed. This kind of arrivals are termed as encouraged arrivals. As a pandemic is overwhelming the world, it could be suggested that, for upbringing of declining businesses, this concept, now, deserves to be taken into account more than ever in the past. In order to describe the encouraged arrival process mathematically, a Markovian queuing model is used and the parameter that represents the arrival rate is modified with percentage increase in the arrival rate of customers. In this paper, we investigate the behavior of measures of performances with and without encouraged arrivals for multi-server finite capacity queuing system. In the analysis it was possible to identify that a significant number of customers compared to the normal arrival process is engaged with the system when it is affiliated with the encouraged arrival process. As well as it shows that customers engage more and more with the system irrespective of the high rates of arrivals and low rates of services. In addition to that under the economic analysis, it was uncovered that the profit increment due to encouraged arrivals is very higher than that due to normal arrivals.

Keywords

Covid-19, Economic Recession, Encouraged Arrivals, Queuing System

Introduction

The advancement of the cutting-edge technology and the rising concept of globalization has influenced businesses so that the environment of businesses gets more competitive than ever before. As well as customers have become more selective and the availability of different brands in each specific product has been resulted in brand switching more frequently. So, it has become a more decisive challenge for every business to maintain a more attractive environment for drawing the attention of as many customers as possible. As a business becomes more copious, the attraction of customers is involuntarily drawn to it and as more customers get engaged with the business, the development of business is ensured. In that case, customer management plays a more catalytic role to ensure a high degree of interest in customers. As well as in the contemporary situation of COVID 19 pandemic, businesses are one of the most affected areas. Varieties of solutions are suggested to overcome from this unpleasant condition and in this case also encouraged arrivals can be regarded as a more effective solution.

Considering customer management, queueing theory deserves to be paid special attention as on many occasions waiting lines are formed when the arrival rate of customers outpaces the service rate of firms. Erlang has initially introduced the concept of queuing theory in the context of telephone traffic engineering (Erlang, 1909). By now, that concept is made use in various fields.

In depth study of queuing theory, we were able to identify number of research carried out regarding different practical approaches such as queuing systems with limited and unlimited length of waiting lines (Jiang, Khattak, Hu, Zhu, & Yao, 2016), and queuing systems with one service point (Som & Seth, An M/M/1/N queuing system with encouraged arrivals, 2017). However, as one of the most practical applications of waiting lines, we decided to study the behavior of a queuing system having multiple service points.

In addition to that, the effects of applicable measures that are usually taken by businesses to increase the number of customers who visit the business were mainly investigated. The arrivals of customers under such stimulations such as lucrative deals and various offers are called encouraged arrivals. The effect of encouraged arrivals was introduced into the model by making a slight change to parameters. In this paper we compare the differences of such encourage arrivals and normal arrivals of multiple server - finite capacity (M/M/c/N) queuing system under steady state probabilities in different aspects such as average number of customers gathered in the queue, profit that could be earned and cost of making that profit.

Methodology

A model that describes (M/M/c/N) queuing system was created and results were plotted against ranges of arrival rates and service rates.

Assumptions of the model:

(i)   The arrivals occur one by one in accordance with the Poisson process with parameter $\lambda(1+\eta)$, where 'η' represents the percentage increase in the arrival rate of customers, calculated from past or observed data.
(ii)   Service times are exponentially distributed with parameter 'μ'.
(iii)   Customers are serviced in the order of their arrival.
(iv)   There are 'c' servers through which the service is provided.
(v)   The capacity of the system is finite, say 'N'.

A. Steady-State Probabilities

The probability of 'n' customers in the system (Som & Seth, An M/M/1/N queuing system with encouraged arrivals, 2017)

$$P_n = \{\frac{1}{n!}r^n P_0, \qquad 0 \le n < c \quad \frac{1}{c^{n-c}\,c}r^n P_0, \qquad c \le n \le N$$

The probability of no customers in the queue

$$P_0 = \{\left[\sum_{n=0}^{c-1} \frac{r^n}{n!} + \frac{r^c}{c!}(1-\rho^{N-c+1})\frac{c}{c-r}\right]^{-1},$$

$$\rho \ne 1 \quad \left[\sum_{n=0}^{c-1} \frac{r^c}{n!} + \frac{r^c}{c!}(N-c+1)\right]^{-1}, \qquad \rho = 1$$

B. Measures of performance

Based on the steady-state probabilities, formulae for measures of performances were obtained.

Average number of customers in the system

$$L_s = \sum_{n=0}^{N} nP_n = L_q + c - P_0 \sum_{n=0}^{c-1} \frac{(c-n)(\rho c)^n}{n!}$$

Average number of customers in the queue

$$L_q = \frac{P_0 r^c \rho}{c! \, (1-\rho)^2} [1 - \rho^{N-c+1} - (1-\rho)(N-c+1)\rho^{N-c}] \qquad where \; \rho \neq 1$$

Average waiting time in the system $\qquad W_s = \frac{L_s}{r\mu(1-P_N)}$

Average waiting time in the queue $\qquad W_q = \frac{L_q}{r\mu(1-P_N)}$

where,

$\rho = \frac{\lambda}{c\mu}$ and $r = \frac{\lambda}{\mu}$ for normal arrivals, and $\rho = \frac{\lambda(1+\eta)}{c\mu}$ and $r = \frac{\lambda(1+\eta)}{\mu}$ for encouraged arrivals.

For same measures, the difference between with and without encouraged arrivals, were investigated

C. Economic model

C_s = Cost per service per unit time.

C_h = Holding cost per unit per unit time.

C_L = Cost associated with each lost unit per unit time.

R = Revenue earned per unit per unit time.

Following economic parameters were calculated using steady-state probabilities and measures of performances. (Som & Seth, An M/M/2/N Queuing System with Encouraged Arrivals, Heterogenous Service and Retention of Impatient Customers, 2017).

Total Expected Cost $\quad TEC = C_s\mu + C_h L_s + C_L \lambda(1+\eta)P_N$

Total Expected Revenue $\quad TER = R\mu(1 - P_0)$

Total Expected Profit $\quad TEP = TER - TEC$

Measures of performances, costs and profits were simulated for arrival rates ranging from 2 to 3.7 and service rates ranging from 3 to 4.7. Values for C_s, C_h, C_L and R were taken according to previous studies (Som & Seth, An M/M/1/N queuing system with encouraged arrivals, 2017). Simulation was carried out using Microsoft excel.

Results

We have observed the variation in measures of performance with respect to arrival rate and service rate.
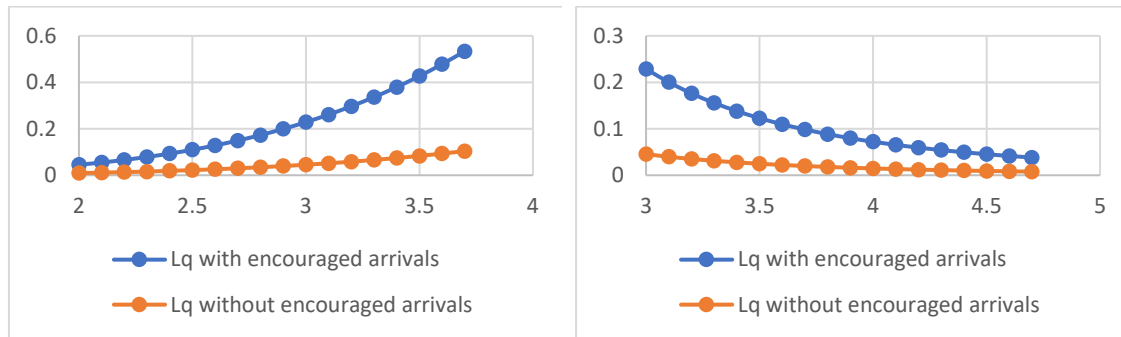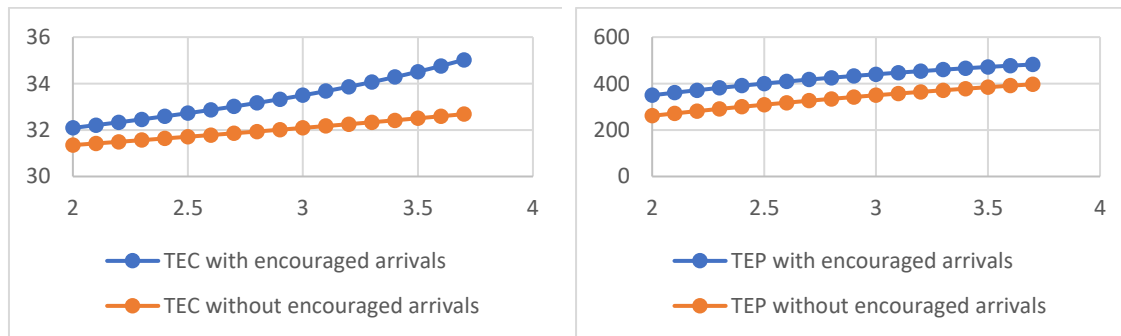

a. Lq Vs λ when $\mu = 3$ b. Lq Vs μ when $\lambda = 3$

Figure 1. *Simulation results when $N = 10, c = 3, \eta = 0.5$*

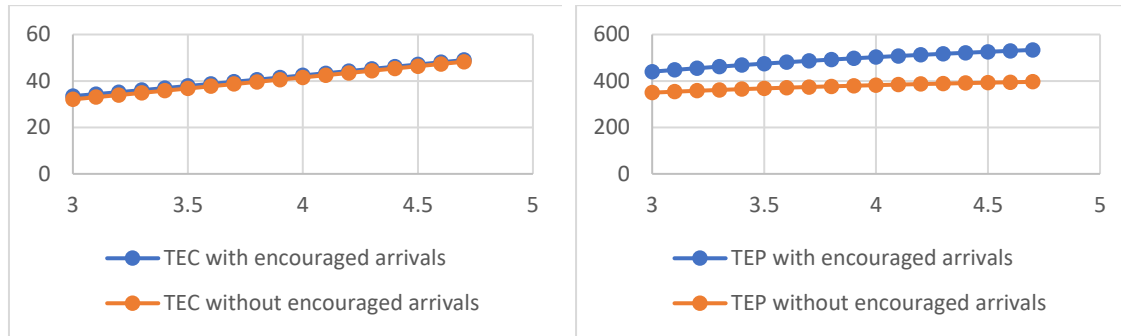Then we observed the variation in economic parameters with respect to arrival rate.

a. TEC Vs λ b. TEP Vs λ

Figure 2. *Simulation results when $N = 10, c = 3, \eta = 0.5, \mu = 3, C_s = 10, C_L = 15, C_h = 2, R = 200$*

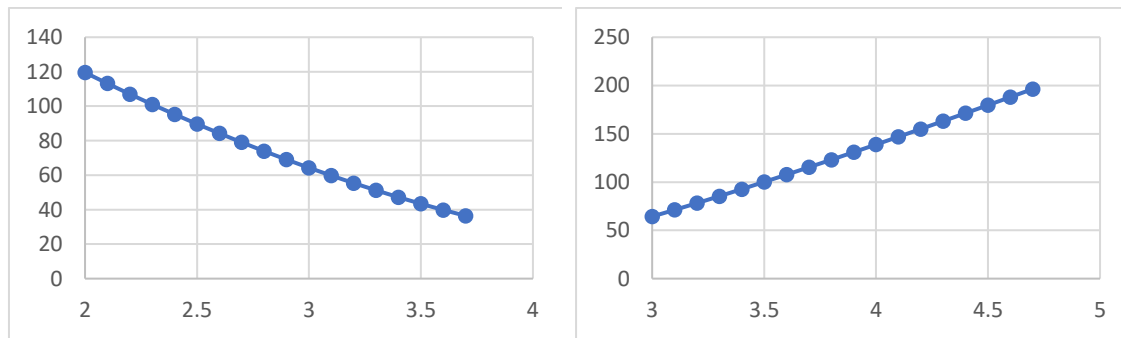Variation in economic parameters with respect to service rate is also observed.

a. $TEC\ Vs\ \mu$ b. $TEP\ Vs\ \mu$

Figure 3. *Simulation results for* $N = 10, c = 3, \eta = 0.5, \lambda = 3, C_s = 10, C_L = 15, C_h = 2, R = 200$

In addition to that the ratio between profit increment to cost increment due to the encouraged arrivals versus arrival rate and service rate are also investigated.

a. (Profit increment / Cost increment) Vs λ when $\mu = 3$ b. (Profit increment / Cost increment) Vs μ when $\lambda = 3$

Figure 4. *Simulation results for* $N = 10, c = 3, \eta = 0.5, C_s = 10, C_L = 15, C_h = 2, R = 200$

Discussion

All the measures of performances always maintain a higher value when it is with encouraged arrivals. As the arrival rate increases, all the measures of performances increase, whereas as the service rate increases, all the measures of performances decrease. As well as it is conspicuous, there are significant differences between measures of performances (Lq) with and without encouraged arrivals in Figure 1.a and 1.b. Though the arrival rate becomes more and more high, the number of customers joining to the queue with an encouraged arrival process does not reduce; it becomes more higher compared to the number of customers joining to the normal arrival process (Figure 1.a). In a similar manner, it is possible to notice a very high number of customers in the encouraged arrival process compared to the normal process even at low service rates (Figure 1.b). The difference of these two situations can be considered as the willingness of customers to engage with a system with encouraged arrivals irrespective to the high arrival rates and low service rates.

Considering the cost analysis, both cost and profit always maintain a higher value for encouraged arrivals than normal arrivals. Yet the cost increased due to encouraged arrivals can be taken for granted compared to the profit increased due to encouraged arrivals. Having calculated according to the data taken from previous studies, it is possible to observe that the increment of TEP/increment of TEC due to encouraged arrivals is almost higher than 60 for many numbers of cases (considerable range of arrival rates and service rates) according to Figure 4.a and 4.b. As well as according to the Figure 3.a, the cost of encouraged and unencouraged arrivals almost remained undeferred, yet the profit shows a considerable increment due to encouraged arrivals. Furthermore, comparing Figures 2.a and 3.a, it is possible to witness that the cost increment due to encouraged arrivals as service rate changes is much lower than that as arrival rate changes. However, it is difficult to see a considerable change of differences between profits with and without encouraged arrivals when arrival or service rate changes as per Figure 2.b and 3.b.

Conclusion

More customers will retain in the system when the firm releases various offers and discounts so that it makes encouraged arrivals. That is drastically increased as the arrival rate increases and takes a considerable higher value though the service rate takes a low value. That represents the stimulation of customers when they see many numbers of customers are getting engaged with the firm and the interest due to the encouragement of them though they see the slowness of serving process. The profit that can be earned by encouraged arrivals is considerably larger compared to the amount of cost paid on it. As well as the profit is considerably developed by a slight increment of service cost. Considering all these aspects, it can be concluded that the concept of encouraged arrivals is preferable for upholding declining business and further developing undeveloped business. Furthermore, this concept could be taken into consideration to face successfully against the economic recession in this era due to COVID-19 pandemic.

References

Erlang, A. K. (1909). The theory of probabilities and telephone conversations. *Nyt Tidsskrift for Matematik, 20*, 33.

Jiang, Y., Khattak, A., Hu, L., Zhu, J., & Yao, Z. (2016). Analytical modeling of two-level urban rail transit station elevator system as phase-Type bulk service queuing system. *European Transport* (62), 5.

Som, B. K., & Seth, S. (2017). An M/M/1/N queuing system with encouraged arrivals. *Global Journal of Pure and Applied Mathematics, 13*, 3443-3453.

Som, B. K., & Seth, S. (2017). An M/M/2/N Queuing System with Encouraged Arrivals, Heterogenous Service and Retention of Impatient Customers. *Advanced Modeling and Optimization, 19*, 97-104.